FITNESS FOR SERVICE ASSESSMENT OF CORRODED PIPELINES

RAM KUMAR BALAKRISHNAN

FITNESS FOR SERVICE ASSESSMENT OF CORRODED PIPELINES

BY

RAM KUMAR BALAKRISHNAN

A THESIS

SUBMITTED TO THE SCHOOL OF GRADUATE STUDIES

IN PARTIAL FULFILLMENT OF THE

REQUIREMENTS FOR THE DEGREE OF

MASTER OF ENGINEERING

FACULTY OF ENGINEERING AND APPLIED SCIENCE

MEMORIAL UNIVERSITY OF NEWFOUNDLAND

St. John's, Newfoundland, Canada

December 2005

Your file Votre référence
ISBN: 978-0-494-30448-8
Our file Notre référence
ISBN: 978-0-494-30448-8

ABSTRACT

Pipelines provide the safe and economic means of transporting oil and gas. Ageing of these pipelines leads to the gradual loss of pipe strength and degradation of performance, because of the development of corrosion defects. Assessment of the corroded pipeline for fitness for service purposes remains as a critical activity of the transmission pipeline integrity management program. Several Level 2 assessment methods have been developed so far to evaluate the remaining strength of corroded pipelines. Most of these methods are based on a semiempirical fracture mechanics approach. Although the ASME B31G criterion for the evaluation of corroded pipelines seems to be adequate for design, it is known to be conservative. The use of high toughness pipeline materials with good post yield characteristics has enabled the application of limit load estimation techniques based on net section collapse criterion for the evaluation of corroded pipelines.

This thesis discusses the application of an improved lower bound limit load estimation technique that is based on variational concepts in plasticity, obtained by invoking the concept of integral mean of yield criterion as it relates to the integrity assessment of corroded pipelines. Decay lengths derived using classical shell theory have been used to define the kinematically active reference volume. The reference volume approach overcomes the limitations posed by most of the current evaluation procedures with respect to the effect of circumferential extent of corrosion. The limit pressure and the remaining strength factor of pipelines, with both external and internal corrosion sites,

subjected to internal pressure loading have been estimated. The results obtained have been found to be in good agreement with three-dimensional inelastic finite element analysis. The results of this study has shown that the variational method provides an improved assessment of the effect of corrosion damage on the integrity of the pipeline in terms of remaining strength factor (RSF). This method has also yielded a better understanding of the behavior and consequence of damage than the ASME B31G criterion. An improved estimation of the limit pressures have been obtained in most cases.

Acknowledgements

The author wishes to thank his supervisor Dr. R. Seshadri, for his technical support and intellectual guidance in carrying out this research. The author acknowledges the financial support provided by Dr. Seshadri, and the Faculty of Engineering and Applied Science, during the course of his graduate studies.

The author also extends his acknowledgements to his friends in the Asset Integrity Management Research Group for their kind assistance and support. The author would also like to thank Mrs. Lisa O'Brien for her support in the documentation and printing activities.

CONTENTS

List of Tables

List of Figures

Nomenclature

Symbols

A	area of the crack or defect in the longitudinal place through the wall thickness
A_0	original cross-sectional area
A'	damage parameter according to ASME B31G
A^i	area of the individual subdivision in the API 579 assessment procedure
A_o^i	original cross-sectional area corresponding to A^i
B, n	creep parameters for power law of creep
E	elastic modulus
E_s	secant modulus
d	depth of corrosion
D	outer diameter of the pipe
E	longitudinal joint factor or joint efficiency
F	design factor
$f(s_{ij})$	yield function
K	rigidity
k	yield stress of a material in pure shear
L	maximum allowable longitudinal extent of corrosion
L_m	measured axial length of corrosion
L_{msd}	distance between the flaw and any major structural discontinuity

L^i	length of the individual subdivision in the API 57 procedure
L_i	length of the individual subdivision in the RSTRENG method
m	exact limit load multiplier or safety factor
M	folias factor
M^i	folias factor corresponding to λ^i
M_{BG}	folias factor calculated using the British Gas equation
m'	Mura's lower bound multiplier
m_1^0	upper bound multiplier corresponding to applied load P based on constant flow parameter
m_2^0	upper bound multiplier corresponding to applied load P based on variable flow parameter
m_α	improved lower bound limit load multiplier
$m_{\alpha d}$	improved lower bound limit load multiplier for corroded pipe
m_u	upper bound limit load multiplier
m_L	lower bound limit load multiplier
p	applied pressure
P_u	limit pressure of plain or undamaged pipe
P'	limit pressure of corroded or damaged pipe
$P_{failure}$	failure pressure of corroded pipe
$P_{long\ groove}$	failure pressure of pipe with long groove like defect
P	applied external load
P_L	limit pressure
r_o	outer radius of the pipe

r_i	inner radius of the pipe
R_L, R_o, R', R_U	normalized variables of limit load multipliers
R_t	remaining thickness ratio
R_i,	lagrangian multiplier representing reaction force
R_m	mean radius of the cylinder
s	coordinate in the circumferential direction
s_{ij}	deviatoric Stress Component
S_T	surface over which traction is prescribed
S_V	surface with fixed boundary condition
t	wall thickness of the pipe
T	temperature derating factor
T_i	applied surface traction
t_{mm}	minimum measured remaining wall thickness
t_{min}	minimum required wall thickness in accordance to the original construction code
t_c	thickness of the remaining ligament
u	displacement
v	velocity
V	volume of the component or structure
V_i	volume of each element
$v_{i,j}$	strain rate
V_R	reference volume in a component or structure
V_T	total volume of the component or structure

V_C	volume of the corroded region
V_U	volume of the uncorroded region
w	radial displacement
X_L	decay length in the longitudinal direction
X_C	decay length in the circumferential direction
δ_{ij}	kronecker delta
λ	metal loss damage parameter
λ^i	metal loss damage parameter for subdivision of length L^i
η	remaining thickness ratio
ϕ	damage parameter used by Kannien et. al.
β	angle representing the circumferential extent of the defect
ε_{crit}	critical strain
ε_e	equivalent strain
$\dot{\varepsilon}$	strain rate at reference state
ζ	linear elastic iteration variable
υ	poisson's ratio
θ	circumferential angle
λ	metal loss damage parameter
μ	plastic flow potential
φ	point function defined in conjunction with the yield function
σ_y	yield stress
σ_f	failure stress
σ_{flow}	flow stress of the material

σ_{max}	maximum stress in the component or structure
σ_{ult}	ultimate stress
σ	hydrostatic stress for an actual stress distribution
σ_e	equivalent stress
σ_{ij}	stress distribution
σ_R	reference stress
σ^0	hydrostatic stress for an assumed stress distribution
σ_M	maximum stress intensity is a component
$(\sigma_e^0)_M, (\sigma_e)_M$	maximum equivalent stress in a component or structure for any arbitrary load P for an elastic stress distribution.
$\sigma_{\theta U}$	circumferential stress for undamaged pipe
$\sigma_{\theta C}$	circumferential stress in the LTA
$\sigma_{\varphi U}$	longitudinal stress for undamaged pipe
$\sigma_{\varphi C}$	longitudinal stress in the LTA
σ_{eU}	equivalent stress for undamaged pipe
σ_{crit}	critical stress
σ_{eC}	equivalent stress for corroded pipe
σ	lagrangian multiplier representing mean stress

Subscripts

e	von Mises equivalent
i, j	tensorial indices

L	limit
R	reference
y	yield
U	uncorroded
c	corroded

Superscripts

0	assumed quantities

Acronyms

LTA	Locally Thinned Area
MAOP	Maximum Allowable Operating Pressure
DF	Design Factor
RSF	Remaining Strength Factor
MAWP	Maximum Allowable Working Pressure
OPS	Office of Pipeline Safety
ASME	American Society of Mechanical Engineers
ANSI	American National Standards Institute
API	American Petroleum Institute
CSA	Canadian Standards Association
CTP	Critical Thickness Profile
FCA	Future Corrosion Allowance
FEA	Finite Element Analysis

CHAPTER 1

INTRODUCTION

1.1 General Background

Pipelines are used to provide safe, efficient and economical means of transporting oil and gas. There are over 500,000 kms of natural gas and hazardous liquid transmission, pipelines in United States and Canada [1, 2]. From the instance a pipeline is commissioned it begins to deteriorate. In spite of the exceptional performance of pipelines, failures due to corrosion defects have become a significant, recurring and an expensive operational, safety and environmental concern, particularly for ageing pipelines. External corrosion occurs due to environmental conditions on the exterior surface of the steel pipe (e.g., from the natural chemical interaction between the exterior of the pipeline and the soil, air, or water surrounding it). Internal corrosion occurs due to chemical attack on the interior surface of the steel pipe due to the commodity transported or other materials carried along. Corrosion results in a gradual reduction of the wall

thickness of the pipe and an eventual loss of pipe strength. This loss of pipe strength could then result in a leakage or rupture of the pipeline due to internal pressure stresses unless the corrosion is repaired, the affected pipeline section is replaced, or the operating pressure of the pipeline is suitably reduced. Apart from the occurrence of leak or rupture, the weaker locations created by corrosion are also more susceptible to third party damage, overpressure events etc.

Corrosion is one of the most prevalent causes of pipeline leaks or failures. For the period 2003 through 2004, incidents attributable to corrosion have represented more than 25% of the incidents reported to the Office of Pipeline Safety (OPS), for both Natural Gas Transmission Pipelines and Hazardous Liquid Transmission Pipelines [3]. Over this same period, 1.8% of the incidents reported to OPS for Gas Distribution Pipelines were due to corrosion.

Significant maintenance costs for pipeline operation is associated with corrosion control and integrity management. The driving force for maintenance expenditures is to preserve the asset of the pipeline and to ensure safe operation without failures that may jeopardize public safety, result in product loss, or cause property and environmental damage. The majority of general maintenance is associated with monitoring and repairing problems, whereas integrity management focuses on fitness for service assessment, corrosion mitigation, life assessment, and risk modeling.

1.2 Factors Influencing the Behavior of Locally Thinned Area (LTA)

Corrosion spots in pipelines are considered to be a locally thinned area (LTA) for the purpose of evaluation. An accurate analysis of residual strength of the corroded pipe becomes difficult due to many variables affecting failure, e.g., pipe and corrosion geometry, material properties, loading and service conditions. The applied loadings, pipe geometry, corrosion profile and its material characteristics all drive the failure of the locally thinned area, as shown in Figure 1.1. Failure occurs when the driving force overcomes the resistance offered by the material (Figure 1.2). The applied loads include internal pressure, loads and bending moments. Material characteristics, geometry of the pipe and the damaged area influence the stress and the strain field controlling the way in which the corroded areas deform and resist the applied loading. Theoretically, the failure mechanism of a damaged component will be different from an undamaged component. Most of the damage prediction models developed assume that the theoretical limiting criterion for the LTA is the same as the limiting criterion for undamaged component. Historically it has been assumed that the LTA would fail due to an unstable ductile tearing process, similar to ultimate rupture of a vessel in pressurized burst test, although recent research suggests the mechanism may be toughness limited in some cases. Prediction of the limit pressure of a corroded pipeline remains an important objective for integrity assessment purposes.

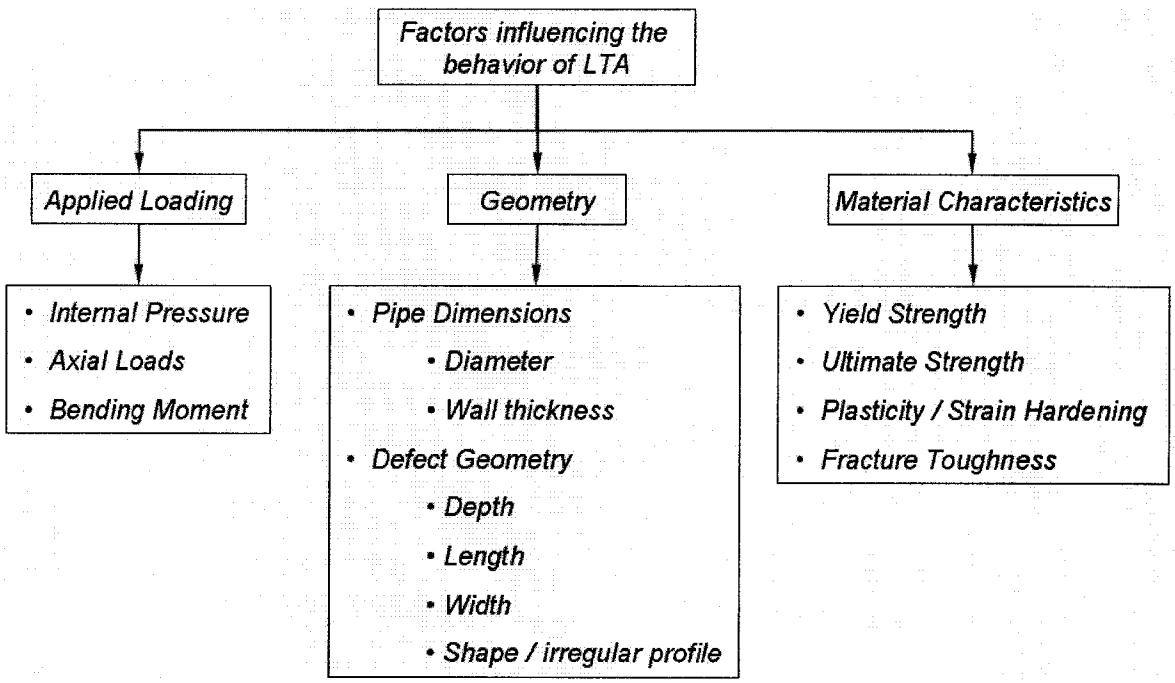

Figure 1.1: Factors Influencing the Behavior of LTA

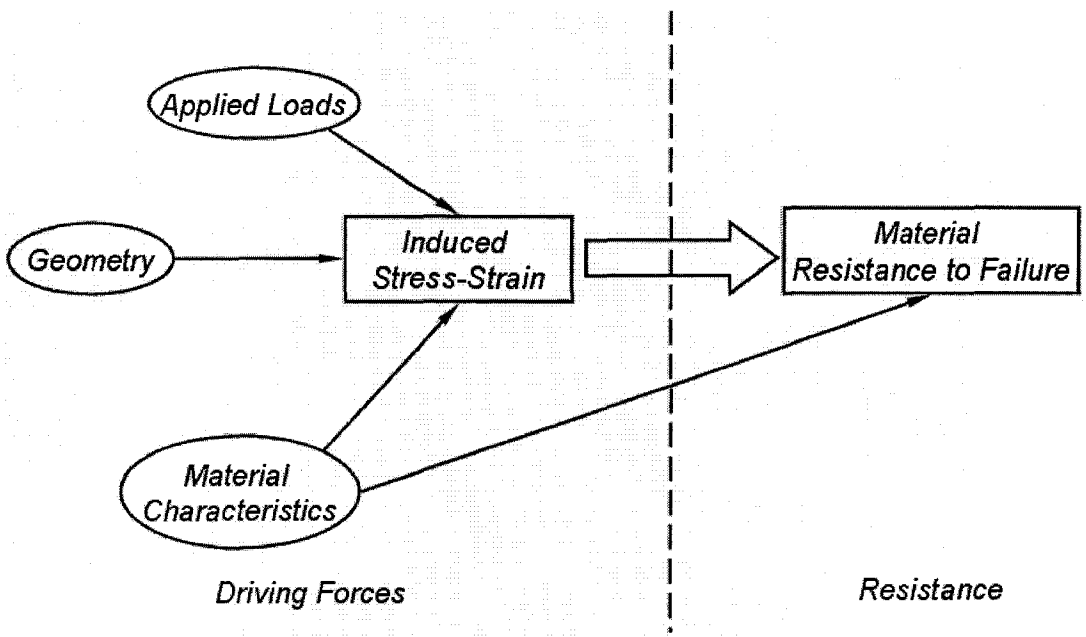

Figure 1.2: Schematic Diagram of Primary Factors Controlling the Behaviour of LTA **[4]**

1.3 Failure of Corroded Pipelines

Metal loss corrosion defects in steel pipelines are characterized as isolated pitting, contiguous pitting, or general corrosion, which present smooth profiled areas of metal loss on the surface of the pipe wall. Metal loss disrupts primary membrane action (by which the pipe normally resists the internal pressure) and induces localized bending and bulging. The stresses due to localized bending are treated as secondary and/ or peak. The influence of bulging is incorporated in the ANSI/ASME B31G procedures [5] by the inclusion of the so-called "Folias factor" for crack like defects.

Experimental investigations show that the failure of corroded pipelines can occur either by ductile failure or toughness related failure.

- Ductile failure – The remaining ligament elongates and achieves complete ductility prior to failure. The pipe has sufficient fracture toughness to ensure that the failure of the defect is governed primarily by its tensile properties rather than fracture toughness. The remaining ligament exhibits three types of behaviour: (1) elastic deformation (2) the spread of plasticity and (3) post-yield hardening. The first type is elastic behaviour which progresses to a point until the elastic limit is reached. Once the elastic limit is reached, the plastic flow commences, and spreads through the thickness. When the third stage is reached, the entire ligament deforms plastically. However, the failure does not occur immediately. A steep increase in the through ligament stress occurs once the stress level corresponding

to the ultimate tensile strength is reached and the failure follows with a further small increment in the load. The usage of materials with sufficient ductility and fracture toughness for the fabrication of pipelines enables the evaluation of corroded pipelines using net section collapse criterion, as the pipeline would encounter ductile failure rather than brittle fracture.

- Toughness dependent failures - Pipelines are also prone to failure due to the initiation of cracks at the base of the remaining ligament. This failure mechanism can be expected in pipelines made of low toughness materials. A stable crack growth may start as the pressure continues to increase after the defect deforms plastically. Unstable crack growth through the wall leads to the creation of a through-wall defect. This through-wall defect can fail either as a leak or rupture.

1.4 Structural Integrity Assessment

Pipeline integrity management is a four phase program consisting of pipeline assessment, inspection management, defect and repair assessment, and rehabilitation and maintenance management. Defect assessment for fitness for service purposes, carried out in order to appraise the operability of the pipeline in the context of its structural integrity, forms a key part of pipeline integrity management. Structural integrity assessment in the oil and gas industry is practiced in three levels. Level 1 assessment procedures provide conservative screening criteria that can be used with a minimum quantity of inspection data or information about the component. Level 2 is intended for use by facilities or field

engineers, although some owner-operator organizations consider it suitable for a central engineering evaluation. Level 3 assessments require sophisticated analysis by experts, where advanced computational procedures are often carried out. The Pipeline industry has developed several integrity assessment procedures (ASME B31G, API 579 etc.) to evaluate the remaining strength of pipelines with corrosion defects. These methods are semi-empirical in nature because of their validation on the basis of experimental results. These methods could become invalid or unreliable if applied outside these empirical limits. Development of a more comprehensive assessment criterion for the corroded pipelines becomes difficult because of the numerous variables (pipe geometry, defect geometry, material properties, etc.) influencing the behaviour and failure of the corroded region. Chouchaoui and Pick [6] have proposed a three level fitness for service assessment procedure for corroded pipelines by incorporating the work done by various researchers, and have also suggested that Level 2 methods need to be developed from a physical model rather than empirical one to allow an understanding of the influence of various parameters.

1.5 Objective of the Research

The main objective of this research is to develop an improved Level 2 assessment procedure for corroded pipelines. This research should provide a more comprehensive method to evaluate the structural integrity of pipelines with both external and internal corrosion sites in the fitness-for-service perspective. An assessment procedure is to be

presented to determine the remaining strength factor and limit pressure of a corroded pipeline, which may be used to derate or rerate the maximum allowable operating pressure of the pipeline if deemed necessary. A more accurate determination of remaining strength of the corroded pipeline, and its maximum allowable operating pressure (MAOP), would enable rationalization of the conservatism embedded in the existing criteria. This can be of value in avoiding costs of unnecessary repairs, or the costs of early replacement of corroded pipelines. The results obtained from the proposed Level 2 assessment procedure are to be validated with inelastic finite element analysis and compared with the current ASME B31G criterion.

1.6 Organization of the Thesis

This thesis is divided into five chapters. The second chapter of the thesis presents a review of literature. A brief outline of most of the existing criteria used by the pipeline industry is provided, along with other research by various investigators. Chapter three presents a complete theoretical basis for the robust limit load estimation techniques using variational concepts in plasticity. This chapter also presents the concept of reference volume which will be employed in conjunction with the variational method as a Level 2 assessment method. The chapter four discusses the practical application of the robust limit load solutions and reference volume for the fitness for service assessment of corroded pipelines using various failure criterions. This chapter also describes the Level 3 inelastic finite element analysis performed as a validation of the proposed Level 2

assessment procedure. Further the results are also compared with the ASME B31G criterion, which is a benchmark for the comparison of all procedures. Graphical plots comparing the results obtained by applying the Level 2 method, inelastic FEA and ASME B31G criterion are also presented in this chapter. The concluding chapter, chapter 5, contains a summary of the findings of the thesis, and a discussion on future research.

CHAPTER 2

REVIEW OF LITERATURE

2.1 Introduction

This chapter presents a summary of the primary investigations made by various researchers and their results reported in the literature on the failure of corroded pipelines. The literature referred in this chapter corresponds to the integrity assessment of the oil and gas transmission pipeline industry. This chapter also presents terminologies involved in the design and operation of oil and gas transmission pipelines. A number of methods have been proposed for the assessment of pipelines with LTA subjected to internal pressure. This literature review incorporates a detailed elucidation of the well established evaluation methods like ASME B31G, RSTRENG [7], modified B31G and API 579 procedures [8], widely used by the transmission pipeline industry. The semi-empirical models and solutions based on fracture mechanics approach has resulted in the development of the above stated methods. Few theoretical models are proposed as an

enhancement to these established methods. This chapter focuses on the Level 2 methods proposed by other investigators, since the objective of this research is to recommend new and improved Level 2 methods for the fitness for service assessment of corroded pipelines.

2.2 Design Factor

The term design factor (DF), most commonly used by the pipeline industry, is the inverse of the term factor of safety widely used in mechanical design. The value of design factor is chosen on the basis of the nature of the fluid transported in the pipeline, the geographical locations through which the pipeline passes and other logistical considerations. These values for different cases are defined in the pipeline design codes (Liquid Pipelines – ASME B31.4, Gas Pipelines – ASME B31.8 and CSA Z662-03 for liquid and gas pipelines). The design factor is used to calculate the maximum allowable stress when the pipeline is designed on an allowable stress basis.

The maximum allowable stress is given by:

$$\text{Maximum Allowable Stress} = (\sigma_y)\,(\text{DF}) \tag{2.1}$$

where σ_y is the yield stress.

The maximum design factor used in ASME B31.4 is 0.72, which corresponds to a factor of safety of 1.39, i.e., when a transmission pipeline operates at its highest allowable stress, there is a 39% margin of safety on yielding due to the effects of

pressure. Canadian pipelines that are governed by CSA Z662-03 have a maximum design factor of 0.8.

2.3 Maximum Allowable Operating Pressure

The maximum allowable operating pressure or the maximum allowable working pressure is defined as the maximum pressure at which the pipeline can be operated. The calculation of maximum allowable operating pressure (MAOP) is made in pipeline design codes by using the following expression:

$$MAOP = \frac{2\,(\sigma_y)\;t}{D}\;(F\;E\;T) \tag{2.2}$$

It can be seen from the above equation that the limit pressure calculated as the hoop stress at failure is derated using a design factor (F), temperature derating factor (T) and longitudinal joint factor or joint efficiency (E) to obtain the maximum allowable operating pressure. Therefore, when no design and temperature factor are used, i.e., F = 1, T = 1, and E = 1 the MAOP calculated from the above expression corresponds to the limit pressure, i.e., hoop stress at failure for a Tresca-based failure criterion.

When a corrosion damage is discovered, the immediate concern is to evaluate whether the pipeline is structurally sound to be operational at the same maximum allowable operating pressure (MAOP). Corrosion damage reduces the capacity of the pipeline to contain internal pressure, and if the corrosion is allowed to proceed it will eventually leak or rupture.

A number of analysis techniques and procedures have been developed and prescribed in design codes in order to determine whether a defect will affect the pipeline's capability to operate at the same MAOP. Some of these techniques will be discussed in the later sections of this chapter.

2.4 Remaining Strength Factor (RSF)

Sims et al. [9] proposed to use the term remaining strength factor (RSF) as a basis for the evaluation of thinned areas in pressure vessels and storage tanks. RSF is defined as:

$$RSF = \frac{\text{Limit / Collapse Load of the Damaged Component}}{\text{Limit / Collapse Load of the Undamaged Component}} \tag{2.3}$$

The calculation of the remaining strength factor provides a direct means of comparing the strength the corroded pipeline with the undamaged pipeline. An allowable RSF of 0.9 implies that the strength of the pipe containing the flaw can be no less than 90% of the original design. In case the damaged pipe does not meet the RSF requirements, the pipeline is derated to operate at a reduced MAWP given by,

$$\begin{aligned} MAWP_r &= MAWP(RSF/RSF_a) && \text{for } RSF < RSF_a \\ MAWP_r &= MAWP && \text{for } RSF \geq RSF_a \end{aligned} \tag{2.4}$$

2.5 Effective Area Methods

The ASME B31G, modified B31G and RSTRENG methods form a class of evaluation methods that replace the actual metal loss with an "effective" cross sectional area. The remaining pressure carrying capacity of the pipeline is calculated based on the amount and distribution of metal loss, and the yield strength of the pipeline steel. The ASME B31G approach is a simple method, which requires the least amount of information on the metal loss in order to calculate the failure pressure of the corroded pipeline. Approximations that lead to the simplification of the method have resulted in excessive conservatism. The modified B31G method and the RSTRENG technique have been developed to reduce the conservatism in the ASME B31G method, by proposing an improved means of considering the area of metal loss and material characteristic. The effective area method assumes that the loss of strength due to corrosion is proportional to the amount of metal loss, measured axially along the pipe, as shown in figure 2.1.

The basic equation leading to the ANSI/ASME B31G criterion that emanated from the Battelle Memorial Institute study [10] is obtained by treating the metal loss due to corrosion as a part through flaw or crack, and the nominal pipe hoop stress at failure in the flaw is given by the following equation:

$$\sigma_f = \sigma_{flow} \left[\frac{1 - (A/A_0)}{1 - (A/A_0)(M^{-1})} \right] \tag{2.5}$$

where σ_f is the failure stress (hoop stress at failure)

σ_{flow} is the flow stress of the material; a material property related to its yield strength;

A is the area of the crack or defect in the longitudinal plane through the wall thickness; and

A_0 is the original longitudinal cross-sectional area of the corroded region

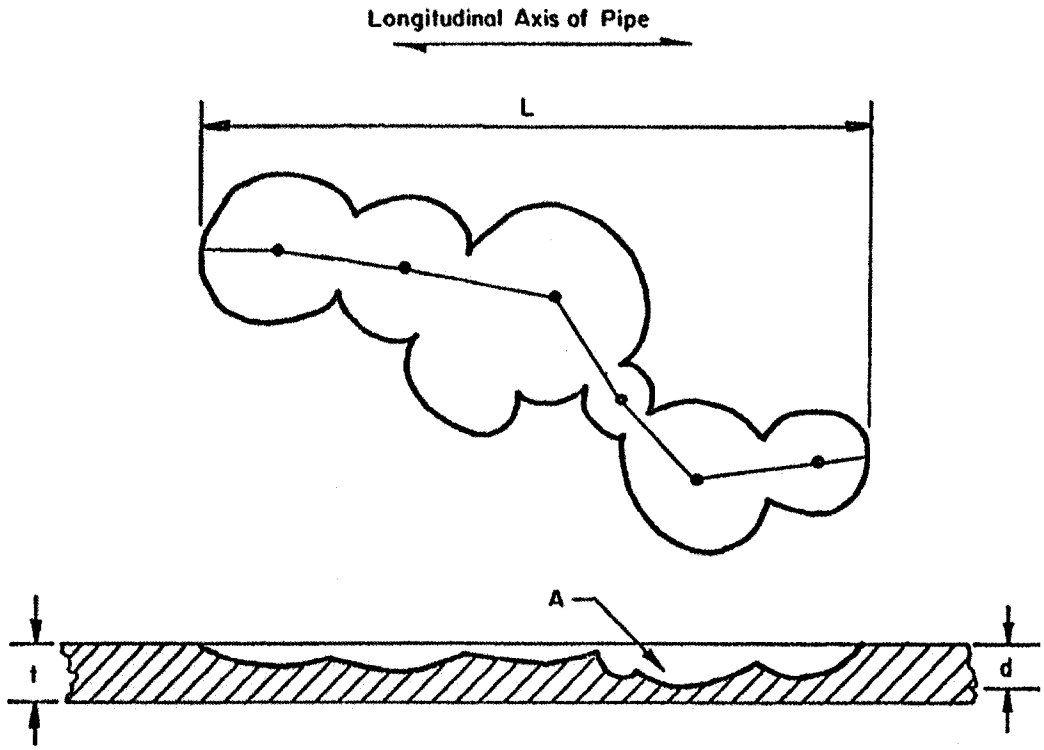

***Figure 2.1: Parameters of Metal Loss used in the Analysis of Remaining Strength* [11]**

In the equation (2.5), M is the "Folias factor" for crack like defects, introduced to account for bulging of the damaged region of the pressurized cylinder. This approach

assumes that the pipe fails when the stress in the flaw reaches the flow stress of the pipe. To accommodate irregular corrosion profiles, the flaw profile is measured, and the deepest points are projected to a single axial plane for analysis, since the effective area methods assume that the profile of corrosion lies in one plane along the axis of the pipe.

2.5.1 Evaluating a Corroded Region using ASME B31 G Criterion

A contiguous corroded area having a maximum depth of more than 10% but less than 80% of the nominal wall thickness of the pipe should not extend along the longitudinal axis of the pipe for a distance greater than that calculated from:

$$L = 1.12\ B\ \sqrt{D\,t} \tag{2.6}$$

where, L – Maximum allowable longitudinal extent of corroded area in inches

D – Nominal outside diameter of the pipe in inches

The value of B is calculated using the following expression:

$$B = \sqrt{\left(\frac{d/t}{1.1\ d/t\ -\ 0.15}\right)^2 - 1} \tag{2.7}$$

except that "B" may not exceed a value of 4. If the corrosion depth is between 10% and 17.5%, use B = 4 in equation (2.6).

The corrosion spots with depths more than 80% of the wall thickness are not permitted because of the chances that very deep corrosion sites may develop leaks. If the

measured maximum depth of the corroded area is greater than 10% of the nominal wall thickness, and the measured longitudinal extent (L_m) of the corroded area is greater than the value determined by equation (2.6), then calculate

$$A' = 0.893\left(\frac{L_m}{\sqrt{Dt}}\right) \tag{2.8}$$

where, A' is the damage parameter

L_m is the measured longitudinal extent of corroded area in inches

t is the nominal wall thickness in inches

Difficulties in determining the exact area of metal loss lead to the approximation by applying effective area techniques. Two shapes, rectangle ($A = L_m\, d$) and the parabola ($A = (2/3)\, L_m\, d$), shown in figure 2.2, were considered in the development of the original B31G criterion on the basis of 47 burst tests [12]. Predictions made using the rectangular profile were found to be too conservative for shorter corrosion profiles, but the assumption of parabolic profile consistently yielded lower bound prediction when compared with the actual failure stress levels. The ratios of the actual to the predicted failure stress levels range from 1.07 to 3.07. For values of $A' < 4$, the safe maximum pressure of the pipe is calculated by assuming a parabolic profile (figure 2.2 b). Hence, equation (2.5) in conjunction with (2.8) will yield

$$P' = 1.1\, P_u \left[\frac{1 - \frac{2}{3}\left(\frac{d}{t}\right)}{1 - \frac{2}{3}\left(\frac{d}{t\sqrt{(A')^2 + 1}}\right)}\right] \tag{2.9}$$

where, $\sqrt{(A')^2 + 1}$ is the Folias factor same as that will be shown in equation (2.10)

P_u is the limit pressure for an undamaged pipe calculated using equation (2.2), and

P' may not exceed P.

It can be observed from the equations (2.8) and (2.9) that the "Folias bulging factor" is approximated by a two-term expression:

$$M = \left[1 + \frac{0.8\, L_m^2}{D\, t}\right]^{1/2} \tag{2.10}$$

In reality, the assumption of parabolic profile has significant limitations. If the corroded area is very long, the assumption of parabolic metal loss profile will lead to an underestimation of the corrosion damage and overestimation of the remaining strength of the pipeline. Hence for values of A > 4, the failure pressure of the pipe calculated by assuming a rectangular profile (figure 2.2 c) is given by,

$$P' = 1.1 \quad P_u \left[1 - \frac{d}{t}\right] \tag{2.11}$$

except that P' may not exceed P_u.

It can be seen from equations (2.9) and (2.11) that the flow stress of the material to calculate the failure pressure of the corroded pipe is assumed as 1.1 σ_y i.e., 10% more than yield stress. Figure 2.3 shows the assumed material curve in ASME B31G.

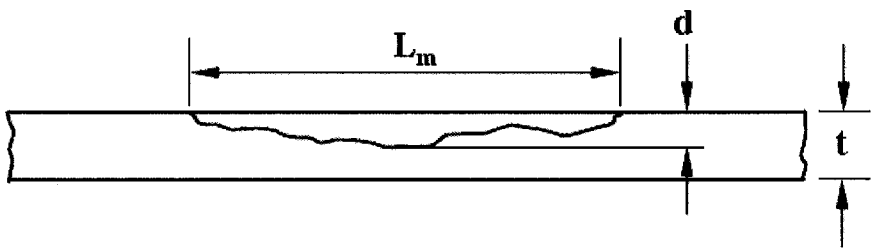

(a): Irregular Corrosion Profile

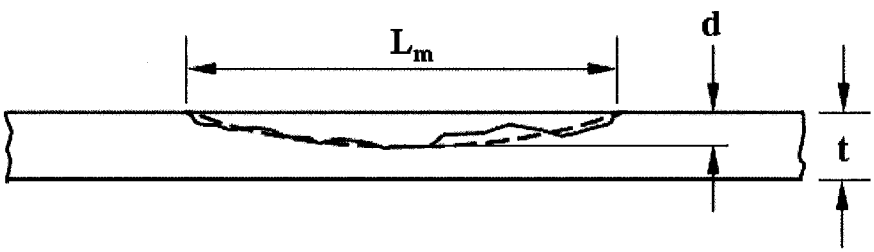

(b): Parabolic Approximation

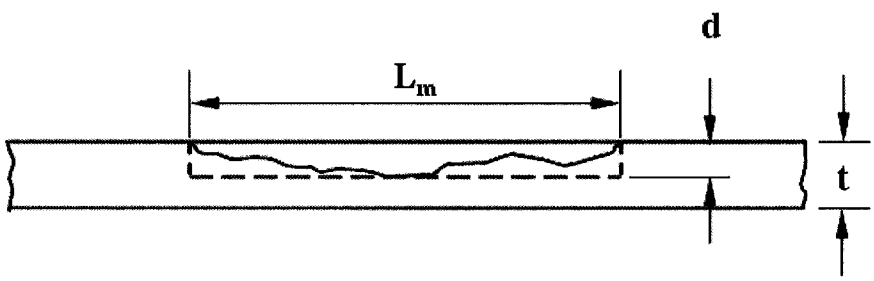

(c): Rectangular Approximation

Figure 2.2: Approximation of Corrosion Profile

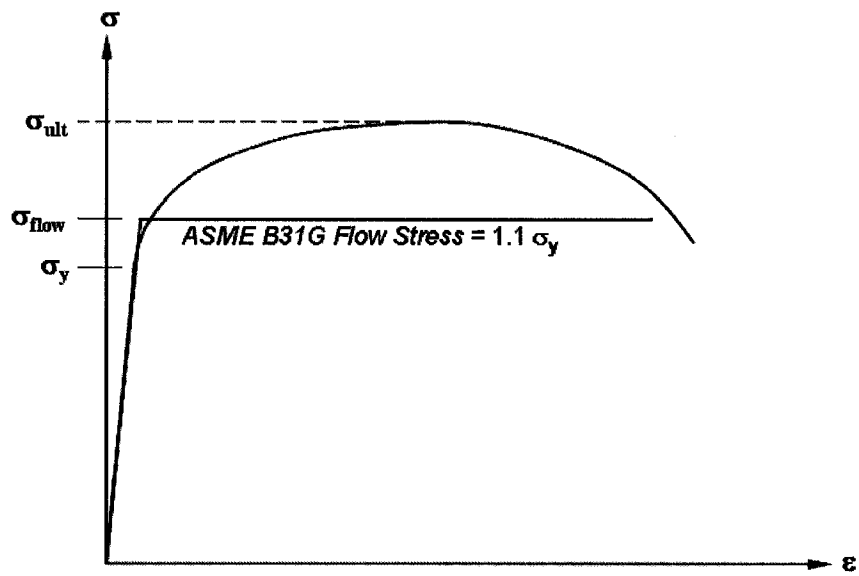

Figure 2.3: Flow Stress Representation for Typical Pipeline Steel

2.5.2 Limitations of B31 G Criterion and Sources of Conservatism

The various limitations and sources of excess conservatism in the ASME B31G criterion are:

- Application of the "Folias bulging factor" and its approximation:
    - Using the Folias bulging factor derived for sharp crack like defects in a internally pressurized cylinder for evaluating LTA's which are usually more blunt adds to the conservatism in B31G method. Furthermore, the

Folias factor is represented by a simplified two-term expression in B31G criterion.

- Approximation of metal loss profile:
    - The inability of the ASME B31G method to consider the metal loss in the circumferential direction because of its fundamental basis on the fracture mechanics consideration of the LTA is a significant limitation. Further the axial metal loss profile is being approximated by a rectangle or parabola which leads to a conservative estimate when compared with the estimation based on actual corrosion profile.
- Estimation of the failure pressure by considering a biaxial stress state (longitudinal and hoop stress) will provide an improved estimation of the failure pressure when compared with the uniaxial stress state (hoop stress) as done in ASME B31G method.
- The expression for flow stress:
    - If the LTA in a pipeline is located away from any major structural discontinuities, such as weld junctions in long transmission pipelines, and if the LTA is expected to fail by ductile tearing as in the case of high toughness pipelines, then the assumption of flow stress as 1.1 σ_y is expected to give a more conservative estimate of the limit pressure.

2.5.3 RSTRENG Technique and Modified B31 G Criterion

A more accurate means of predicting the failure stress was achieved by the development of a computer program, RSTRENG, which overcomes few of the above stated limitations of the ASME B31G method. The basis of RSTRENG is the multiple evaluation of the predicted limit pressure based on subsections of affected area rather than total area as done in B31G criterion. A more realistic representation of the exact profile of metal loss is made by plotting points along the "river bottom" path of a contour map of pit depths as shown in figure 2.4 (a). The "equivalent axial profile" corresponding to the dashed (river bottom) path in figure 2.4 (a) is shown in figure 2.4 (b). This figure illustrates 16 possible flaw lengths for analysis. Each calculation involves determining the area of metal loss beneath a particular length L_i. RSTRENG computes the failure pressure based on all 16 possible flaw geometries and reports the lowest as its final result.

The RSTRENG technique uses a modified expression for folias factor as below:

For $\frac{L^2}{Dt} \leq 50$,

$$M = \left[1 + 0.6275 \frac{L^2}{Dt} - 0.003375 \frac{L^4}{D^2 t^2} \right]^{1/2} \qquad (2.12)$$

For $\frac{L^2}{Dt} > 50$,

$$M = 0.032 \frac{L^2}{Dt} + 3.3 \qquad (2.13)$$

The authors [2] have also proposed to use a higher flow stress of $\sigma_{flow} = \sigma_y + 10{,}000$ psi to reduce the excess conservatism.

Because of the tedious procedure involved in the RSTRENG method, an alternative method was proposed by Kiefner and Veith [7], known as the modified B31G criterion. In this method the effective area is calculated with the following expression:

$$A = 0.85\ dL_m \tag{2.14}$$

This criterion also termed as the 0.85 dL method, uses a higher flow stress and folias factor as in the case of RSTRENG technique. The Folias factor is computed by substituting $L = L_i$ in eqn. (2.12) and (2.13) for RSTRENG technique and $L = L_m$ for modified B31G method.

ASME B31G criteria and RSTRENG technique have become established methods for evaluating single corrosion defects oriented in axial plane and loaded by internal pressure and are the standards against which other methods are compared. Specific areas of concern include application to high strength steels, axial and bending loads, circumferentially oriented defects, spirally oriented defects and problems with separated LTA's and defect interactions.

Cronin and Pick [13] have also created an experimental database after performing burst tests on more than 40 pipes removed from service. They have shown that predictions by ASME B31G and RSTRENG methods are conservative when compared with the actual burst pressure from experiments.

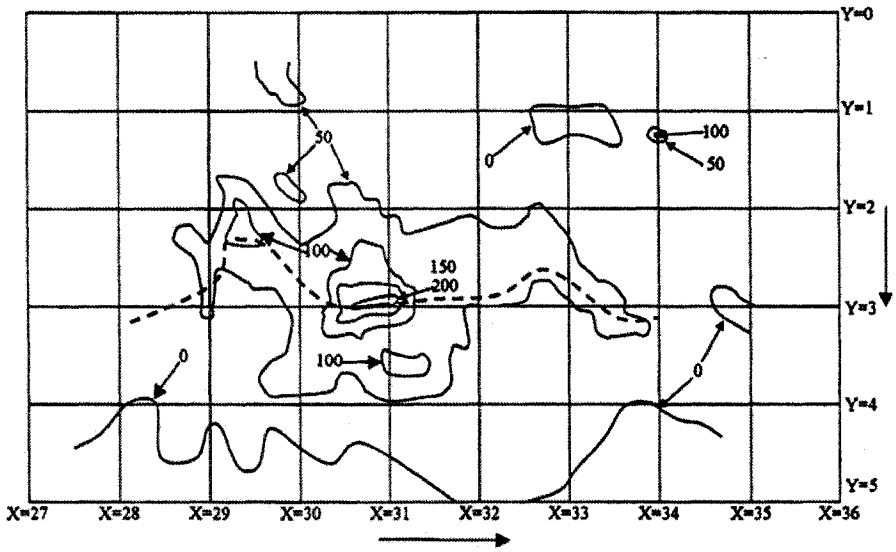

(a): Contour Map of Pit Depths

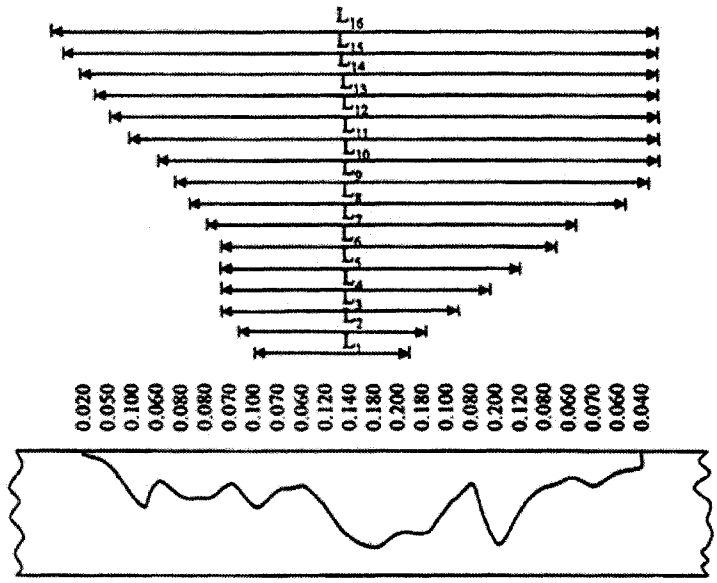

(b): Profile of Pit Depths along "River Bottom" Path in (a)

Figure 2.4: Effective Area Estimation in RSTRENG Method (Dimensions in inches) **[11]**

2.5.4 API 579 Evaluation Procedure

API 579 assessment procedure is primarily classified as

- General metal loss rules
- Local metal loss rules

The general metal loss rules are based on the average depth of metal loss while the local metal loss rules are based on more accurate metal loss profiles, known as the critical thickness profiles (CTP's), obtained in both longitudinal and circumferential direction using the "river bottom" approach as in the case of RSTRENG method. It is to be noted that the RSTRENG technique did not consider the thickness profile in the circumferential direction. Both general and local metal loss rules provide guidelines for Level 1 and Level 2 assessments. The LTA is also evaluated to prevent leakage on the basis of the minimum measured thickness readings. Measurement of the depth of metal loss at 15 different points in the LTA is recommended to confirm whether the metal loss is general or local.

The local metal loss rules of the API 579 procedures require the computation of the RSF which can then be used to calculate the limit pressure and maximum allowable working pressure of the corroded pipeline.

2.5.4.1 Local Metal Loss Rules

The following geometric limitations on the region of metal loss need to be satisfied in order to apply local metal loss rules for assessment:

$$R_t \geq 0.20$$

$$t_{mm} - FCA \geq 2.5 \text{ mm } (0.10 \text{ inches}) \qquad (2.15)$$

$$L_{msd} \geq 1.8 \sqrt{D\, t_{min}}$$

where, $R_t = \dfrac{t_{mm} - FCA}{t_{min}}$ is the remaining thickness ratio

t_{mm} is the minimum measured remaining wall thickness.

t_{min} is the minimum required wall thickness in accordance with original construction code

L_{msd} is the distance between the flaw and any major structural discontinuity.

D is the outer diameter of the cylinder

It will be seen that L_{msd} is the same as the relaxation length X_L that will be introduced in the concept of reference volume.

2.5.4.2 Level 1 Assessment Procedure

The Level 1 assessment procedure involves the definition of the metal loss damage parameter, which is used to calculate the Folias bulging factor. The Level 1

assessment criterion of API 579 uses the same Folias factor as the ASME B31G criterion to compute the RSF. The metal loss damage parameter λ is given by:

$$\lambda = \frac{1.285\, L_m}{\sqrt{D\, t_{min}}} \tag{2.16}$$

where, L_m is the measured axial extent of corrosion

RSF is calculated by:

$$RSF = \frac{R_t}{1 - \frac{1}{M}(1 - R_t)} \tag{2.17}$$

where $M = \sqrt{1 + 0.48\,\lambda^2}$

2.5.4.3 Level 2 Assessment Procedure

Level 2 assessment procedure can be used to obtain a better estimate of the RSF than that computed in Level 1 for a component subject to internal pressure, if there are significant variations in the thickness profile. This procedure ensures that the weakest ligament is identified and properly evaluated. If the limitations stated in equations (2.15) are satisfied, and if $\lambda \leq 5$, then the RSF is computed for each of the subsections (Figure 2.5) of the critical thickness profile in both longitudinal and circumferential directions using the following expression:

$$RSF^i = \frac{1 - \left(\frac{A^i}{A_o^i}\right)}{1 - \frac{1}{M^i}\left(\frac{A^i}{A_o^i}\right)} \tag{2.18}$$

where

$A_o^i = L^i t_{min}$ is the original area based on L^i

$$M^i = \left[\frac{1.02 + 0.4411 (\lambda^i)^2 + 0.006124 (\lambda^i)^4}{1 + 0.02642 (\lambda^i)^2 + 1.533 (10^{-6}) (\lambda^i)^4} \right]^{1/2} \tag{2.19}$$

and 'i' corresponds to each subdivision

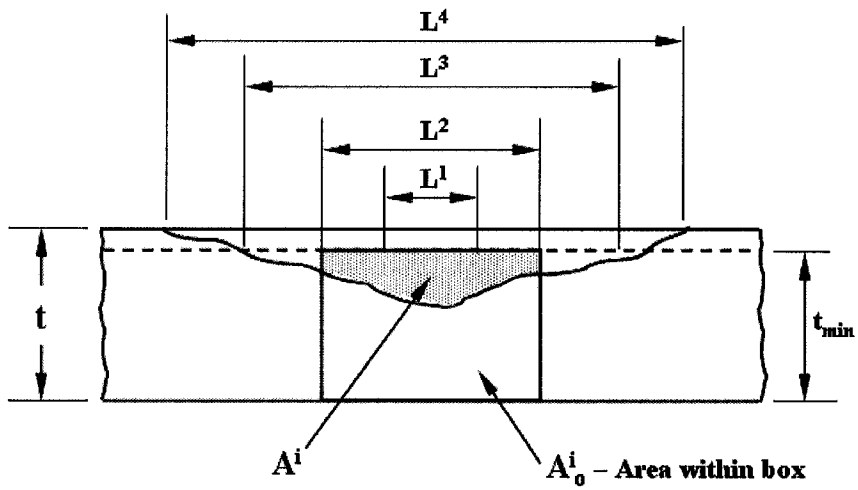

Figure 2.5: Subdivisions to Determine RSF

The RSF to be used in the assessment is the minimum value of all the subsections. Smaller the size of the subsection, more accurate will be the result. This follows the approach similar to the RSTRENG method.

The Maximum Allowable Working Pressure (MAWP) for the corroded pipeline is calculated by taking into account the internal pressure and all the supplemental loads that may result in net section axial force, bending moment and torsion. The supplemental loads will contribute to the longitudinal membrane, bending and shear stresses acting on the flaw in addition to the primary membrane hoop and longitudinal stress due to pressure.

Advanced assessment of LTA's based on elastic-plastic nonlinear finite element analysis to determine the collapse load may provide a more accurate assessment of the safe load carrying capacity of the pipeline. This analysis will account for the redistribution of the stresses as a result of inelastic deformations. A local failure criterion can be defined to specify failure in the vicinity of the LTA. API 579 recommends limiting the maximum peak strain at any point to 5% when a Level 3 analysis is performed. Alternatively the code also permits limiting the net section stress in the LTA when strain hardening is included in the analysis by considering the material ductility, hydrostatic stress, effect of localized strain and the effects of environment, which can result in increased material hardness zones.

2.6 Other Investigations

Researchers at Southwest Research Institute [14] developed a theoretical rather than empirical model to assess local thin areas in pipelines. They used elastic shell theory in conjunction with their assumption of an axisymmetric metal loss of uniform depth,

which would correspond to a "ring" of metal loss, as shown in the figure 2.6 to derive a modified expression for the bulging factor. The nomenclature used in this model is the same as that in ASME B31G. The model begins with a set of elastic shell bending equations, which are solved to satisfy the continuity conditions (continuity of displacement, slope and moment) at the transition region from the full thickness area to the thinned area. This model results in the following expression for the bulging factor:

$$
\begin{aligned}
M = [(1+\eta^4)\ & (\cosh\phi.\sinh\phi + \sin\phi.\cos\phi) + 2\,\eta^{3/2}\,(\cosh^2\phi - \cos^2\phi) \\
& + 2\,\eta^2\,(\cosh\phi.\sinh\phi - \sin\phi.\cos\phi) + 2\,\eta^{5/2}\,(\cosh^2\phi - \cos^2\phi)] \\
& \Big[(\cosh\phi.\sin\phi + \sinh\phi.\cos\phi) + 2\,\eta^{5/2}\cosh\phi.\cos\phi \\
& + \eta^2\,(\sinh\phi.\cos\phi - \cosh\phi.\sin\phi)\Big]^{-1}
\end{aligned}
\tag{2.20}
$$

where,

$$\phi = \frac{0.9306\ L_m}{\sqrt{D\,(t-d)}} \quad \text{is the damage parameter}$$

$$\eta = 1 - \frac{d}{t} \quad \text{is the remaining thickness ratio}$$

The RSF is calculated using the following expression:

$$RSF = \left[\frac{1 - (d/t)}{1 - (d/t)\,M}\right] \tag{2.21}$$

Adapting axisymmetric elastic theory to the problem of LTA in cylindrical shell has resulted in more detailed and complex relationship for bulging factor than those obtained by Folias. The above expression for bulging factor considers the length and depth of corrosion, when compared with the Folias bulging factor, which is dependent only on the length of the corrosion.

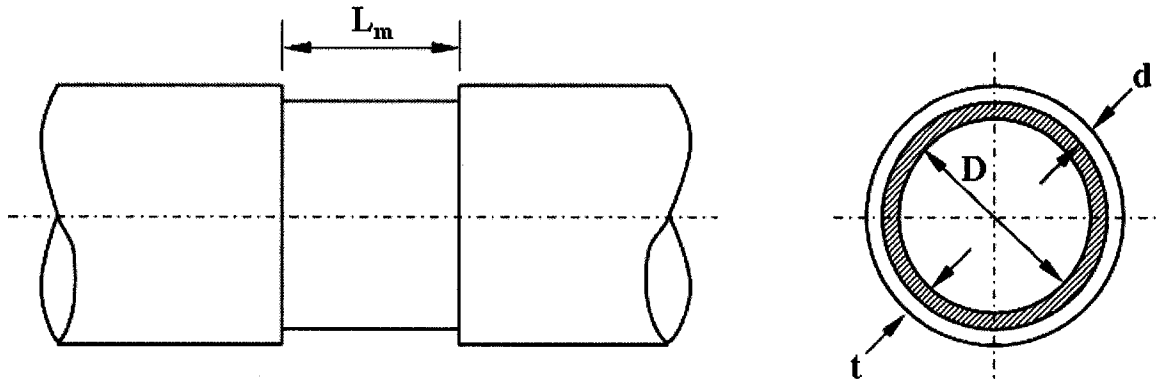

Figure 2.6: Axisymmetric Corrosion Model

Kanninen et al. [14] also proposed a plane strain solution to determine the failure stress of the corroded pipeline, which was used when the length of the corroded region was relatively long. It is known that the maximum bulging is seen at the center of the LTA, and hence maximum stress including membrane and bending is given by,

$$\sigma_{max} = \frac{p\,R}{t_c}\left[1 + 3\,(1+\varepsilon)\left(1-\frac{t_c}{t}\right)\right] \qquad (2.22)$$

where, $t_c = t - d$ is the remaining thickness of the ligament

and 2β is the angle representing the circumferential extent of the defect

$$\varepsilon = \frac{B(\beta - \sin\beta) - (C)\beta}{(A)(C) - B^2}$$

$$A = \beta + (\pi - \beta)\eta^3$$

$$B = \beta - \sin\beta + (\pi - \beta + \sin\beta)\eta^3$$

$$C = \frac{3}{2}\beta - 2\sin\beta + \frac{1}{4}\sin 2\beta + \left[\frac{3}{2}(\pi - \beta) + 2\sin\beta - \frac{1}{4}\sin 2\beta\right]\eta^3$$

$$\eta = 1 - \frac{d}{t}$$

The authors have suggested using the plane strain solution when the axial extent of corrosion is critical, and axisymmetric metal loss solution if the circumferential extent of corrosion is critical to obtain lower bound results. They have also performed full-scale experiments on simulated corrosion defects.

Cronin and Pick [15] proposed a method of predicting the failure pressure of pipelines with corrosion defects by employing a weighted depth difference approach in conjunction with an expression for failure pressure developed as an extension of the model proposed by Svensson [16]. Svennson's model predicts the failure pressure of a homogeneous pipe made of high toughness material exhibiting strain hardening behaviour. This model is based on the assumption that geometric instability is a result of decreasing wall thickness and increasing pipe radius, which leads to increasing stress and strain in the material at the point of instability. This model is modified in order to accomodate the Ramberg-Osgood material model. Regression analysis was applied to

compare with the experimental results. A factor was introduced to take account of the inhomogenity in the material properties of the pipe and reduce the predicted failure pressure accordingly. Cronin and Pick adopted this method to determine the failure pressure of pipe with a long groove like defect and assumed that the failure pressure of any corroded pipeline lies between predicted failure pressures of undamaged pipe and pipe with a long groove i.e., failure pressures of plain pipe and pipe with long groove serve as the upper and lower bounds for the failure pressure of the actual corroded pipeline. Hence,

$$P_{failure} = P_{Long\,Groove} + [P - P_{Long\,Groove}]\,g \tag{2.23}$$

The value of g ranges from 0 to 1.0 corresponding to pipe with long groove and undamaged pipe respectively. A weighted depth difference method is used in estimating the value of g. The corrosion defect is considered as metal loss projected on to the longitudinal axis of the pipe, and the value of g is calculated at each evaluation point by considering the depth of metal loss in the adjacent regions.

Assuming that the deformation of the plain pipe and defect bulging are negligible in comparison to the pipe radius, the failure pressure for pipe with long groove is given by,

$$P_{Long\,Groove} = \frac{\sigma_{Crit}}{r_o \sqrt{\frac{3}{4}}}\, t_c \left[\exp\left(-\sqrt{\frac{3}{4}}\ \varepsilon_{crit} \right) \right] \tag{2.24}$$

It can be observed from the above equation that the failure pressure is calculated based on the reduction in thickness of the ligament with the increase in pressure, and the ligament is said to fail when the stress and strain reach the critical state, which corresponds to the ultimate state in the assumed material model. Hence the original thickness of the ligament (t_c) is reduced by an exponential factor dependent on critical strain. This estimation of the failure pressure is done at various evaluation points along the actual measured corrosion profile. By assuming an ultimate stress state as the failure criteria, this method implies that the failure of the thinned section is only by ductile tearing and is toughness independent. Hence this model is suitable only for high toughness materials.

Chouchaoui and Pick [6] proposed a three level assessment criteria for the residual strength of the corroded line pipe incorporating the work done by various investigators. The authors proposed to use B31G and other effective area methods like the modified ASME B31G and RSTRENG as Level 1 methods because of the limitations in applying these methods and also the degree of conservatism embedded in them. The limitations include:

- Inability to consider the circumferential extent of corrosion.
- ASME B31G found to be unconservative for long corrosion defects and overly conservative for corrosion not aligned longitudinally.

- Ignoring the effect of longitudinal stresses because of the end conditions and bending of pipes. This may lead to overestimation of limit pressure when compressive longitudinal stresses are present.
- Externally corroded pipe is found to fail earlier than the internally corroded pipe. Assessing both external and internal corrosion similarly would lead to a slightly conservative prediction for internal corrosion.

Chouchaoui and Pick suggested that the Level 2 solutions need to be developed from a physical model rather than empirically to allow an understanding of the influence of various parameters. In addition, simplified calculations are desirable for Level 2 solutions. The authors also suggested using the reduced modulus methods with elastic finite element analysis as an alternative Level 2 method to more accurate Level 3 solution from complete nonlinear FEA. The authors have also emphasized the importance of considering the strain hardening behaviour of high strength pipeline steels when corrosion geometries are simulated for evaluations.

A detailed study was carried out by British Gas [17] to determine the failure pressure of pipelines made of high strength steel. The program included numerical analysis by inelastic finite element analysis and validation by full-scale pipe burst tests on machined corrosion specimens. This study identified the ultimate stress as the limiting stress in the defect. The results of three-dimensional inelastic FEA with large deformation effects was found to be in good agreement with experiments when true stress strain relationship was used to define the material property in the finite element model.

For the pipe to fail at ultimate stress, the material should exhibit sufficient ductility and fracture toughness for the LTA to elongate fully before failure.

Batte et al. [17] proposed to use the following expression to determine the failure pressure of the corroded pipe as:

$$P_{failure} = \frac{2\,t\,\sigma_{ult}}{D}\left[\frac{1 - (d/t)}{1 - (d/t)\,(M_{BG})^{-1}}\right] \tag{2.25}$$

Failure pressure of the undamaged pipe is taken as,

$$P = \frac{2\,t\,\sigma_{ult}}{D} \tag{2.26}$$

The RSF can be computed using:

$$RSF = \left[\frac{1 - (d/t)}{1 - (d/t)\,(M_{BG})^{-1}}\right] \tag{2.27}$$

A modified expression for the bulging factor (M_{BG}) was proposed by a curve fit between experimental and analytical results.

$$M_{BG} = \sqrt{1 + 0.31\,\frac{L_m}{\sqrt{Dt}}} \tag{2.28}$$

Leis and Stephen [18] have shown that not all corrosion defects achieve full ductility at failure. They suggested that low toughness pipes might fail at net section stresses below ultimate stress by the initiation of cracks at the base of the corrosion defects resulting in failure pressures lower than predicted by models based on fully

ductile failure. As a consequence there is a likelihood that corrosion defects fail by more than one mechanism and the existing databases have combined multiple mechanisms into a single group. They suggested that ultimate stress might be taken as the failure stress only for those pipes with high ductility and moderate to high fracture toughness, which will enable the pipe to achieve full ductility before failure. This essentially follows the ultimate strength design philosophy with the determination of plastic collapse load.

2.7 Closure

This chapter contains an overview of the evaluation methods currently employed by the oil and gas transmission pipeline industry and a few other criteria proposed by various researchers for the assessment of residual strength of corroded pipelines. Irrespective of the method of solution involved, it is observed that most of the evaluation methods considered only the longitudinal extent of corrosion and assumed the LTA to achieve full ductility at failure. The reasons for their inability to consider the circumferential extent of corrosion include their dependence on fracture mechanics approach and the simplified representation of LTA as circumferential groove-like defect. The circumferential extent of corrosion may be important when a short defect with more circumferential extent is to be assessed. The assumption that LTA fails by ductile tearing restricts the application of these solutions to low toughness materials or to pipelines that encounter loss of ductility due to service environment conditions. While sufficient margin exists between yield and ultimate stress, allowing the primary load more than that required for net section yielding would result in stress strain fields much different

compared to elastic state because of the large deformations. Though the present criteria, employed by the industry are conservative because of their inherent assumptions, an improved Level 2 procedure can be developed to overcome these limitations thereby enabling a better understanding of the behavior of LTA.

CHAPTER 3

LIMIT LOAD ESTIMATION USING VARIATIONAL METHODS

3.1 Introduction

Limit analysis offers a more realistic design and assessment methodology taking into account the material nonlinearity by assuming an elastic perfectly plastic material model. The estimation of limit load for mechanical components provides a better means of structural integrity assessment and fitness for service evaluation. Limit load solutions based on net section collapse criterion for the LTA (locally thinned area) have been extensively used in integrity assessment. Theoretical limit load expressions for damaged components are difficult to obtain when the defect geometry has a significant influence on the load carrying capacity of the component. In this case, application of lower and upper bound theorems of plasticity has proven to be a viable alternative for the estimation of collapse load. The classical upper and lower bound theorems still play an important

role in engineering design. Lower bound limit load solutions obtained from "equilibrium distributions" are of interest from a design standpoint to ensure safe designs and avoid operational failures due to primary loads. However, the upper bound theorems are suitable for metal forming processes where a load more than the exact limit load is needed to estimate the power requirements and drive selection. Mura et al. [19] proposed an alternate method to determine the limit load by applying variational concepts in plasticity and invoking the concept of "integral mean of yield criterion". This concept has been extended by Seshadri and Mangalaramanan [20] to obtain improved lower bound limit load estimates by the introduction of the m_α method.

The design of mechanical components is usually achieved on the basis of an allowable stress with the maximum allowable stress specified as a fraction of the yield stress as shown in the previous chapter. In many practical cases, the local plastic flow occurs at locations of stress raisers and geometric discontinuities such as LTA. This localized plastic flow, which occurs because of the deformation controlled secondary stresses and peak stresses redistribute. The ductility of the material offers adequate reserve strength beyond initial yield by permitting some local plastic flow. It is important to assess whether the structure will be able to resist the primary load in order to avoid catastrophic failure. Hence, the limit load can be used as a realistic basis for assessing the permissible working load on a structure by using a factor of safety. Hence better prediction of limit load would lead to a less conservative estimate of working pressure in the case of pipelines. Robust limit load estimation methods based on variational concepts in plasticity have been applied in this thesis to obtain better estimates of the limit load.

3.2 Classical Limit Theorems

3.2.1 Upper Bound Theorem

The upper bound estimate of the limit load is obtained from kinematically admissible strain distributions. A strain field is called kinematically admissible, if it is derived from a velocity field which satisfies the compatibility or continuity conditions.

The upper bound theorem states that, "If an estimate of the limit load of a component or structure is made by equating the internal rate of dissipation of energy to the rate of external work in any postulated mechanism of deformation, the estimate will either be high or correct.

3.2.2 Lower Bound Theorem

The lower bound limit load solutions are derived from statically admissible stress distributions that satisfy equilibrium. A stress field is said to be statically admissible if for the given loads, the system is in a state of equilibrium and the stress at any location in the structure lies within the yield surface.

The classical lower bound theorem states that, "If any stress distribution throughout the component or structure can be found, which is everywhere in equilibrium internally and balances the external loads and at the same time does not violate the yield condition, then these loads will at least be equal or less than the exact limit load and will be carried safely".

The classical lower bound limit load for an arbitrary load P calculated from the maximum equivalent stress assuming a statically admissible stress distribution may be expressed as:

$$P_L = P \frac{\sigma_y}{(\sigma_e)_{max}} \tag{3.1}$$

3.3 Theorem of Nesting Surfaces

Consider a body of volume V bounded by surface S and acted upon by a generalized system of loads Q_k (k = 1, 2, 3...) as shown in figure 3.1. A stress field σ_{ij} and a corresponding strain rate field $\dot{\varepsilon}_{ij}$ is setup in the structure. The material behaviour is governed by the power law for the steady state creep given by,

$$\dot{\varepsilon}_{ij} = B \sigma_e^n \tag{3.2}$$

The generalized effective stress of this structure is given by,

$$Q_e = F_n(\sigma_{ij}) = \left[\frac{1}{V} \int_V \sigma_e^{n+1} \, dV \right]^{\frac{1}{n+1}} \tag{3.3}$$

The theorem of nesting surfaces [21] states that the above functional is strictly monotonically increasing with the exponent n. It is bounded below by the result n = 1 (elastic) and the above by the limiting functional as $n \to \infty$ (perfectly plastic). Thus if we consider the hypersurfaces $F_n(\sigma_{ij})$ = constant in stress space then they must 'nest' inside each other for increasing n.

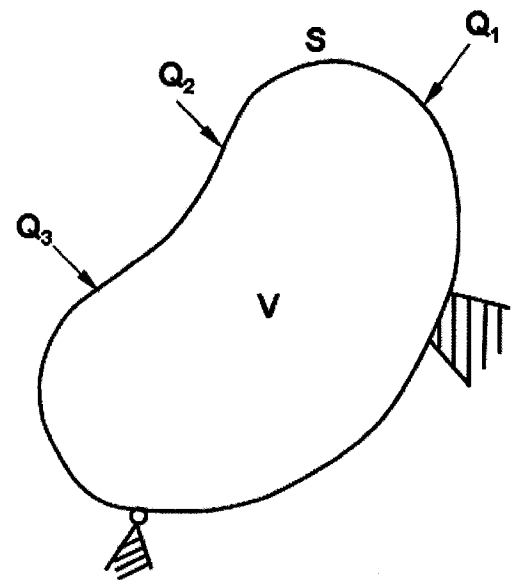

Figure 3.1: Body with prescribed loads

When the reference stress is interpreted on the basis of energy dissipation, such that the dissipation rate in a component or a structure under a system of loads is equated to the average dissipation rate at the 'reference stress state', then,

$$\sigma_R \, \varepsilon_R \, V = \int_V \sigma_{ij} \, \varepsilon_{ij} \, dV \tag{3.4}$$

Using equivalent stress and strain to represent the three dimensional stress states, and using equation (3.2),

$$\sigma_R^{n+1} \, V = \int_V \sigma_e^{n+1} \, dV \tag{3.5}$$

Hence the equation for reference stress as obtained from the theorem of nesting surfaces can be written as

$$\sigma_R = \left[\frac{1}{V}\int_V \sigma_e^{n+1}\, dV\right]^{\frac{1}{n+1}} \tag{3.6}$$

In terms of the finite element discretization scheme, it can be written as

$$\sigma_R = \sqrt{\frac{\sum_{i=1}^{N} \sigma_{ei}^2\, \Delta V_i}{V}} \tag{3.7}$$

It is known from the theorem of nesting surfaces that the stress space is bounded by surfaces with exponent n = 1 and n = ∞ corresponding to elastic and limit state. The nesting surfaces of a two bar pin-jointed structure is shown in figure 3.2.

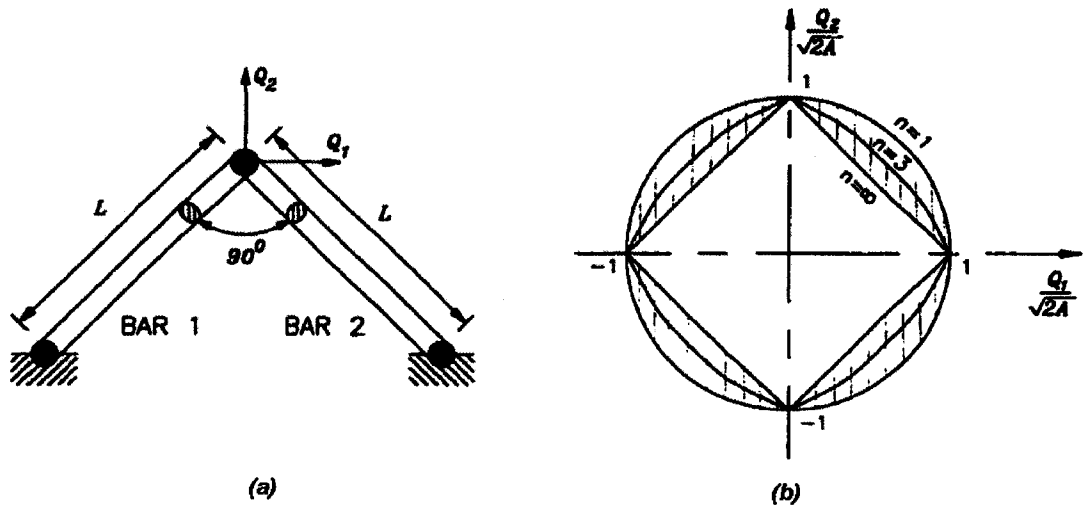

Figure 3.2: (a) A pin jointed two bar structure
***(b) Nesting Surfaces in generalized load space* [22]**

3.4 Extended Variational Theorems of Limit Analysis

Mura and Lee [23] showed by means of variational principles that the safety factors, the kinematically admissible multiplier and statically admissible multiplier for a body made of perfectly plastic isotropic material and subjected to a given surface traction are actually extremum values of the same functional under different constraint conditions.

The statically admissible stress field associated with the lower bound limit load cannot lie outside the hypersurface of the yield criterion. Mura et. al. [19] introduced the integral mean of yield criterion as an alternate approach to determine the upper and lower bound limit loads utilizing the pseudo-elastic distribution of stresses.

Consider a body of volume 'V' bounded by surfaces S_T and S_V as shown in figure 3.3. Assume the body to be fixed on the surface S_V and a surface traction T_i acting on the surface S_T of the volume 'V'. They showed that the safety factor, m, for this body can be obtained by rendering the following functional, F, stationary, i.e.,

$$F_2\left[v_i, s_{ij}, \sigma, R_i, \mu, m, \varphi\right] = \int_V s_{ij} \frac{1}{2}(v_{i,j} + v_{j,i})\, dV + \int_V \sigma\, \delta_{ij}\, v_{i,j}\, dV - \int_{S_v} R_i\, v_i\, dS$$
$$- m\left(\int_{S_T} T_i\, v_i\, dS - 1\right) - \int_V \mu\left[f(s_{ij}) + \varphi^2\right] dV \tag{3.8}$$

with the constraint condition that $\mu \geq 0$.

In the equation 3.8, v_i is the velocity, s_{ij} is the deviatoric stress and σ, μ, R_i, m, and φ are the Lagrangian multipliers. The yield function is given by,

$$f(s_{ij}) = \frac{1}{2} s_{ij}\, s_{ij} - k^2 \tag{3.9}$$

Setting the first variation of the functional F equal to zero, the following conditions are obtained:

$$\frac{1}{2}(v_{i,j} + v_{j,i}) = \mu \frac{\partial f}{\partial s_{ij}} \qquad \text{in V with } \mu \geq 0 \tag{3.10}$$

$$(s_{ij} + \sigma\, \delta_{ij})_{,j} = 0 \qquad \text{in V} \tag{3.11}$$

$$(s_{ij} + \sigma \delta_{ij})\, n_j = m T_i \qquad \text{on } S_T \tag{3.12}$$

$$(s_{ij} + \sigma\, \delta_{ij})\, n_j = R_i \qquad \text{on } S_V \tag{3.13}$$

$$f(s_{ij}) + \varphi^2 = 0 \qquad \text{in V} \tag{3.14}$$

$$\mu\, \varphi = 0 \qquad \text{in V} \tag{3.15}$$

$$\delta_{ij}\, v_{i,j} = 0 \qquad \text{in V} \tag{3.16}$$

$$v_i = 0 \qquad \text{on } S_V \tag{3.17}$$

$$\int_{S_T} T_i\, v_i\, dS = 1 \tag{3.18}$$

Equations (3.10) to (3.18) represent the conditions for incipient plastic flow. Equation (3.10) is the plastic flow potential, equations (3.11) to (3.13) are the equilibrium conditions, and equations (3.16) to (3.18) define a kinematically admissible velocity

field. It should be noted that the Lagrangian multipliers σ, R_i, m, μ and φ are respectively the mean stress, the reaction on S_V, the safety factor, the positive scalar proportionality and the yield parameter. Equations (3.14) and (3.15) define the admissible domain of stress space i.e.,

$$f(s_{ij}) = 0 \qquad \text{if } \mu > 0 \tag{3.19}$$

$$f(s_{ij}) \leq 0 \qquad \text{if } \mu = 0 \tag{3.20}$$

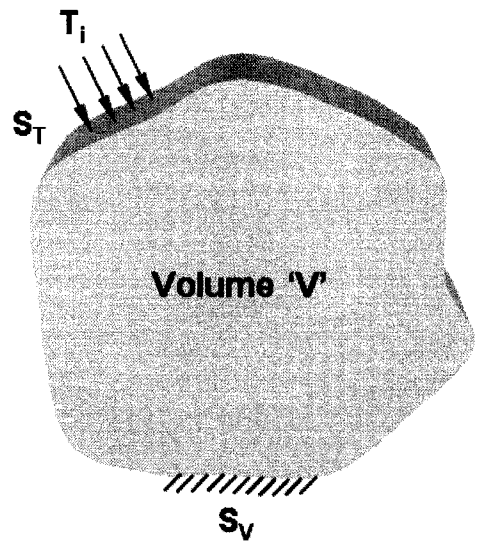

Figure 3.3: Representation of Solid with Boundary Conditions & Loading

Condition (3.13) can be used to determine the reaction at the boundary. Condition (3.18) is no more restrictive than the requirement

$$\int_{S_T} T_i \, v_i \, dS > 0 \tag{3.21}$$

Setting the work done in the expression (3.18) as unity only determine the otherwise arbitrary size of the velocity vector v_i.

Considering arbitrary arguments,

$$v_i^0 = v_i + \delta v_i,\ s_{ij}^0 = s_{ij} + \delta s_{ij} \ldots\ldots \tag{3.22}$$

in which v_i, s_{ij}.... denote the stationary set of arguments of the equation (3.8) and δv_i, δs_{ij},..... denote the corresponding variations. If the arguments of the equation (3.8) are substituted by equation (3.22) taking account of conditions specified by equations (3.10) to (3.18), the functional F can be written as,

$$\begin{aligned} F_2\left[v_i^0, s_{ij}^0, \sigma^0, R_i^0, \mu^0, m^0, \varphi^0\right] &= m + \int_V \delta s_{ij}\,\frac{1}{2}(\delta v_{i,j} + \delta v_{j,i})\,dV \\ &+ \int_V \delta\sigma.\delta_{ij}.\,\delta v_{i,j}\,dV - \int_{S_v} \delta R_i.\delta v_i\,dS - \delta m \int_{S_T} T_i\,\delta v_i\,dS \\ &- \int_V \mu\left[\frac{1}{2}\delta s_{ij}\,\delta s_{ij} + (\delta\varphi)^2\right]dV - \int_V \delta\mu\left[f(s_{ij}^0) + (\varphi^0)^2\right]dV \end{aligned} \tag{3.23}$$

Making use of equations (3.11) to (3.13), the requirements of a statically admissible stress field can be written as,

$$(s_{ij}^0 + \sigma^0\,\delta_{ij})_{,j} = 0 \tag{3.24}$$

$$(s_{ij}^0 + \sigma^0\,\delta_{ij})\,n_j = m^0\,T_i \tag{3.25}$$

$$(s_{ij}^0 + \sigma^0\,\delta_{ij})\,n_j = R_i^0 \tag{3.26}$$

equation (3.23) can be written as,

$$F = m - \int_V \mu\left[\frac{1}{2}\delta s_{ij}\,\delta s_{ij} + (\delta\varphi)^2\right]dV - \int_V \delta\mu\left[f(s_{ij}^0) + (\varphi^0)^2\right]dV \tag{3.27}$$

R_i^0 denotes the reaction of the stress field on the surface S_V. Also integrating equation (3.8) with arbitrary arguments v_i^0, s_{ij}^0, σ^0, R_i^0, m^0, μ^0 and φ^0 and using constraint conditions given by equations (3.24) to (3.26), the following expression can be obtained:

$$F = m^0 - \int_V \mu^0 \left\{ f(s_{ij}^0) + (\varphi^0)^2 \right\} dV \tag{3.28}$$

The integral mean of yield criterion can be expressed as

$$\int_V \mu^0 \left\{ f(s_{ij}^0) + (\varphi^0)^2 \right\} dV = 0 \tag{3.29}$$

$$\text{where} \qquad \mu^0 \geq 0 \tag{3.30}$$

Substitution of equation (3.29) into (3.28) results in

$$F = m^0 \tag{3.31}$$

Since $\mu^0 = \mu + \delta\mu$, equation (3.29) can be written as

$$-\int_V \delta\mu \left\{ f(s_{ij}^0) + (\varphi^0)^2 \right\} dV = \int_V \mu \left\{ f(s_{ij}^0) + (\varphi^0)^2 \right\} dV \tag{3.32}$$

Equation (3.32) can be substituted into (3.27) to obtain

$$F = m - \int_V \mu \left[\frac{1}{2} \delta s_{ij}\, \delta s_{ij} + (\delta\varphi)^2 \right] dV + \int_V \mu \left[f(s_{ij}^0) + (\varphi^0)^2 \right] dV \tag{3.33}$$

Since second term on the right hand side of the equation (3.33) is always a positive quantity, equations (3.31) and (3.33) can be related by an inequality as

$$m^0 \leq m + \int_V \mu \left\{ f(s_{ij}^0) + (\varphi^0)^2 \right\} dV$$

$$\leq m + \max \left\{ f(s_{ij}^0) + (\varphi^0)^2 \right\} \int_V \mu \, dV \qquad (3.34)$$

where $\max \left\{ f(s_{ij}^0) + (\varphi^0)^2 \right\} \geq 0$ because of conditions (3.29) and (3.30).

The safety factor can be expressed as

$$m = m \int_{S_T} T_i \, v_i \, dS = \int_S (s_{ij} + \delta_{ij} \sigma \, n_j) \, v_i dS$$

$$= \int_V (s_{ij} + \delta_{ij} \, \sigma) \, v_{i,j} \, dV + \int_V (s_{ij} + \delta_{ij} \, \sigma) \, v_{j,i} \, dV$$

$$= \int_V s_{ij} \frac{1}{2} (v_{i,j} + v_{j,i}) \, dV$$

$$= \int_V s_{ij} \, \mu \, s_{ij} \, dV$$

$$= 2k^2 \int_V \mu \, dV$$

Rearranging we get,

$$\int_V \mu \, dV = \frac{m}{2k^2} \qquad (3.35)$$

From (3.34) and (3.35), a new lower bound multiplier m′ for the safety factor m can be obtained as,

$$m' = \frac{m^0}{1 + \left\{ \dfrac{\max \left[f(s_{ij}^0) + (\varphi^0)^2 \right]}{2k^2} \right\}} \leq m \qquad (3.36)$$

which holds for any set of s_{ij}^0, σ^0, m^0, μ^0 and φ^0 satisfying equations 3.24, 3.25, 3.29, and 3.30.

Equation (3.36) includes the classical definition of the lower bound, wherein if $\max \left\{ f(s_{ij}^0) + (\varphi^0)^2 \right\} = 0$, equation (3.36) reduces to

$$m^0 \leq m \tag{3.37}$$

In equation (3.28), the linear elastic stress distribution s_{ij}^0 corresponds to an applied traction, $m^0 T_i$. If $\bar{s}_{ij}^0$ is a statically admissible stress distribution corresponding to an applied traction T_i, then $m^0 \bar{s}_{ij}^0$ would correspond to $m^0 T_i$. Therefore,

$$s_{ij}^0 = m^0 \bar{s}_{ij}^0 \tag{3.38}$$

Hence equation (3.28) is rewritten as,

$$F = m^0 - \int_{V_T} \mu^0 \left[\frac{1}{2} (m^0)^2 \bar{s}_{ij}^0 \bar{s}_{ij}^0 - k^2 + (\varphi^0)^2 \right] dV \tag{3.39}$$

Mura and co-workers have shown that m^0, μ^0 and φ^0 can be determined by rendering the functional F in equation (3.39) stationary leading to a set of equations,

$$\frac{\partial F}{\partial m^0} = 0 \quad ; \quad \frac{\partial F}{\partial \mu^0} = 0 \quad ; \quad \frac{\partial F}{\partial \varphi^0} = 0 \tag{3.40}$$

The von Mises equivalence for uniaxial state of stress can be written as follows:

$$\frac{1}{2} \bar{s}_{ij}^0 \bar{s}_{ij}^0 = \frac{(\sigma_e^0)^2}{3} \tag{3.41}$$

and

$$k^2 = \frac{\sigma_y^2}{3} \tag{3.42}$$

Equation (3.39) becomes,

$$F = m^0 - \int_{V_T} \frac{\mu^0}{3} \left[\left\{ (m^0)^2 (\sigma_e^0)^2 - \sigma_y^2 \right\} + 3 (\varphi^0)^2 \right] dV \qquad (3.43)$$

Applying (3.43) in conjunction with (3.40), Seshadri and Mangalaramanan [20] derived the expression of m^0 for a constant flow parameter. This expression is shown below as m_1^0. Pan and Seshadri [24] have derived an expression, m_2^0 taking into account the variable flow parameter μ^0. The expressions for m_1^0 and m_2^0 are given as

$$m_1^0 = \frac{\sigma_y \sqrt{V_T}}{\sqrt{\int_{V_T} (\sigma_e^0)^2 \, dV}} \qquad (3.44)$$

$$m_2^0 = \frac{\sigma_y \sqrt{\int_{V_R} \frac{dV}{E_s}}}{\sqrt{\int_{V_R} \frac{\sigma_e^2 \, dV}{E_s}}} \qquad (3.45)$$

where, $E_s = \frac{\sigma_e}{\varepsilon_e}$

Finite element implementation of the equation 3.44 was made from the statically admissible stress distributions as below:

$$m_1^0 = \frac{\sigma_y \sqrt{V_T}}{\sqrt{\sum_{k=1}^{N} (\sigma_{ek}^0)^2 \, \Delta V_k}} \qquad (3.46)$$

where the quantities σ_{ek}^0 and ΔV_k are the von Mises equivalent stresses and volumes of respective elements in the FEA discretization scheme.

Comparing the expressions for m_l^0, as obtained from equation (3.44), and equation (3.7) for reference stress, it can be seen that

$$m_l^0 = \frac{\sigma_y}{\sigma_R} \tag{3.47}$$

A monotonic increase in the value of the reference stress implies monotonic decrease in the value of m_l^0, with increasing n. Since equation (3.6) gives a lower bound on the reference stress for n =1, m_l^0 corresponding to n = 1 is an upper bound multiplier for limit loads. It is to be noted that equation (3.6) was developed on the basis of the average rate of energy dissipation at reference state.

Equation (3.36) can be simplified further using equations (3.41) and (3.42) as,

$$m' = \frac{2\, m^0\, \sigma_y^2}{\sigma_y^2 + (m^0)^2 \left(\sigma_e^0\right)_M^2} \leq m \tag{3.48}$$

Equation (3.44) and (3.48) can be readily obtained on the basis of linear elastic FEA. $(\sigma_e^0)_M$ is the maximum equivalent stress in a component or structure for a traction T_i.

The lower bound limit load (P_L) can therefore be expressed as:

$$P_L = m' P \tag{3.49}$$

$$\text{Hence,} \qquad m' \leq m \leq m^0 \tag{3.50}$$

3.5 Improved Lower Bound Estimates: The m_α method

The lower bound limit load multiplier (m′) obtained from Mura's extended variational theorem was shown to be less than that obtained by applying classical lower bound theorem. Hence the m_α-method was introduced by Seshadri and Mangalaramanan [20] by invoking the notion of reference volume to account for localized collapse and the technique of "leapfrogging" to a limit state.

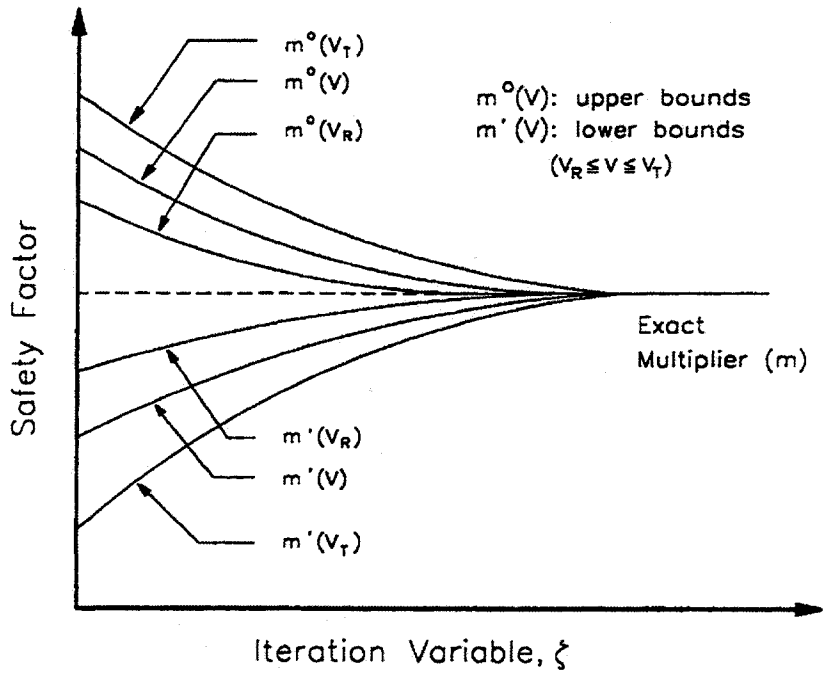

***Figure 3.4: Variation of* m′ *and* m^0 *with Iteration Variable* ζ **[20]**

An iteration variable ζ was introduced in such a manner that infinitesimal changes to the elastic modulus of various elements in successive analysis would induce a corresponding change Δζ. As ζ increases with the iterations, m^0 and m′ should ideally

converge uniformly to the exact value of the safety factor, m. A schematic variation of m^0 and m′ with ζ is shown in figure 3.4.

3.5.1 Local Plastic Collapse – The Reference Volume

When plastic collapse occurs over a localized region of a component or structure, the value of m_l^0 will be overestimated if it is calculated on the basis of the total volume, V_T, as in equation (3.44). Furthermore, the corresponding m′ will be underestimated. The reference volume was introduced to identify the "kinematically active" portion of the structure that participates in plastic action. If V_R is the reference volume, then $V_R \leq V_T$ (figure 3.5).

Hence,

$$m_l^0(V_R) = \frac{\sigma_y \sqrt{V_R}}{\sqrt{\sum_{k=1}^{\alpha} (\sigma_{ek}^0)^2 \, \Delta V_k}} \tag{3.51}$$

where $V_R = \sum_{k=1}^{\alpha} (\Delta V_k)$, and $\alpha < N$.

The elements are arranged in the following sequence,

$$(\sigma_{e1}^0)^2 \, \Delta V_1 > (\sigma_{e2}^0)^2 \, \Delta V_2 > \ldots\ldots\ldots\ldots > (\sigma_{en}^0)^2 \, \Delta V_n \tag{3.52}$$

In terms of the iteration variable ζ, Mura's lower bound multiplier can be expressed as,

$$m'(\zeta) = \frac{2\, m^0(\zeta)\, \sigma_y^2}{\sigma_y^2 + \left[m^0(\zeta)\right]^2 \left[\sigma_M^0(\zeta)\right]^2} \tag{3.53}$$

where $\sigma_M^0(\zeta)$ is the maximum equivalent stress at the iteration number "i". The quantities m', m^0 and σ_M^0 are all functions of ζ.

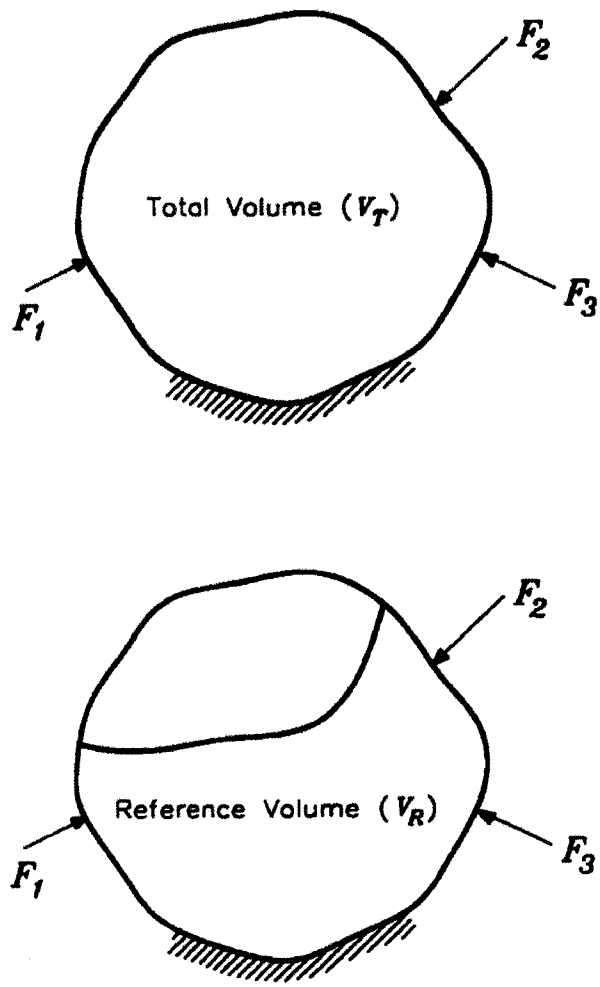

Figure 3.5: Representation of Reference Volume

Differentiating both sides of the above equation with respect to ζ, we get,

$$\frac{dm'}{d\zeta} = \frac{\partial m'}{\partial m^0}\frac{dm^0}{d\zeta} + \frac{\partial m'}{\partial \sigma_M^0}\frac{d\sigma_M^0}{d\zeta} \tag{3.54}$$

In terms of finite difference, equation (3.54) can be expressed as,

$$\Delta m' = \left.\frac{\partial m'}{\partial m^0}\right|_{\zeta_i} .(\Delta m^0) + \left.\frac{\partial m'}{\partial \sigma_M^0}\right|_{\zeta_i} .(\Delta \sigma_M^0) \tag{3.55}$$

where $\zeta = \zeta_i$ corresponds to the i-th iteration.

For a limit type state (ζ_∞), we define,

$$\left.\begin{aligned} \Delta m' &= m_\alpha - m_i' \\ \Delta m^0 &= m_\alpha - m_i^0 \\ \text{and } \sigma_M^0 &= \frac{\sigma_y}{m_\alpha} - \sigma_{Mi}^0 \end{aligned}\right\} \tag{3.56}$$

m_α is the value to which m' and m^0 are expected to converge to.

Combining equations (3.55) and (3.56) and carrying out the necessary algebraic manipulations, the following quadratic equation can be obtained:

$$A m_\alpha^2 + B m_\alpha + C = 0 \tag{3.57}$$

where

$$A = (m_i^0\ \bar{\sigma}_{Mi}^0)^4 + 4\ (m_i^0\ \bar{\sigma}_{Mi}^0)^2 - 1$$

$$B = -8\, m_i^0\ (m_i^0\ \bar{\sigma}_{Mi}^0)^2 \qquad (3.58)$$

$$C = 4\,(m_i^0)^3\ \bar{\sigma}_{Mi}^0$$

$$\text{and } \bar{\sigma}_{Mi}^0 = \frac{\sigma_{Mi}^0}{\sigma_y}$$

The coefficients A, B, C and finally m_α can be evaluated from the results of any linear elastic FEA. Although the m_α method was intended for two iterations at first, increasing iterations would give better estimations provided certain conditions are satisfied.

To ensure real roots for equation (3.57), the discriminant must be greater than zero, i.e.,

$$m_i^0\ \bar{\sigma}_{Mi}^0 \leq 1+\sqrt{2} \qquad (3.59)$$

3.5.2 Expression for Lower Bound Multiplier m_α

Reinhardt and Seshadri [25] derived an expression for the lower bound multiplier m_α, from the equation $m' = f(m_L, m^0)$. If m_L and m^0 are derived from a series of stress and strain distributions that converge to collapse, then m' is assumed to follow a line that ends at $m = m_L = m' = m^0$. From the current iteration ζ, the estimate of the final solution is

made by linear extrapolation along the tangent to the curve m′ (ζ). The differentiation of the equation $m' = f(m_L, m^0)$ with respect to the iteration variable ζ is as below:

$$\frac{dm'}{d\zeta} = \left(\frac{\partial m'}{\partial m^0}\right)_{\zeta_i} \frac{dm^0}{d\zeta} + \left(\frac{\partial m'}{\partial \frac{1}{m_L}}\right)_{\zeta_i} \frac{d\frac{1}{m_L}}{d\zeta} \tag{3.60}$$

It is postulated that the trajectory ends at $m = m_L = m' = m^0$ and by doing so m_α is expected to give a reasonable estimate of the multiplier m if the values of m_L and m^0 are sufficiently close to the exact limit load multiplier m. In terms of finite differences, equation (3.60) is written as,

$$m' - m_\alpha = 2\frac{1-\left(\frac{m^0}{m_L}\right)^2}{\left[1+\left(\frac{m^0}{m_L}\right)^2\right]^2}(m^0 - m_\alpha) - 4\frac{(m^0)^3}{m_L\left[1+\left(\frac{m^0}{m_L}\right)^2\right]^2}\left(\frac{1}{m_L} - \frac{1}{m_\alpha}\right) \tag{3.61}$$

Solving the above equation for m_α gives,

$$m_\alpha = 2m^0 \frac{2\left(\frac{m^0}{m_L}\right)^2 + \sqrt{\frac{m^0}{m_L}\left(\frac{m^0}{m_L}-1\right)^2\left(1+\sqrt{2}-\frac{m^0}{m_L}\right)\left(\frac{m^0}{m_L}-1+\sqrt{2}\right)}}{\left(\left(\frac{m^0}{m_L}\right)^2+2-\sqrt{5}\right)\left(\left(\frac{m^0}{m_L}\right)^2+2+\sqrt{5}\right)} \tag{3.62}$$

3.6 Bounds on Multipliers

3.6.1 Bounds on m′ and m^0

Mura's lower bound multiplier, m′, can be shown to be equivalent to

$$m' = \frac{2\,m^0}{1 + \left(\frac{m^0}{m_L}\right)^2} \leq m \tag{3.63}$$

where m_L is the classical lower bound multiplier.

By using the true collapse load multiplier, the following normalized variables are defined:

$$R_L = \frac{m_L}{m} \; ; \; R_u = \frac{m_u}{m} \; ; \; R' = \frac{m'}{m} \text{ and } R_0 = \frac{m^0}{m} \tag{3.64}$$

where m_u is the classical upper bound multiplier.

By virtue of equation (3.64), equation (3.63) can be written as

$$R' = \frac{2\,R_0}{1 + \left(\frac{R_0}{R_L}\right)^2} \leq 1 \tag{3.65}$$

It is now easily shown, in the following hypothesis, that R′ is not only a lower bound, but even that it is smaller than R_L.

$$\frac{2R_0}{1+\left(\frac{R_0}{R_L}\right)^2} \le R_L \Leftrightarrow 2\frac{R_0}{R_L} \le 1+\left(\frac{R_0}{R_L}\right)^2 \Leftrightarrow 0 \le 1-2\frac{R_0}{R_L}+\left(\frac{R_0}{R_L}\right)^2 = \left(1-\frac{R_0}{R_L}\right)^2$$

(3.66)

For the m^0 multipliers, bounds can be derived as well. The multiplier m_1^0, defined in equation (3.44), is shown to be greater than m_L by,

$$m_1^0 = \frac{\sigma_y \sqrt{V_T}}{\sqrt{\int_{V_T} (\sigma_e)^2 \, dV}} = \frac{\frac{\sigma_y}{\sigma_{max}}\sqrt{V_T}}{\sqrt{\int_{V_T}\left(\frac{\sigma_e}{\sigma_{max}}\right)^2 dV}} = m_L \sqrt{\frac{\int_{V_T} 1^2 \, dV}{\int_{V_T}\left(\frac{\sigma_e}{\sigma_{max}}\right)^2 dV}} \ge m_L \qquad (3.67)$$

The relationship (3.67) holds everywhere because $\sigma_e \le \sigma_{max} = \max(\sigma_e)$. The multiplier m_1^0 may not converge to the limit multiplier m, meaning $R_1^0 \ge 1$ at the exact limit state. From equation (3.67), it is clear that $R_1^0 = 1$ can occur only if $\sigma_e = \sigma_{max}$ everywhere in the volume V_T. If localized plastic hinges form in the structure, that condition is generally not satisfied. As a remedy, the idea of the reference volume introduced by Seshadri and Mangalaramanan [20].

For a restricted class of materials, namely those of the linear elastic type with homogeneous properties throughout V_T, m_1^0 can be shown to be an upper bound. The proof makes use of the Schwarz inequality, according to which the inner product of linear operators of a fairly general class satisfies

$$(x, y) \leq \|x\| \|y\| \tag{3.68}$$

where (x, y) is the inner product of x and y, and $\|x\|$ is the norm of x. Integrals for which the integrand is bounded are operators suitable for the application of the Schwarz inequality, and $(x, y) \leq \int xy\,dz$, $\|x\| = \sqrt{\int x^2\,dz}$. Therefore, the following relationship can be derived:

$$\sqrt{\int_{V_T} \sigma_e^2\,dV}\ \sqrt{\int_{V_T} 1^2\,dV} \geq \int_{V_T} \sigma_e .1\,dV \Leftrightarrow \sqrt{V_T} \geq \frac{\int_{V_T} \sigma_e\,dV}{\sqrt{\int_{V_T} \sigma_e^2\,dV}} \tag{3.69}$$

By substituting the right expression in equation (3.69) into equation (3.44), it follows that

$$m_1^0 = \frac{\sigma_y \sqrt{V_T}}{\sqrt{\int_{V_T} \sigma_e^2\,dV}} \geq \frac{\sigma_y \int_{V_T} \sigma_e\,dV}{\int_{V_T} \sigma_e^2\,dV} = \frac{\sigma_y \int_{V_T} E\,\varepsilon_e\,dV}{\int_{V_T} E\,\sigma_e\,\varepsilon_e\,dV} \tag{3.70}$$

If the material is homogeneous, the elastic modulus in the rightmost expression is constant and can be cancelled. Furthermore, for an isotropic-elastic material, the principal axis of stress and strain are coincident, and $\sigma_e\,\varepsilon_e = \sigma_{ij}\,\varepsilon_{ij}$. By virtue of classical upper bound theorem, the right most expression of equation (3.70) equals m_u, and hence it follows that $m_1^0 \geq m_u$, meaning that it is guaranteed to be an upper bound for a homogeneous, isotropic-elastic material.

A more general upper bound property can be derived for the multiplier m_2^0, defined by equation (3.45). The proof uses again the Schwarz inequality, this time with

the linear operator $\int_{V_T} \frac{1}{E_s} \ldots\ldots dV$, with the requirement $0 < \frac{1}{E_s} < \infty$, which is always satisfied in practical numerical applications. The Schwarz inequality becomes

$$\sqrt{\int_{V_T} \frac{1}{E_s} \sigma_e^2 \, dV} \sqrt{\int_{V_T} \frac{1}{E_s} 1^2 \, dV} \geq \int_{V_T} \frac{1}{E_s} \sigma_e . 1 \, dV \Leftrightarrow \sqrt{\int_{V_T} \frac{1}{E_s} 1^2 \, dV} \geq \frac{\int_{V_T} \frac{1}{E_s} \sigma_e \, dV}{\sqrt{\int_{V_T} \frac{1}{E_s} \sigma_e^2 \, dV}} \tag{3.71}$$

Again, substituting the right expression in equation (3.71) into equation (3.45) gives,

$$m_2^0 = \frac{\sigma_y \sqrt{\int_{V_T} \frac{1}{E_s} dV}}{\sqrt{\int_{V_T} \frac{1}{E_s} \sigma_e^2 \, dV}} \geq \frac{\sigma_y \int_{V_T} \frac{1}{E_s} \sigma_e \, dV}{\int_{V_T} \frac{1}{E_s} \sigma_e^2 \, dV} = \frac{\sigma_y \int_{V_T} \varepsilon_e \, dV}{\int_{V_T} \sigma_e \varepsilon_e \, dV} \tag{3.72}$$

In this inequality, the possibility of an inhomogeneous material has been considered (that is, E_S can be function of the location in the material). Therefore, assuming isotropic elastic behaviour, equation (3.72) gives rise to the inequality $m_2^0 \geq m_u$, meaning that m_2^0 is guaranteed to be an upper bound for any inhomogeneous, isotropic-elastic material.

3.6.2 Estimation of Bounds on m_α

The expression for m_α written in terms of the normalized multipliers (equation 3.64) is given as $R_\alpha = \frac{m_\alpha}{m}$ with

$$R_\alpha = 2R^0 \frac{2\left(\frac{R_0}{R_L}\right)^2 + \sqrt{\frac{R_0}{R_L}\left(\frac{R_0}{R_L}-1\right)^2\left(1+\sqrt{2}-\frac{R_0}{R_L}\right)\left(\frac{R_0}{R_L}-1+\sqrt{2}\right)}}{\left(\left(\frac{R_0}{R_L}\right)^2+2-\sqrt{5}\right)\left(\left(\frac{R_0}{R_L}\right)^2+2+\sqrt{5}\right)} \tag{3.73}$$

Due to normalization, it is clear that $R_\alpha < 1$ means that m_α is effectively a lower bound, whereas $R_\alpha > 1$ denotes an upper bound. The above equation describes R_α as a function of two variables, and it is therefore possible to represent the boundary between the upper and lower bound regions as a line in two-dimensional space. This is done in figure 3.6, which represents a section through the R_α surface at $R_\alpha = 1$ as function of R_0 and R_0 / R_L. In the region below the line $R_\alpha = 1$, m_α is a lower bound, and above it is not. Since the normalizing factor m is unknown, a known combination of m^0 and m_L is a vertical line in R_0 versus R_0 / R_L space that connects the point where $R_0 = 1$ ($m = m^0$) to the point where $R_0 = R_0 / R_L$ ($m = m_L$). In other words, the line denotes the allowed range of m, which is between the upper bound m^0 and the lower bound m_L. The lower part of this line lies in the region where $R_\alpha \leq 1$ and the rest in the region where $R_\alpha > 1$. The length of the respective segments is a measure of the likelihood of whether or not R_α is a lower bound. Note that the multiplier m_α is guaranteed to be above the classical lower bound multiplier m_L.

The use of the diagram (figure 3.6) is as below:

- From the FE model that gives the stress and strain distributions in the body, get the ratio R_0/R_L (which equals the ratio m^0/m_L).
- Plot a vertical line at the given R_0 / R_L.
- Since m is unknown, R_0 could theoretically have any value between 1 and R_0 / R_L as indicated by the length of the vertical line. Generally, the 45 degree line in figure indicates the maximum value of R_0. The admissible region (domain) for R_0 thus lies between the horizontal axis and the 45 degree line.
- The portion of the vertical line that lies below the line $R_\alpha = 1$ is the range of possible values R_0 for which m_α is a lower bound. It can be seen that this region is large when the ratio R_0 / R_L is high. This is desirable in the sense that the probability that m_α is a lower bound is high, but at the same time indicates that the true value m is likely underestimated by m_α. When R_0 / R_L is close to 1, the likelihood of overestimating m with m_α is relatively high, but the amount by which it may be overestimated is low because the bounds are good. Figure shows a curve ($R_\alpha = 1.05$) for which m_α could be 5% on the upper bound side, which may be considered as acceptable within engineering accuracy. Another interpretation would be that $\frac{m_\alpha}{1.05} \leq m$. If this line is adopted as the limit, it is seen that the region in which m_α gives acceptable estimates of the limit load is quite large.

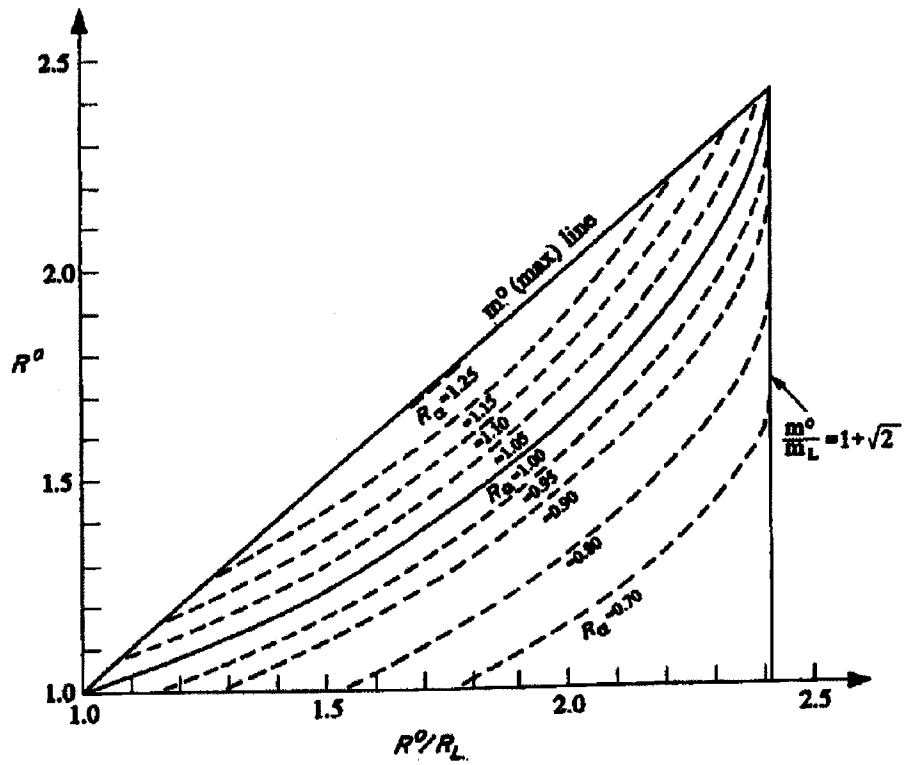

Figure 3.6: Region of lower and upper boundedness of m_α **[25]**

In practice, the m_α estimate for the initial iterations turns out to be a lower bound in the great majority of cases. Lower bound solutions are obtained if the quality of the upper and lower bounds entering the equation (3.62) is roughly the same. Lower bound m_α estimates may not be obtained if a lower bound multiplier of very good quality is obtained while the upper bound multiplier is not so close to m. Clearly, the mesh sizes should be such that peak stresses are predicted accurately so that m_L and, therefore m_α is estimated properly. Coarse meshes tend to underestimate the peak stresses and overestimate m_α.

3.7 Lower Bound Limit Loads for Damaged Cylinders

3.7.1 Reference volume

The concept of reference volume in the context of localized behaviour of thermal hotspots has been introduced by Seshadri [26]. The reference volume in the context of damaged cylinder identifies the 'kinematically active' portion of the cylinder that participates in the plastic action due to the presence of the damage. The extent to which this localized effect is observed in a cylindrical shell is defined by the decay lengths, X_C (in the circumferential direction) and X_L (in the longitudinal direction).

For a thin cylindrical shell as shown in figure 3.7, Donnell's equations in the absence of surface loadings are expressed as:

$$\frac{t^2}{12}(\nabla^8 w^c) + \frac{(1-\upsilon^2)}{R_m^2}\left(\frac{\partial^4 w^c}{\partial x^4}\right) = 0 \qquad (3.74\ a)$$

$$\nabla^4 u_s^c = -\frac{(2+\upsilon)}{R_m}\left(\frac{\partial^3 w^c}{\partial x^2\,\partial s}\right) - \frac{1}{R_m}\left(\frac{\partial^3 w^c}{\partial s^3}\right) \qquad (3.74\ b)$$

$$\nabla^4 u_x^c = -\frac{\upsilon}{R_m}\left(\frac{\partial^3 w^c}{\partial x^3}\right) + \frac{1}{R_m}\left(\frac{\partial^3 w^c}{\partial x\,\partial s^3}\right) \qquad (3.74\ c)$$

Where t is the shell thickness, R_m is the mean radius, υ is the Poisson's ratio, x is the coordinate along the axis (meridional direction), s is the coordinate along the circumferential direction; u_x is the displacement along the x-coordinate, u_s is the

displacement along s, and w is the radial displacement. The superscript c refers to the complementary component of the solution.

The following nondimensional variables were defined by substituting s with $R_m\theta$ as below:

$$y = \frac{x}{R_m} \; ; \; v = \frac{u_s^c}{R_m} \; ; \; u = \frac{u_x^c}{R_m} \text{ and } \overline{w} = \frac{w^c}{R_m} \tag{3.75}$$

Based on the transformations,

$$\nabla^2 = \frac{\partial^2}{\partial y^2} + \frac{\partial^2}{\partial \theta^2} \tag{3.76 a}$$

$$\text{and} \qquad 4K^4 = 12(1-\upsilon^2)\left(\frac{R_m}{t}\right)^2 \tag{3.76 b}$$

In the absence of surface loading, the displacement was assumed to be of the form:

$$\overline{w} = A\, e^{p\theta} (\cos ny) \tag{3.77}$$

Considering displacements that decreases as θ increases, the general solution was expressed as:

$$\begin{aligned}\overline{w} = [&A_1 e^{-\alpha_1\theta} \cos(\beta_1\theta) + A_2 e^{-\alpha_1\theta} \cos(\beta_1\theta) + A_3 e^{-\alpha_2\theta} \cos(\beta_2\theta) \\ &+ A_4 e^{-\alpha_2\theta} \cos(\beta_2\theta)] \cos(ny)\end{aligned} \tag{3.78}$$

where A_1, A_2, A_3, A_4, α_1, α_2, β_1, and β_2 are constants.

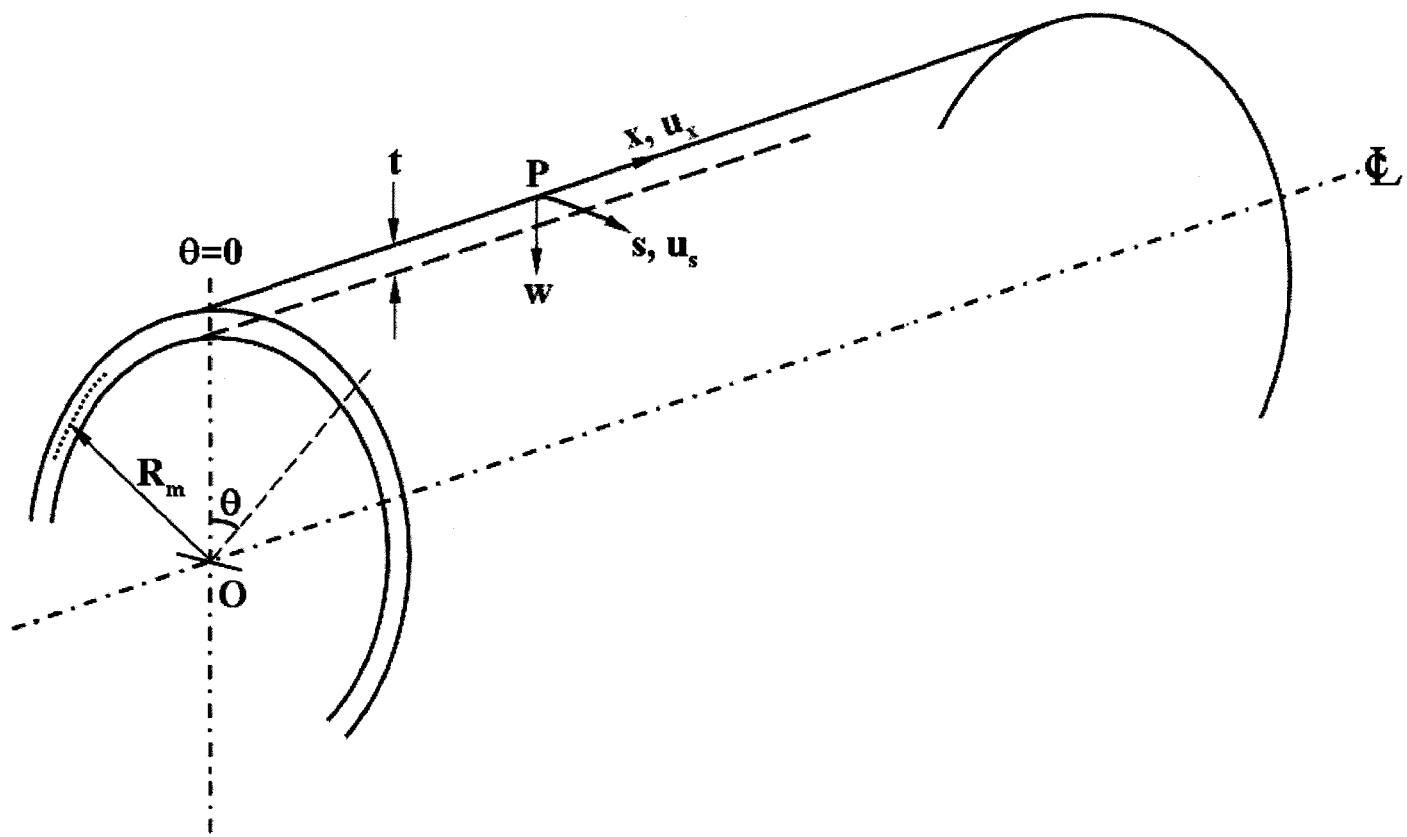

Figure 3.7: Thin Cylindrical Shell

The following relationships were used for α:

$$\begin{Bmatrix} \alpha_1^2 \\ \alpha_2^2 \end{Bmatrix} = \frac{n}{2} \begin{Bmatrix} (n+k) + [(n+k)^2 + k^2]^{1/2} \\ (n-k) + [(n-k)^2 + k^2]^{1/2} \end{Bmatrix} \tag{3.79}$$

where 'n' refers to the nth harmonic of a Fourier series expansion.

Since, the displacements in the circumferential direction behave as $e^{-\alpha_i \theta}$, the critical angle (θ_c) occurs when $\alpha_i \theta = \pi$, or $\theta_c = \frac{\pi}{\alpha_i}$. θ_c will assume a maximum value when α_i is minimum. It can be observed from equation (3.79) that α_i is a minimum when n = 1.

For n = 1 and larger values of k, $\alpha_2 < \alpha_1$. Hence,

$$\alpha_2^2 \approx \left(\frac{\sqrt{2} - 1}{2} \right) k \tag{3.80}$$

For $\upsilon = 0.3$, using equation (3.76 b),

$$\alpha_2 \approx 0.516 \left(\frac{R_m}{t} \right)^{1/4} \tag{3.81}$$

Since, $\theta_c = \pi / \alpha_2$ and $X_c = a\theta_c$, the circumferential decay length is derived as:

$$X_C = 6.1 \, (R_m^3 \, t)^{1/4} \tag{3.82}$$

The following well-known equation for axisymmetric longitudinal bending, in the absence of surface loading was used in deriving the decay length in the meridional direction.

$$\frac{d^4 w^c}{dx^4} + 4\beta^4 w^c = 0 \tag{3.83}$$

where $\beta = \dfrac{3(1-\upsilon^2)}{R_m^2 t^2}$

The complementary solution is expressed as:

$$w^c(x) = e^{\beta x}[C_1 \sin(\beta x) + C_2 \cos(\beta x)] + e^{-\beta x}[C_3 \sin(\beta x) + C_4 \cos(\beta x)] \tag{3.84}$$

where C_1 to C_4 are constants of integration. For finite displacements to occur as $x \rightarrow \infty$, it is stipulated that $C_1 = C_2 = 0$. The radial displacement diminishes significantly when $\beta x = \pi$. Hence the decay length is given by,

$$X_L = \frac{\pi}{\beta} = \pi\left[\frac{R_m^2 t^2}{3(1-\upsilon^2)}\right]^{1/4} \tag{3.85}$$

For $\upsilon = 0.3$, $X_L = 2.44 (R_m t)^{1/2}$.

However for practical purposes, X_L is given by,

$$X_L = 2.5 (R_m t)^{1/2} \tag{3.86}$$

It is observed from the above equations that the decay lengths depend on shell geometry. It is to be noted that the expression for X_L is the same as the minimum distance required between the LTA and any major structural discontinuity, L_{msd}, defined in the

local metal loss rules of API 579 evaluation procedure (equation 2.15) as shown by Osage et al. [8].

Considering a LTA of dimensions (2a x 2b) as shown in the figure 3.8, the reference volume or kinematically active volume (where the plastic redistribution is assumed to be confined in a cylinder with LTA) is composed of both the corroded and uncorroded volumes and is computed by the following expressions:

$$V_C = (2a)(2b)\ t_c$$
$$V_U = \left[(2X_C + 2a)(2X_L + 2b) - (2a)(2b)\right] t \tag{3.87}$$

where t_c is the remaining thickness of the LTA.

Hence the reference volume can be expressed as

$$V_R = V_U + V_C \tag{3.88}$$

Although the area of corrosion can be irregular in practice, it has been idealized to be represented by a rectangle of dimensions 2a x 2b for simplicity. The depth of corrosion is assumed to be uniform for this analysis, but the maximum depth of corrosion may be used in the case of irregular corrosion spots to obtain results on the safe side.

Computation of reference volume enables the consideration of both longitudinal and circumferential extent of corrosion, which is a much closer approximation of the actual corroded volume. This overcomes the limitations of other evaluation guidelines.

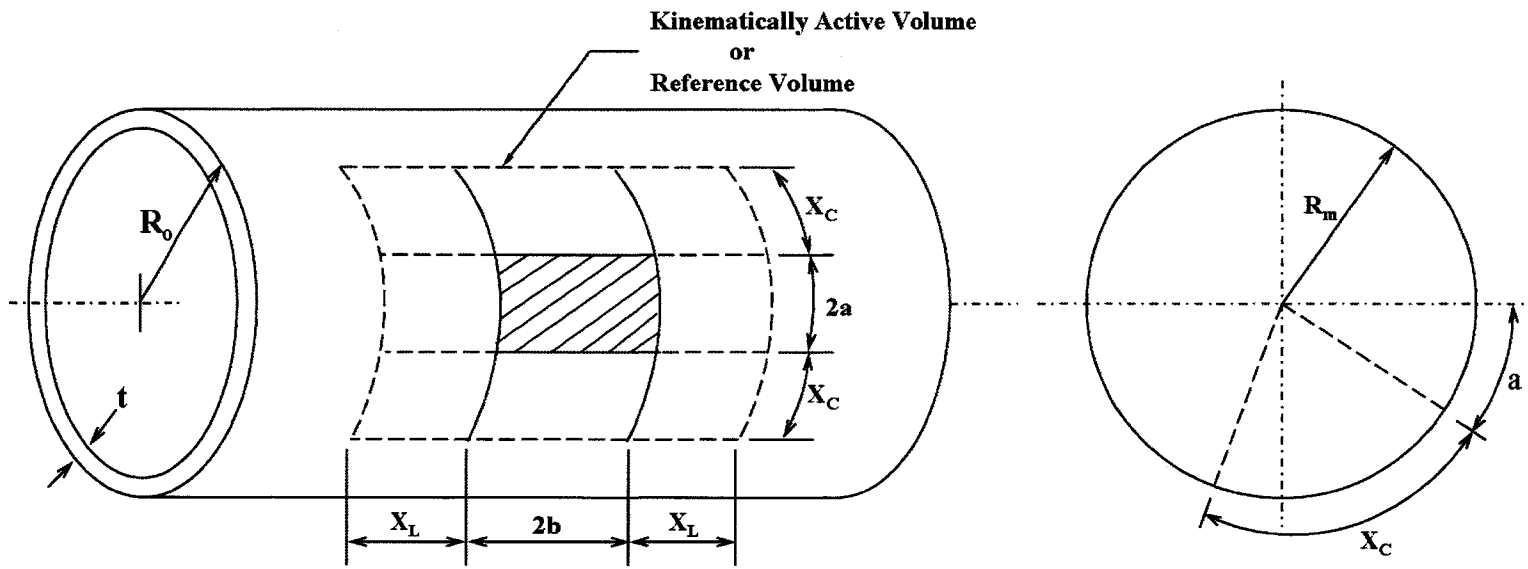

Figure 3.8: Pipe with Locally Thinned Area

3.7.2 Variational Formulation for Limit Load Estimation

It has been shown that for a thin walled cylinder with a LTA as shown in figure 3.9, the integral mean of yield criterion (equation 3.29) using the von Mises criterion can be expressed as [27]:

$$\int_{V_U} \left\{(m_d^0\ \sigma_{eU}^0)^2 - \sigma_y^2\right\} dV + \int_{V_C} \left\{(m_d^0\ \sigma_{eC}^0)^2 - \sigma_y^2\right\} dV = 0 \qquad (3.89)$$

where the subscript C refers to the LTA, and subscript U refers to the region with undamaged thickness or the uncorroded part of the pipe.

If the stresses are assumed constant, yet statically admissible, in V_U and V_C, integration of the above equation leads to

$$\left\{(m_d^0\ \sigma_{eU}^0)^2 - \sigma_y^2\right\} V_U + \left\{(m_d^0\ \sigma_{eC}^0)^2 - \sigma_y^2\right\} V_C = 0 \qquad (3.90)$$

where σ_{eU} is the equivalent stress in the original cylinder and σ_{eC} is the equivalent stress in the LTA.

After carrying out some algebraic manipulations, m_d^0 for the corroded pipeline can be expressed as

$$m_d^0 = \sqrt{\frac{\sigma_y^2\ (V_R)}{\sigma_{eU}^2\ V_U + \sigma_{eC}^2\ V_C}} \qquad (3.91)$$

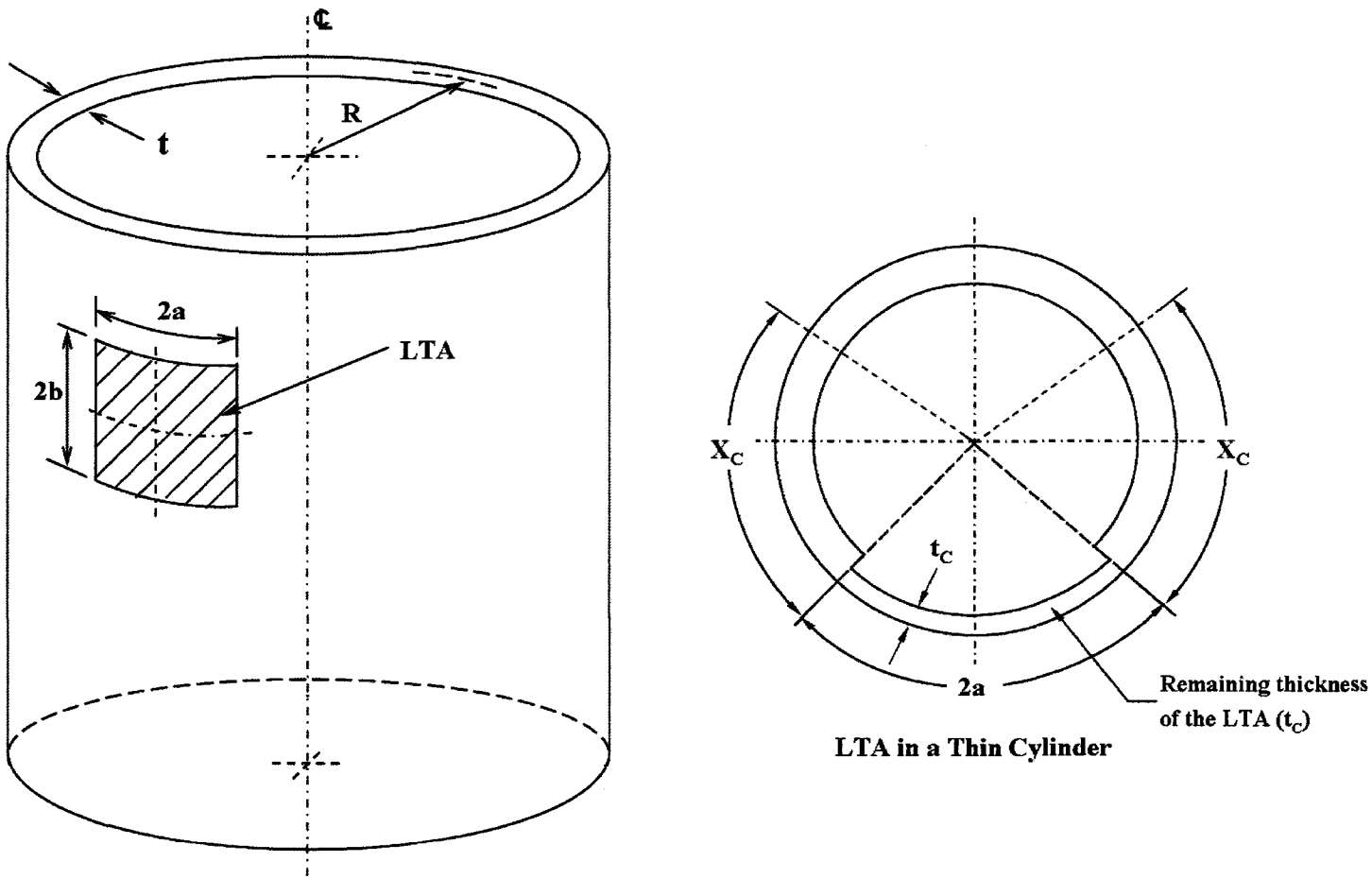

Figure 3.9: LTA in a Thin Cylinder

The lower bound limit load multiplier for the corroded pipeline is given by:

$$m_{\alpha d} = 2m_d^0 \frac{2\left(\frac{m_d^0}{m_{Ld}}\right)^2 + \sqrt{\frac{m_d^0}{m_{Ld}}\left(\frac{m_d^0}{m_{Ld}}-1\right)^2\left(1+\sqrt{2}-\frac{m_d^0}{m_{Ld}}\right)\left(\frac{m_d^0}{m_{Ld}}-1+\sqrt{2}\right)}}{\left(\left(\frac{m_d^0}{m_{Ld}}\right)^2+2-\sqrt{5}\right)\left(\left(\frac{m_d^0}{m_{Ld}}\right)^2+2+\sqrt{5}\right)} \quad (3.92)$$

where $m_{Ld} = \frac{\sigma_y}{\sigma_{eC}}$.

Hence the remaining strength factor (RSF) of the corroded pipeline is given by

$$RSF = \frac{m_{\alpha d}}{m_u^0} \quad (3.93)$$

where $m_u^0 = \frac{\sigma_y}{\sigma_{eU}} = m_L$

The above methodology can be used in conjunction with either the von Mises or the Tresca yield criterion. The "flow stress", defined as the average of the yield stress and equivalent stress at 1% membrane strain, may be used with the Tresca failure criterion as is done in the ASME B31G and other evaluation guidelines to reduce the conservatism.

3.8 Closure

Complete theoretical basis for the Level 2 integrity assessment procedure with reference to literature and earlier research has been outlined in this chapter. Earlier research by Seshadri and Mangalaramanan [20] leads to the development of the m_α

method (which introduced the concept of reference volume in limit analysis) and the application of the integral mean of yield criterion to obtain improved limit load estimates. The work by Reinhardt and Seshadri [25] has provided an expression for the lower bound limit load multiplier m_α, which has been used by Indermohan and Seshadri [27] to determine the limit load of cylinders with internal LTA and thermal hot spots. The application of integral mean of yield criterion has consistently yielded robust and improved estimates of lower bound limit loads. These concepts will be applied in further chapters to determine the RSF and limit load of pipelines with internal and external LTA and will also be shown to provide better prediction when compared with existing ASME B31G criterion, which serves as a basis for the comparison of different criteria and procedures.

CHAPTER 4

ANALYSIS OF CORRODED PIPELINES

4.1 Introduction

Structural analysis requires the concurrent satisfaction of the equilibrium equations, static boundary conditions, strain-displacement relations or compatibility conditions and the kinematic boundary conditions. The stresses and strains are related by approximate material constitutive relationships. Both the equilibrium equations and strain-displacement relations are independent of material property, and need to be satisfied both in the elastic and plastic range. Hence, the difference between elastic and inelastic analysis is the choice of material constitutive relationship, which is linear in elastic range and non-linear in plastic range. The satisfaction of compatibility conditions within the structure demonstrates the continuity of the structure in terms of the main degree of freedom, which is the displacement in structural analysis. Strains can be

determined uniquely in the elastic range from the state of stress, irrespective of how the stress state is reached; whereas determination of strains in the inelastic range requires the knowledge of the loading history. Hence conventional inelastic finite element analysis involves an iterative solution using the Newton-Raphson method.

In this chapter, a detailed parametric study of the pipelines with internal and external corrosion sites has been carried out. Indermohan and Seshadri [27] demonstrated the application of robust limit load solution for internally corroded pipeline with radius to thickness ratio of greater than 50. This method is extended in this thesis to a thicker pipeline with radius to thickness ratio of about 30 with both internal and external corrosion sites. A typical pipeline size made of a generic pipeline steel is chosen for this study. This parametric study involves the computation of the remaining strength factor and the limit pressure of the corroded pipeline of various corrosion configurations. The Level 2 assessment method introduced in the previous chapter is used and comparison of the results with the collapse load obtained from inelastic finite element analysis is carried out. The results are also compared with the ASME B31G criterion, which serves as an industry benchmark for the comparison of all recently developed criteria.

4.2 Finite Element Modeling

The objective of this finite element analysis is to validate the solution obtained by applying the variational method, since FEA remains the most accurate numerical solution that may be obtained for complex engineering problems. Three-dimensional inelastic

finite element analysis incorporating the effect of strain hardening was carried out using ANSYS [28]. Finite element models were created for simulating pipelines containing both internal and external corrosion sites of the same aspect ratio (2a x 2b). The metal loss in corroded pipeline is modeled by a reduced section thickness at the corrosion site, with the other characteristic dimensions being longitudinal and circumferential extent of corrosion. Simplified regular rectangular and square profiles of corrosion were simulated, since the modeling of the highly irregular actual corrosion profiles are extremely difficult. The assumption of uniform depth, rectangular or square corrosion profiles enabled taking advantage of the symmetry by modeling only half of the pipeline circumferentially. Hence, only 180^0 of the pipeline is modeled. The advantage of symmetry is also evident in the longitudinal direction by having the plane of symmetry at the centre of the corrosion. The length of the pipeline is chosen in such a manner that the locations of the boundary conditions do not influence the solution. Accordingly, a longer pipeline is taken.

The three-dimensional solid continuum finite element model was constructed using the eight nodded brick SOLID 185 element. This element has 3 degrees of freedom per node (displacements in X, Y and Z directions) and has enhanced strain formulation to prevent shear locking in bending dominated problems and volumetric locking while simulating nearly incompressible cases. A minimum of four and maximum of six elements were used through the thickness in the corroded region. The maximum number of elements was limited to six to reduce the computational time required for inelastic FEA. The minimum number of elements required across the thickness was chosen on the

basis that the difference in limit load obtained from the current level of refinement to the next higher level is less than or equal to two percent. Since the element that has been used in this study is a linear element without mid-side nodes, more number of elements were needed to simulate the deformation behavior of the thinned area, and the discontinuity regions between the corroded and uncorroded regions of the pipe. Further, such a fine mesh prevents the occurrence of common meshing errors such as the error due to aspect ratio of the elements in the reference volume. A gradually varying mesh was done on the surface of the cylinder with more refinement in the corrosion spot and the regions adjacent to it.

A rate independent plasticity model using the von Mises yield criterion was adopted. A pipeline made of generic pipeline steel such as API 5L Grade A with a yield stress of 30,000 psi was used. An elastic modulus of 30e6 psi and a Poisson's ratio of 0.3 were used. Chouchaoui and Pick [6] have emphasized the importance of considering the strain hardening behavior of the material in predicting the burst strength of the pipe when corrosion geometries are simulated. The effect of strain hardening is included in this analysis to take advantage of the post yield behaviour of high strength pipeline steels. Accordingly, a representative bilinear material model with a plastic modulus of 50e4 psi was assumed. A number of investigators [17, 29-30] have shown that predicting limit load by inelastic FEA using true stress strain curve with ultimate tensile strength as the failure criterion provides a more accurate determination of burst pressure of line pipes close to the experimental results. This essentially follows the ultimate strength design philosophy with the determination of plastic collapse load.

Symmetric boundary conditions existing in this model constrains displacement in two principal directions (X and Z). The other boundary condition (displacement in the third principal direction) is chosen so as provide free expansion when the pipeline is subjected to internal pressure. The iterative solution accounts for the non-linear material behavior beyond yield using incremental application of the loading. Internal pressure and the longitudinal force due to the end-capped condition are applied to one end of the pipe. The load was applied in 200 substeps. More number of substeps will result in better accuracy, but with an increased number of runs. Automatic time stepping has been used to enable ANSYS to invoke the bisection feature if convergence is not achieved. Bisection provides a means of automatically recovering from a convergence failure. This feature will cut a time step size into half whenever equilibrium iterations fail to converge and automatically restart from the last converged substep. If the halved time step again fails to converge, bisection will again cut the time step size and restart, continuing the process until convergence is achieved is reached.

As the LTA is known to yield and fail ahead of the remaining part of the pipe, it is more appropriate to define a local failure criterion for the LTA. The failure of a pipeline subjected to monotonically increasing internal pressure occurs when the pressurized fluid starts to leak through a tear or crack developed through the remaining ligament. It is observed from the finite element analysis that the remaining ligament in the corroded region will bulge and bending effect is seen at the junction to satisfy the continuity of displacements between the corroded and uncorroded parts of the pipe. DePadova and Sims [31] elected to limit the plastic strain to 2% at any location in the LTA in their

analysis using an elastic perfectly plastic material model. It was seen in the previous chapter, API 579 [8] recommends limiting the peak strain at any location of the remaining ligament to 5% when a Level 3 analysis is performed. In the present analysis, the total membrane strain of the LTA is limited to 1% (figure 4.1).

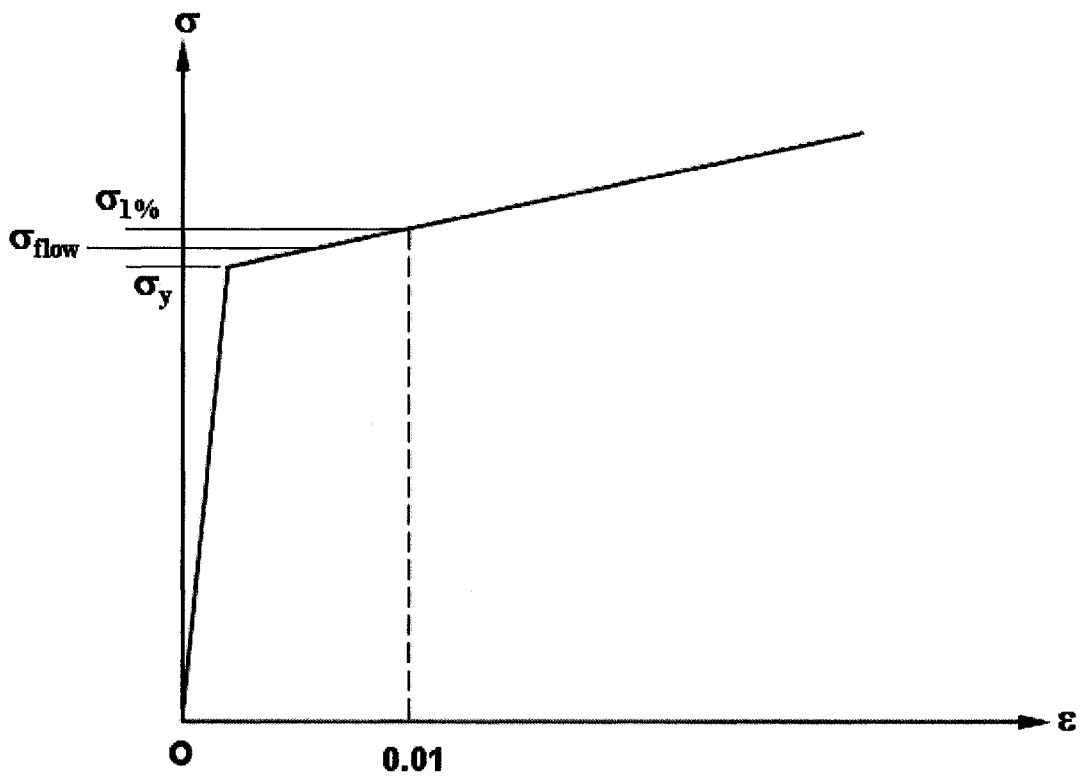

Figure 4.1: Material Model

4.3 Numerical Examples

In this section of the thesis, the estimation of the limit load and remaining strength factor of corroded pipeline with various configurations of the corrosion profile is carried out using the variational method, discussed in the previous chapter. The limit pressure using the variational method is calculated on the basis of three failure criteria: von Mises criterion, Tresca and Tresca with flow stress. The flow stress used in the third criterion as the failure stress level is defined as the average of the yield stress and the stress at 1% strain. The modeling of similar configurations is also done in ANSYS to obtain limit loads for comparison with the analytical solution. Single corrosion profiles are modeled and analyzed since, these serve as the basic configuration for validation. The results are also compared with those obtained by applying the ASME B31G criterion. The pipelines with the internal and external LTA of identical configurations are analyzed so as to obtain a comparison, and define a calculation procedure. The following are the specifications of the line pipe defined in this analysis:

Outer diameter of the pipe (D_0)	-	42 in (1.07 m)
Wall thickness (t)	-	0.625 in (0.016 m)
Operating Pressure (p)	-	600 psi (4.14 MPa)
Yield Stress (σ_y)	-	30 ksi (206.85 MPa)
Elastic Modulus	-	30e6 psi (206.85e3 MPa)
Plastic Modulus	-	50e4 psi (34.5e2 MPa)
Outer radius of the pipe (r_o)	-	21 in (0.533 m)

Inner Radius of the pipe (r_i) - 20.38 in (0.518 m)

Mean Radius of plain pipe (R_m) - 20.69 in (0.526 m)

Decay Lengths:

Longitudinal direction (X_L) - 8.99 in (0.228 m)

Circumferential direction (X_C) - 52.61 in (1.336 m)

The numerical solution procedure using the Level 2 solution based on variational method is demonstrated here for the following configuration of the LTA.

Circumferential extent of corrosion (2a) - 10 in (0.254 m)

Longitudinal extent of corrosion (2b) - 20 in (0.508 m)

Depth of Corrosion (d/t) percent - 25 %

Depth of corrosion d = 0.25 (t) - 0.16 in (0.004 m)

Remaining wall thickness (t_C) = t – d - 0.47 in (0.012 m)

Volume of the LTA (V_C) - 93.75 in^3 (0.002 m^3)

Uncorroded volume (V_U) - 2610.03 in^3 (0.043 m^3)

Reference volume (V_R) - 2703.78 in^3 (0.044 m^3)

4.3.1 Pipeline with Internal LTA

Pipelines with single internal LTA are simulated to give the limit load at 1 % membrane strain. The finite element model showing a typical mesh used in this analysis is shown in figure 4.2. The results obtained by using different methods and criteria for

pipeline with various configurations of the internal LTA are shown in Table 4.1. The numerical calculation procedure for the Level 2 assessment is as shown below:

Calculation Procedure:

Inner Radius of corrosion (R_{iC}) = r_i + d = 20.53 in (0.521 m)

von Mises Yield Criterion:

Stresses in the uncorroded pipe:

Hoop Stress: $\sigma_{\theta U} = \frac{p R_m}{t}$ = 19860 psi (136.93 MPa)

Longitudinal Stress: $\sigma_{\varphi U} = \frac{p R_m}{2t}$ = 9930 psi (68.46 MPa)

Equivalent Stress: $\sigma_{eU} = \sqrt{\sigma_{\theta U}^2 + \sigma_{\varphi U}^2 - \sigma_{\theta U}\,\sigma_{\varphi U}}$ = 17199.26 psi (118.58 MPa)

Stresses in the LTA:

Hoop Stress: $\sigma_{\theta C} = \frac{p R_{iC}}{t_C}$ = 26280 psi (181.19 MPa)

Longitudinal Stress: $\sigma_{\varphi C} = \frac{p R_{iC}}{2 t_C}$ = 13140 psi (90.60 MPa)

Equivalent Stress: $\sigma_{eC} = \sqrt{\sigma_{\theta C}^2 + \sigma_{\varphi C}^2 - \sigma_{\theta C}\,\sigma_{\varphi C}}$ = 22759.15 psi (156.92 MPa)

Multipliers:

$$m_u^0 = \frac{\sigma_y}{\sigma_{eU}} = 1.74$$

$$m_d^0 = \sqrt{\frac{\sigma_y^2 \ (V_R)}{\sigma_{eU}^2 \ V_U + \sigma_{eC}^2 \ V_C}} = 1.72$$

$$m_{Ld} = \frac{\sigma_y}{\sigma_{eC}} = 1.32$$

$$m_{\alpha d} = 2 m_d^0 \frac{2\left(\frac{m_d^0}{m_{Ld}}\right)^2 + \sqrt{\frac{m_d^0}{m_{Ld}}\left(\frac{m_d^0}{m_{Ld}} - 1\right)^2 \left(1 + \sqrt{2} - \frac{m_d^0}{m_{Ld}}\right)\left(\frac{m_d^0}{m_{Ld}} - 1 + \sqrt{2}\right)}}{\left(\left(\frac{m_d^0}{m_{Ld}}\right)^2 + 2 - \sqrt{5}\right)\left(\left(\frac{m_d^0}{m_{Ld}}\right)^2 + 2 + \sqrt{5}\right)}$$

$$= 1.54$$

$$RSF = \frac{m_{\alpha d}}{m_u^0} = 0.88$$

Limit Pressure $P_L = (m_{\alpha d})(p) = 921.35$ psi (6.35 MPa)

Tresca Criterion:

$$\sigma_{eU} = \sigma_{\theta U} = 19860 \text{ psi } (136.93 \text{ MPa})$$

$$\sigma_{eC} = \sigma_{\theta C} = 26280 \text{ psi } (181.19 \text{ MPa})$$

$$m_u^0 = \frac{\sigma_y}{\sigma_{eU}} = 1.51$$

$$m_d^0 = \sqrt{\frac{\sigma_y^2 \ (V_R)}{\sigma_{eU}^2 \ V_U + \sigma_{eC}^2 \ V_C}} = 1.49$$

$$m_{Ld} = \frac{\sigma_y}{\sigma_{eC}} = 1.14$$

$$m_{\alpha d} = 2m_d^0 \frac{2\left(\frac{m_d^0}{m_{Ld}}\right)^2 + \sqrt{\frac{m_d^0}{m_{Ld}}\left(\frac{m_d^0}{m_{Ld}} - 1\right)^2 \left(1 + \sqrt{2} - \frac{m_d^0}{m_{Ld}}\right)\left(\frac{m_d^0}{m_{Ld}} - 1 + \sqrt{2}\right)}}{\left(\left(\frac{m_d^0}{m_{Ld}}\right)^2 + 2 - \sqrt{5}\right)\left(\left(\frac{m_d^0}{m_{Ld}}\right)^2 + 2 + \sqrt{5}\right)}$$

$$= 1.33$$

$$\text{RSF} = \frac{m_{\alpha d}}{m_u^0} = 0.88$$

$$\text{Limit Pressure } P_L = (m_{\alpha d})(p) = 797.91 \text{ psi } (5.50 \text{ MPa})$$

Tresca Criterion with flow stress:

$$\sigma_{flow} = \frac{\sigma_y + (\sigma_e)_{1\% strain}}{2} = 32250 \text{ psi } (222.36 \text{ MPa})$$

$\sigma_{eU} = \sigma_{\theta U} = 19860$ psi (136.93 MPa)

$\sigma_{eC} = \sigma_{\theta C} = 26280$ psi (181.19 MPa)

$$m_u^0 = \frac{\sigma_{flow}}{\sigma_{eU}} = 1.62$$

$$m_d^0 = \sqrt{\frac{\sigma_{flow}^2 \ (V_R)}{\sigma_{eU}^2 \ V_U + \sigma_{eC}^2 \ V_C}} = 1.60$$

$$m_{Ld} = \frac{\sigma_{flow}}{\sigma_{eC}} = 1.23$$

$$m_{\alpha d} = 2m_d^0 \frac{2\left(\frac{m_d^0}{m_{Ld}}\right)^2 + \sqrt{\frac{m_d^0}{m_{Ld}}\left(\frac{m_d^0}{m_{Ld}} - 1\right)^2\left(1 + \sqrt{2} - \frac{m_d^0}{m_{Ld}}\right)\left(\frac{m_d^0}{m_{Ld}} - 1 + \sqrt{2}\right)}}{\left(\left(\frac{m_d^0}{m_{Ld}}\right)^2 + 2 - \sqrt{5}\right)\left(\left(\frac{m_d^0}{m_{Ld}}\right)^2 + 2 + \sqrt{5}\right)}$$

$= 1.43$

RSF = 0.95

Limit Pressure $P_L = (m_{\alpha d})(p) = 857.75$ psi (5.91 MPa)

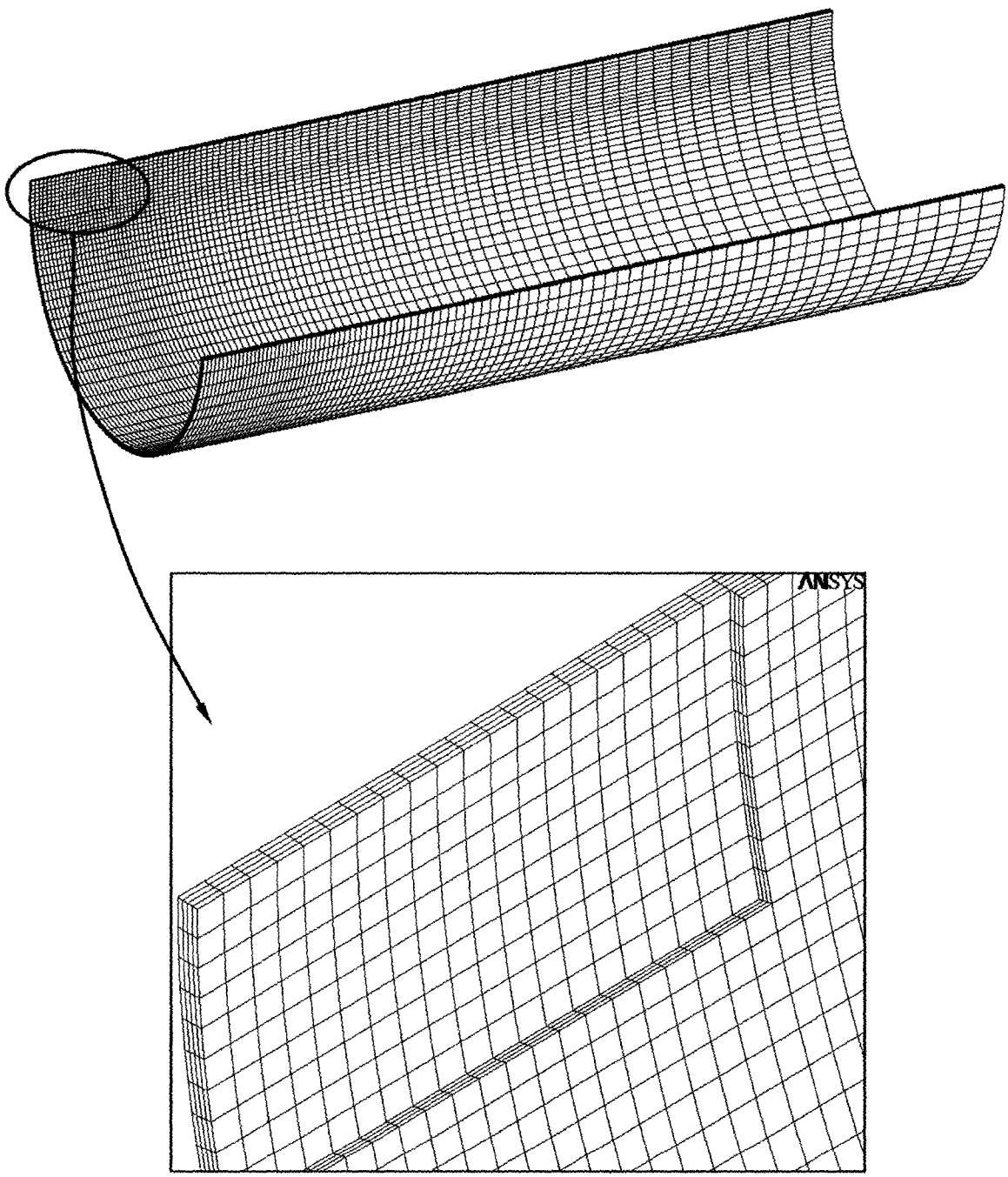

Figure 4.2: Typical Mesh of Internal Corrosion Model

Table 4.1: Results for Pipe with Internal Corrosion

Corrosion Geometry			Inelastic FEA		ASME B31G		m_α (von Mises)		m_α (Tresca)		m_α (Tresca & σ_f)	
2a	2b	% Depth of Corrosion	RSF	P_L	RSF	P_L	RSF	P_L	RSF	P_L	RSF	P_L
10	10	10	1.00	1047.30	1.00	892.86	0.97	1012.33	0.97	876.70	1.00	942.46
10	10	20	1.00	1045.50	1.00	892.86	0.92	957.68	0.92	829.37	0.98	891.57
10	10	25	0.97	1012.00	1.00	892.48	0.88	922.94	0.88	799.29	0.95	859.24
10	10	30	0.92	961.00	0.98	872.56	0.84	882.26	0.84	764.06	0.91	821.36
10	10	35	0.87	914.50	0.95	851.90	0.80	834.73	0.80	722.90	0.86	777.12
10	10	40	0.83	870.00	0.93	830.44	0.74	779.36	0.74	674.95	0.80	725.57
10	10	50	0.72	752.00	0.88	784.98	0.61	639.89	0.61	554.16	0.66	595.72
20	10	10	1.00	1047.30	1.00	892.86	0.97	1010.82	0.97	875.39	1.00	941.05
20	10	20	0.97	1017.00	1.00	892.86	0.91	955.03	0.91	827.08	0.98	889.11
20	10	25	0.93	974.00	1.00	892.48	0.88	920.10	0.88	796.83	0.95	856.59
20	10	30	0.88	919.50	0.98	872.56	0.84	879.54	0.84	761.71	0.90	818.83
20	10	35	0.83	865.50	0.95	851.90	0.80	832.54	0.80	721.00	0.86	775.07
20	10	40	0.78	817.50	0.93	830.44	0.74	778.17	0.74	673.91	0.80	724.46
20	10	50	0.66	695.50	0.88	784.98	0.61	642.78	0.61	556.66	0.66	598.41
10	20	10	1.00	1047.30	1.00	892.86	0.97	1011.48	0.97	875.97	1.00	941.66
10	20	20	0.94	987.00	0.99	883.68	0.91	956.19	0.91	828.09	0.98	890.19
10	20	25	0.90	942.70	0.96	857.88	0.88	921.35	0.88	797.91	0.95	857.75
10	20	30	0.84	883.00	0.93	831.58	0.84	880.74	0.84	762.74	0.90	819.95
10	20	35	0.79	827.70	0.90	804.75	0.80	833.51	0.80	721.84	0.86	775.98
10	20	40	0.74	771.00	0.87	777.40	0.74	778.72	0.74	674.39	0.80	724.97
10	20	50	0.62	648.50	0.81	721.04	0.61	641.59	0.61	555.63	0.66	597.31

4.3.2 Pipeline with External LTA

Externally corroded pipeline with a single corrosion site is simulated to give the limit load at 1% membrane strain. The finite element model showing a typical mesh used in this analysis is shown in Figure 4.3. The results obtained by using different solution methods and criterion for pipeline with various configurations of the internal LTA are shown in Table 4.2. The numerical calculation procedure for the Level 2 assessment is as shown below:

Calculation Procedure:

Outer Radius of corrosion (R_{oC}) = $r_i + t_C$ = 20.84 in (0.529 m)

von Mises Yield Criterion

Stresses in the uncorroded pipe:

Hoop Stress: $\sigma_{\theta U} = \frac{p R_m}{t}$ = 19860 psi (136.93 MPa)

Longitudinal Stress: $\sigma_{\varphi U} = \frac{p R_m}{2t}$ = 9930 psi (68.46 MPa)

Equivalent Stress: $\sigma_{eU} = \sqrt{\sigma_{\theta U}^2 + \sigma_{\varphi U}^2 - \sigma_{\theta U}\,\sigma_{\varphi U}}$ = 17199.26 psi (118.58 MPa)

Stresses in the LTA:

Hoop Stress: $\sigma_{\theta C} = \dfrac{p\,R_{oC}}{t_C} = 26680$ psi (183.95 MPa)

Longitudinal Stress: $\sigma_{\varphi C} = \dfrac{p\,R_{oC}}{2\,t_C} = 13340$ psi (91.98 MPa)

Equivalent Stress: $\sigma_{eC} = \sqrt{\sigma_{\theta C}^2 + \sigma_{\varphi C}^2 - \sigma_{\theta C}\,\sigma_{\varphi C}} = 23105.56$ psi (159.31 MPa)

Multipliers:

$$m_u^0 = \frac{\sigma_y}{\sigma_{eU}} = 1.74$$

$$m_d^0 = \sqrt{\frac{\sigma_y^2\ (V_R)}{\sigma_{eU}^2\ V_U + \sigma_{eC}^2\ V_C}} = 1.72$$

$$m_{Ld} = \frac{\sigma_y}{\sigma_{eC}} = 1.30$$

$$m_{\alpha d} = 2m_d^0 \frac{2\left(\dfrac{m_d^0}{m_{Ld}}\right)^2 + \sqrt{\dfrac{m_d^0}{m_{Ld}}\left(\dfrac{m_d^0}{m_{Ld}} - 1\right)^2\left(1 + \sqrt{2} - \dfrac{m_d^0}{m_{Ld}}\right)\left(\dfrac{m_d^0}{m_{Ld}} - 1 + \sqrt{2}\right)}}{\left(\left(\dfrac{m_d^0}{m_{Ld}}\right)^2 + 2 - \sqrt{5}\right)\left(\left(\dfrac{m_d^0}{m_{Ld}}\right)^2 + 2 + \sqrt{5}\right)}$$

$$= 1.52$$

$$RSF = \frac{m_{\alpha d}}{m_u^0} = 0.87$$

Limit Pressure $P_L = (m_{\alpha d})(p) = 912.87$ psi (6.29 MPa)

Tresca Criterion:

$\sigma_{eU} = \sigma_\theta = 19860$ psi (136.93 MPa)

$\sigma_{eC} = \sigma_{\theta C} = 26680$ psi (183.95 MPa)

$$m_u^0 = \frac{\sigma_y}{\sigma_{eU}} = 1.51$$

$$m_d^0 = \sqrt{\frac{\sigma_y^2 \ (V_R)}{\sigma_{eU}^2 \ V_U + \sigma_{eC}^2 \ V_C}} = 1.49$$

$$m_{Ld} = \frac{\sigma_y}{\sigma_{eC}} = 1.12$$

$$m_{\alpha d} = 2m_d^0 \frac{2\left(\frac{m_d^0}{m_{Ld}}\right)^2 + \sqrt{\frac{m_d^0}{m_{Ld}}\left(\frac{m_d^0}{m_{Ld}} - 1\right)^2 \left(1 + \sqrt{2} - \frac{m_d^0}{m_{Ld}}\right)\left(\frac{m_d^0}{m_{Ld}} - 1 + \sqrt{2}\right)}}{\left(\left(\frac{m_d^0}{m_{Ld}}\right)^2 + 2 - \sqrt{5}\right)\left(\left(\frac{m_d^0}{m_{Ld}}\right)^2 + 2 + \sqrt{5}\right)}$$

$= 1.32$

RSF = 0.87

Limit Pressure $P_L = (m_{\alpha d})(p) = 790.57$ psi (5.45 MPa)

Tresca Criterion with flow stress:

$$\sigma_{flow} = \frac{\sigma_y + (\sigma_e)_{1\% \text{ Strain}}}{2} = 32250 \text{ psi } (222.36 \text{ MPa})$$

$$\sigma_{eU} = \sigma_{\theta U} = 19860 \text{ psi } (136.93 \text{ MPa})$$

$$\sigma_{eC} = \sigma_{\theta C} = 26680 \text{ psi } (183.95 \text{ MPa})$$

$$m_u^0 = \frac{\sigma_{flow}}{\sigma_{eU}} = 1.62$$

$$m_d^0 = \sqrt{\frac{\sigma_{flow}^2 (V_R)}{\sigma_{eU}^2 V_U + \sigma_{eC}^2 V_C}} = 1.60$$

$$m_{Ld} = \frac{\sigma_{flow}}{\sigma_{eC}} = 1.21$$

$$m_{ad} = 1.42$$

RSF = 0.94

Limit Pressure $P_L = (m_{ad})(p) = 849.86$ psi (5.86 MPa)

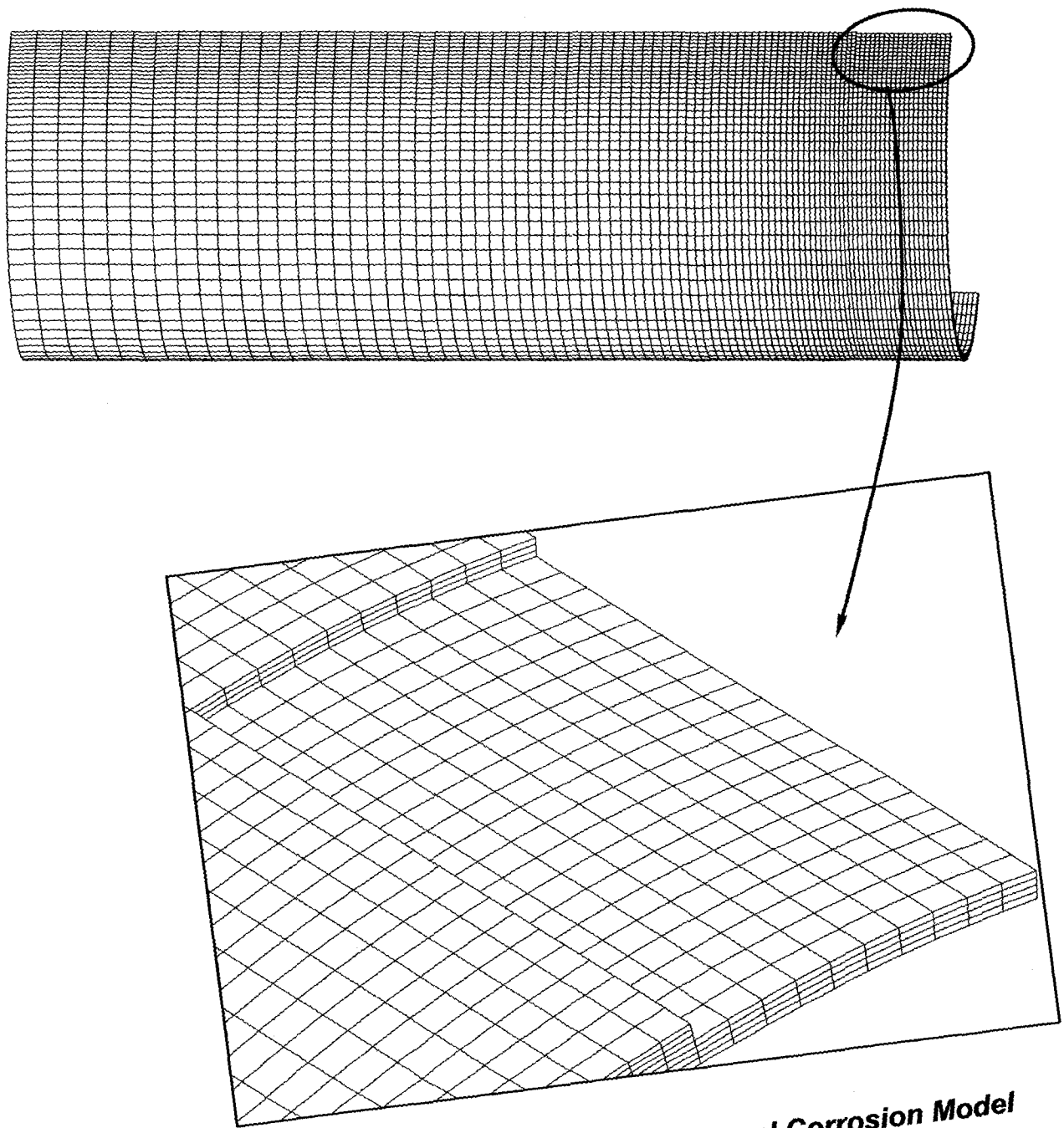

Figure 4.3: Typical Mesh of External Corrosion Model

Table 4.2: Results for Pipe with External Corrosion

Corrosion Geometry			Inelastic FEA		ASME B31G		m_α (von Mises)		m_α (Tresca)		m_α (Tresca & σ_f)	
2a	2b	% Depth of Corrosion	RSF	P_L	RSF	P_L	RSF	P_L	RSF	P_L	RSF	P_L
10	10	10.00	1.00	1047.30	1.00	892.86	0.96	1002.28	0.96	868.00	1.00	933.10
10	10	20.00	0.96	1003.00	1.00	892.86	0.91	948.42	0.91	821.36	0.97	882.96
10	10	25.00	0.91	958.00	1.00	892.48	0.87	914.49	0.87	791.97	0.94	851.37
10	10	30.00	0.87	910.00	0.98	872.56	0.84	874.89	0.84	757.68	0.90	814.50
10	10	35.00	0.82	859.75	0.95	851.90	0.79	828.76	0.79	717.73	0.85	771.56
10	10	40.00	0.77	806.25	0.93	830.44	0.74	775.09	0.74	671.25	0.80	721.59
10	10	50.00	0.66	687.00	0.88	784.98	0.61	639.89	0.61	554.16	0.66	595.72
20	10	10.00	1.00	1047.30	1.00	892.86	0.96	1000.43	0.96	866.40	1.00	931.38
20	10	20.00	0.94	985.00	1.00	892.86	0.90	945.65	0.90	818.96	0.97	880.38
20	10	25.00	0.90	937.80	1.00	892.48	0.87	911.60	0.87	789.47	0.94	848.68
20	10	30.00	0.85	885.00	0.98	872.56	0.83	872.20	0.83	755.35	0.90	812.00
20	10	35.00	0.80	833.00	0.95	851.90	0.79	826.63	0.79	715.89	0.85	769.58
20	10	40.00	0.74	777.00	0.93	830.44	0.74	773.99	0.74	670.29	0.80	720.56
20	10	50.00	0.63	662.50	0.88	784.98	0.61	642.78	0.61	556.66	0.66	598.41
10	20	10.00	1.00	1047.30	1.00	892.86	0.96	1001.24	0.96	867.10	1.00	932.13
10	20	20.00	0.92	964.00	0.99	883.68	0.90	946.87	0.90	820.01	0.97	881.51
10	20	25.00	0.87	909.50	0.96	857.88	0.87	912.87	0.87	790.57	0.94	849.86
10	20	30.00	0.81	852.00	0.93	831.58	0.83	873.39	0.83	756.37	0.90	813.10
10	20	35.00	0.76	795.00	0.90	804.75	0.79	827.58	0.79	716.71	0.85	770.46
10	20	40.00	0.70	735.00	0.87	777.40	0.74	774.50	0.74	670.73	0.80	721.04
10	20	50.00	0.59	618.50	0.81	721.04	0.61	641.59	0.61	555.63	0.66	597.31

4.4 Analysis of Pipelines with Irregular Corrosion Profiles

The development of Level 2 assessment procedures by taking into account the actual profile is difficult because of the numerous variables controlling the behavior of the LTA. Therefore, a few approximations may be made in order to obtain acceptable and conservative predictions of the remaining strength factor and limit pressure using Level 2 procedures for these pipelines. The approximation of the corroded volume enables the application of variational method used in the previous sections for the analysis of pipelines with irregular metal loss. The irregular area of metal loss (on the surface of the pipe) may be approximated by regular shapes such as rectangles enclosing the actual corroded area (figure 4.4). A more accurate approximation of the actual corroded area may be made by dividing the actual metal loss area into finite segments.

Although this method of approximation seems tedious, the more the number of finite segments involved in the approximation the more accurate will be the estimation of the area, and less conservative estimate of the remaining strength and limit pressure. The maximum depth of corrosion can be taken in the evaluation of the corroded volume, leading to conservative results. If the variation of the depth of the corrosion is less, the average thickness may also be assumed. Further study needs to be carried out in order to validate these assumptions.

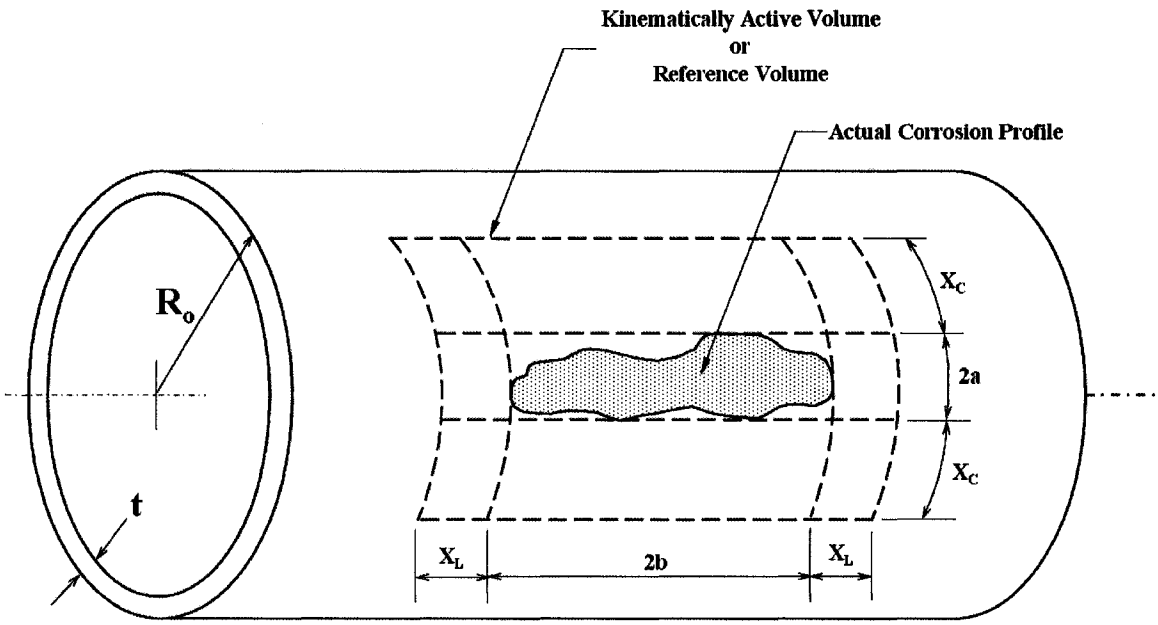

Figure 4.4: Approximation of Actual Corroded Area

4.5 Results and Discussion

Figures 4.5 (a) and 4.5 (b) show the radial displacement plots in the longitudinal and circumferential directions obtained from inelastic FEA at 1% strain for pipe with LTA of aspect ratio 1:2 and certain depths of metal loss. The decay lengths obtained from equation (3.74) are shown in the figures 4.5 (a) and (b) and compared with the inelastic FEA results. It can be seen from the figures that the LTA does not have much influence on the behaviour of the pipe beyond the calculated decay distances X_L and X_C. Hence this serves as a validation of the reference volume concept, which identifies the "kinematically active volume". Similar curves can be generated for pipes with various configurations of LTA.

The remaining strength factor (RSF) for different configurations of internal and external corrosion in a pipeline is presented in figure 4.6. Though the remaining strength factor and limit pressure depend directly on the actual size of the corrosion spot, FE modeling was done for three different aspect ratios to have a basis for the comparison of the results and understand the influence of various variables through this parametric study and validation. The results of RSF based on the m_α method has been compared with inelastic FEA, for corrosion depths up to half the wall thickness. It can be seen that the RSF calculated by the m_α method based on von Mises criterion gives lower bound estimates when compared to the inelastic FEA for all configurations of internal corrosion and most configurations of external corrosion. Beyond the 25% depth of corrosion, the RSF is a slight upper bound in the case of externally corroded pipe with aspect ratio of 1:2. It appears from our study that the RSF implied by ASME B31G points to an underestimation of the corrosion damage. More studies should be carried out to confirm this trend.

The plots of limit pressure for various configurations of internal and external corrosion are shown in Figures 4.7 (a)–(c) and Figures 4.8 (a)–(c). The results are plotted in order to compare the limit pressure obtained from the variational method with inelastic FEA and ASME B31G criterion. Improved estimation of limit pressures is obtained by the m_α method with von Mises yield criterion when compared with the ASME B31G criterion for corrosion configurations with less axial extent (aspect ratios 1:1 and 2:1) and up to 30% depth of metal loss. ASME B31G is found to underestimate the residual strength of the pipe and limit pressure when the length of corrosion is increased (aspect

ratio 1:2). This is due to the absence of the term involving the length of corrosion in equation (2.11) used for the assessment. Hence beyond a certain length of corrosion, ASME B31G value will predict the same RSF and limit pressure. Applying Tresca yield criterion in conjunction with the variational method yields a conservative estimate. Prediction of limit pressure by the m_α method is found to be conservative when compared with inelastic FEA for all configurations of internal corrosion and most configurations of external corrosion. It can also be observed from the plots that the residual strength, and hence the limit pressure of externally corroded pipeline, is less than that of the internally corroded pipeline with the same corrosion geometry.

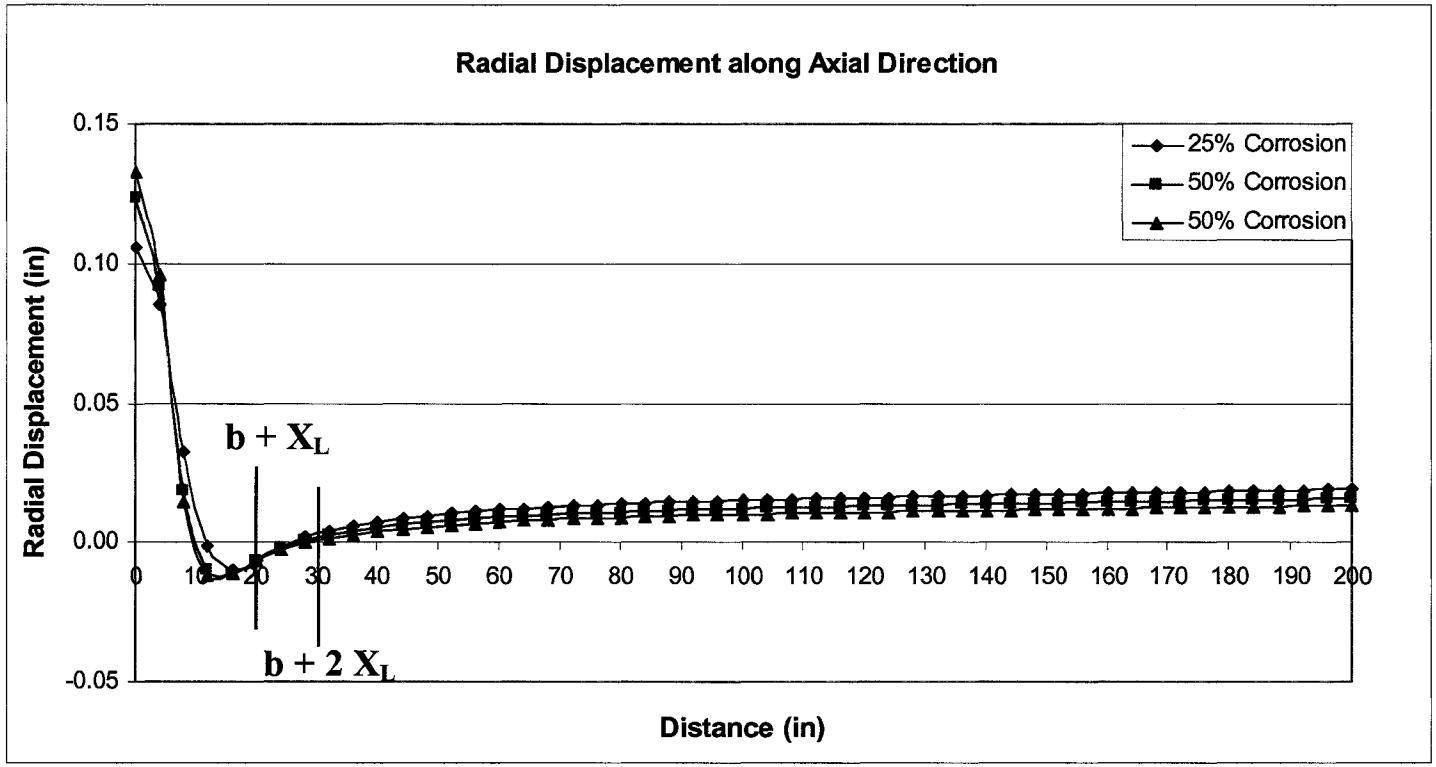
Radial Displacement along Axial Direction
Radial Displacement (in)
0.15
0.10
0.05
0.00
-0.05
0
10
20
30
40
50
60
70
80
90
100
110
120
130
140
150
160
170
180
190
200
Distance (in)
25% Corrosion
50% Corrosion
50% Corrosion
b + X_L
b + 2 X_L

Figure 4.5 (a)

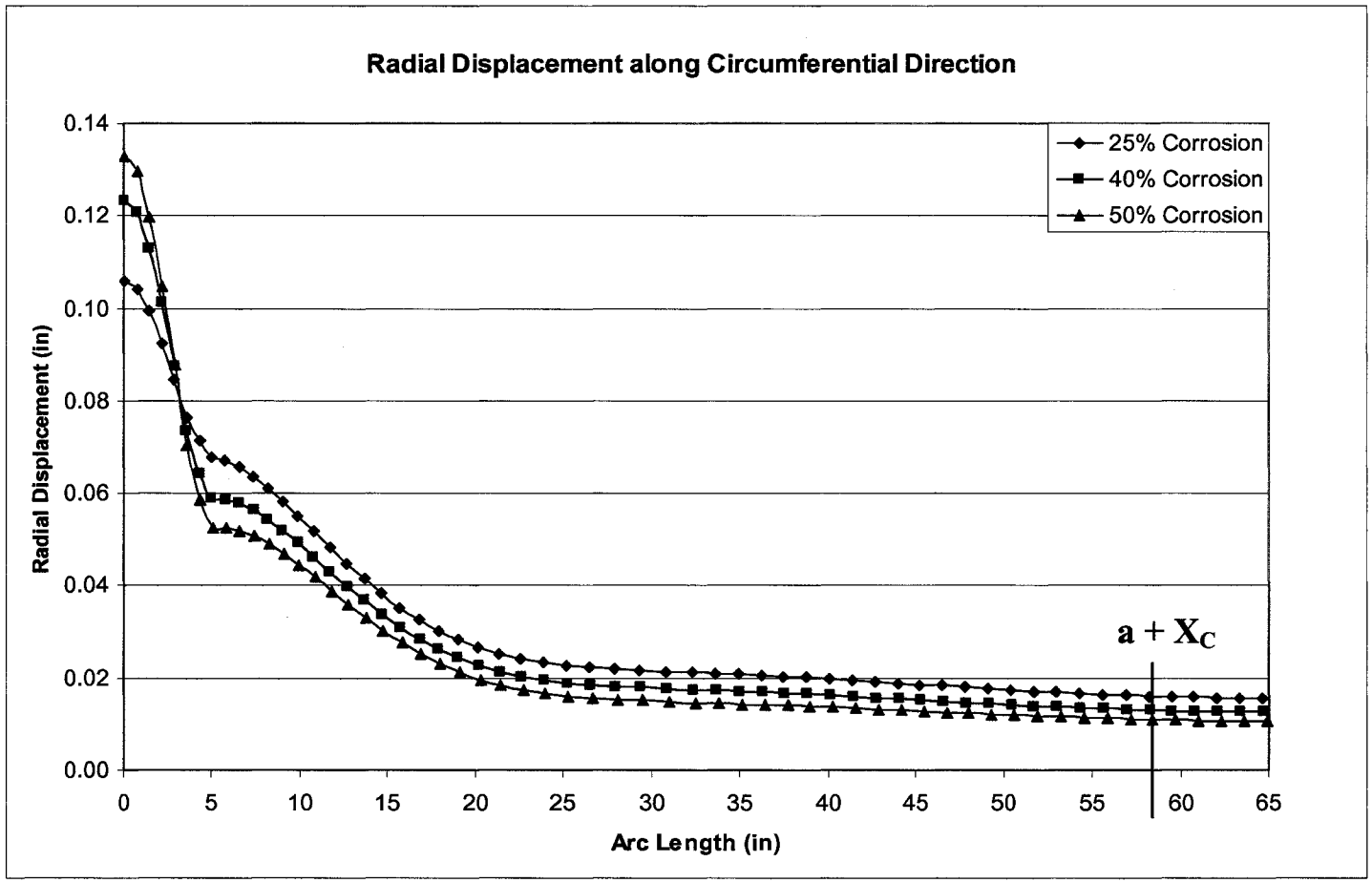
Radial Displacement along Circumferential Direction
Radial Displacement (in)
0.14
0.12
0.10
0.08
0.06
0.04
0.02
0.00
0
5
10
15
20
25
30
35
40
45
50
55
60
65
Arc Length (in)
25% Corrosion
40% Corrosion
50% Corrosion
a + Xc

Figure 4.5 (b)

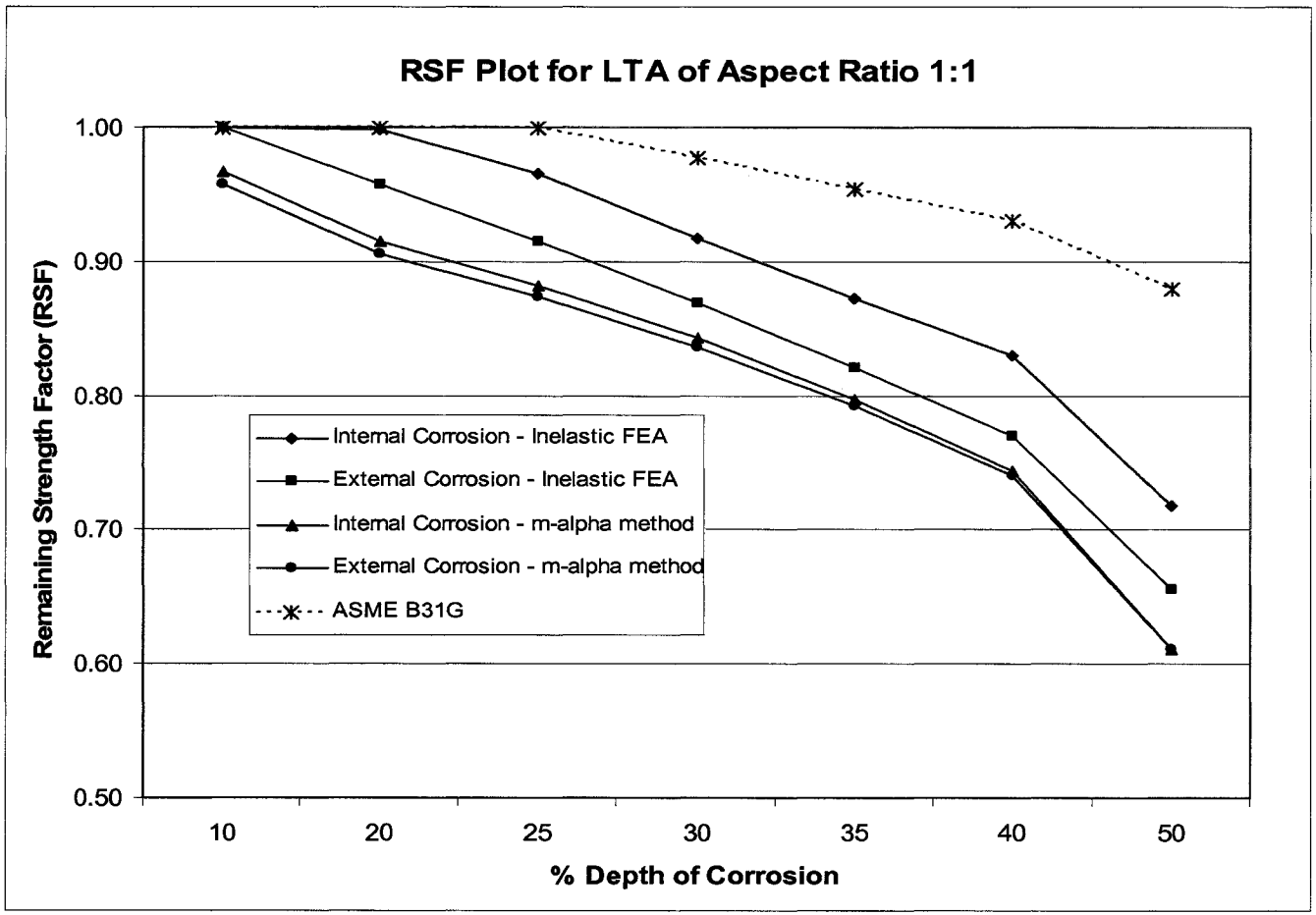
RSF Plot for LTA of Aspect Ratio 1:1
Remaining Strength Factor (RSF)
1.00
0.90
0.80
0.70
0.60
0.50
10
20
25
30
35
40
50
% Depth of Corrosion
Internal Corrosion - Inelastic FEA
External Corrosion - Inelastic FEA
Internal Corrosion - m-alpha method
External Corrosion - m-alpha method
ASME B31G

Figure 4.6 (a)

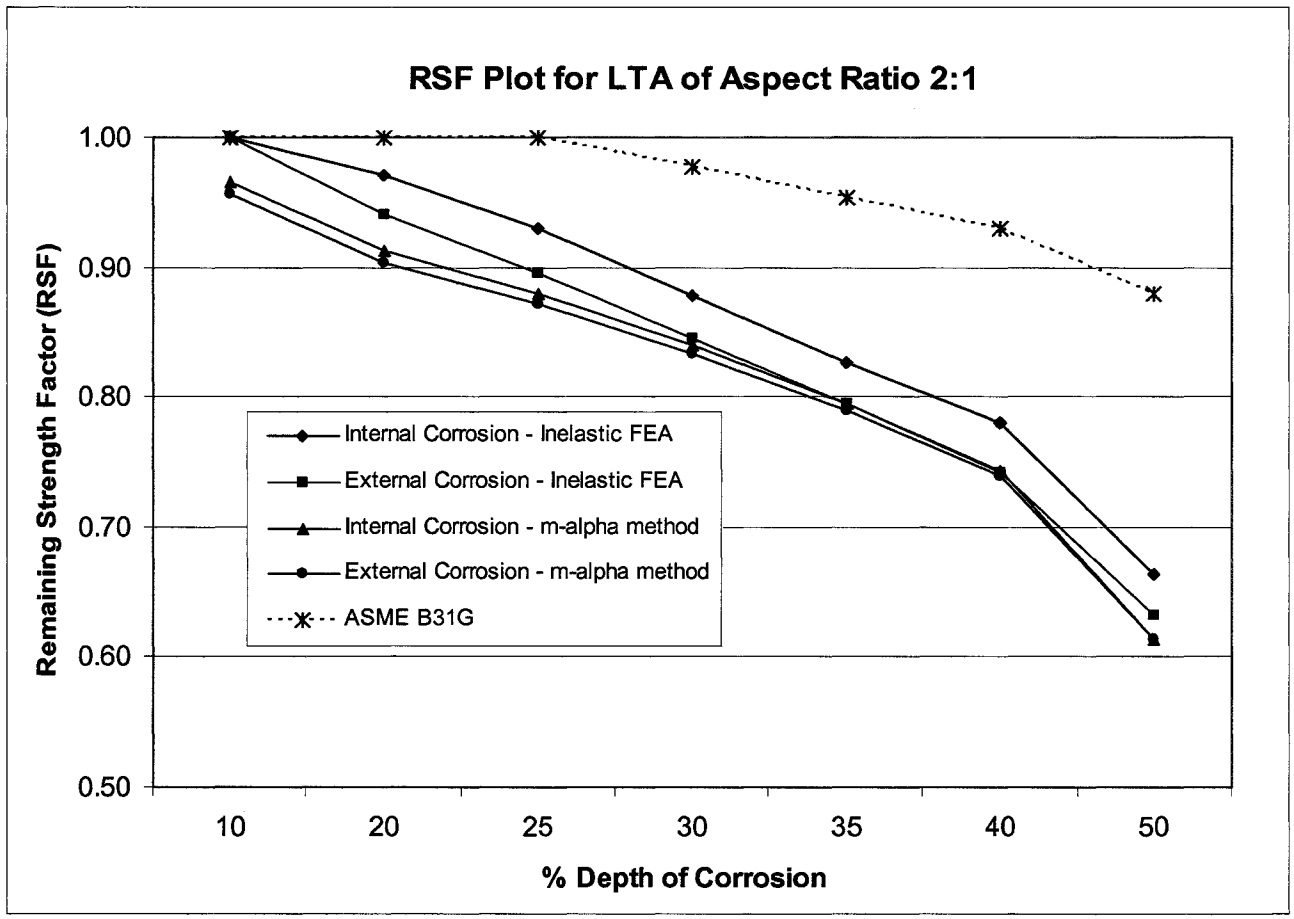
RSF Plot for LTA of Aspect Ratio 2:1
Remaining Strength Factor (RSF)
1.00
0.90
0.80
0.70
0.60
0.50
10
20
25
30
35
40
50
% Depth of Corrosion
Internal Corrosion - Inelastic FEA
External Corrosion - Inelastic FEA
Internal Corrosion - m-alpha method
External Corrosion - m-alpha method
ASME B31G

Figure 4.6 (b)

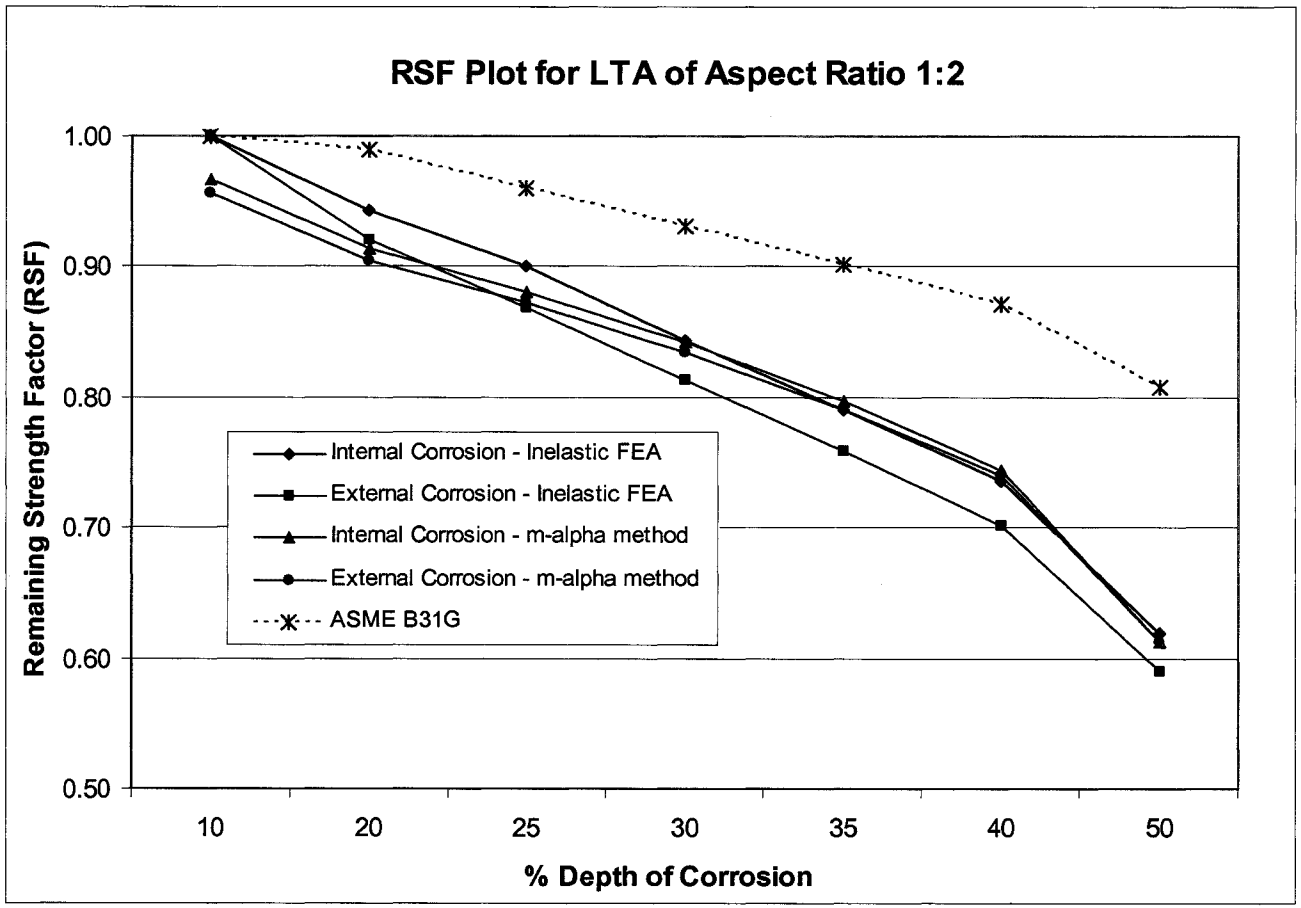
RSF Plot for LTA of Aspect Ratio 1:2
Remaining Strength Factor (RSF)
1.00
0.90
0.80
0.70
0.60
0.50
10
20
25
30
35
40
50
% Depth of Corrosion
Internal Corrosion - Inelastic FEA
External Corrosion - Inelastic FEA
Internal Corrosion - m-alpha method
External Corrosion - m-alpha method
ASME B31G

Figure 4.6 (c)

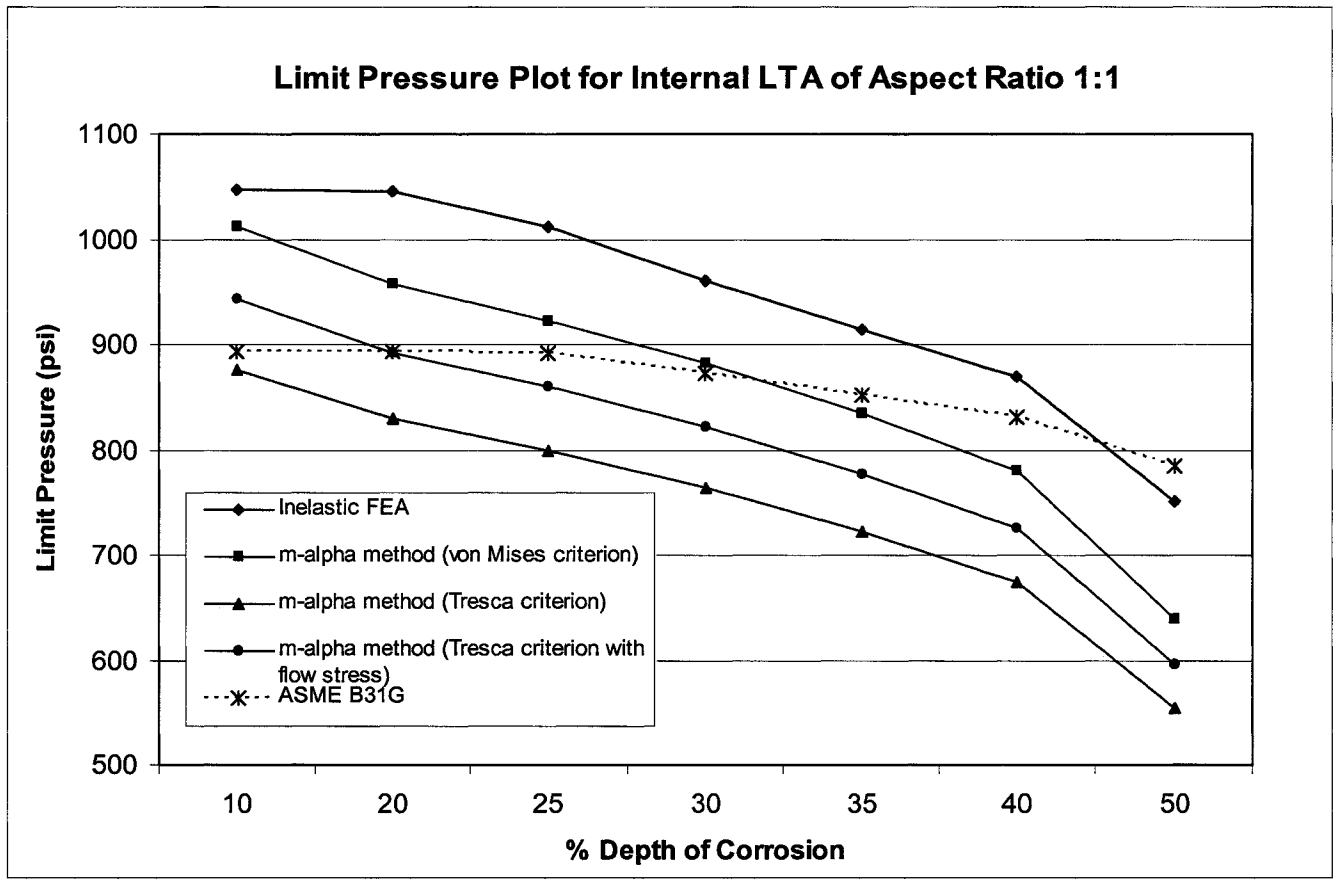
Limit Pressure Plot for Internal LTA of Aspect Ratio 1:1
Limit Pressure (psi)
1100
1000
900
800
700
600
500
10
20
25
30
35
40
50
% Depth of Corrosion
Inelastic FEA
m-alpha method (von Mises criterion)
m-alpha method (Tresca criterion)
m-alpha method (Tresca criterion with flow stress)
ASME B31G

Figure 4.7 (a)

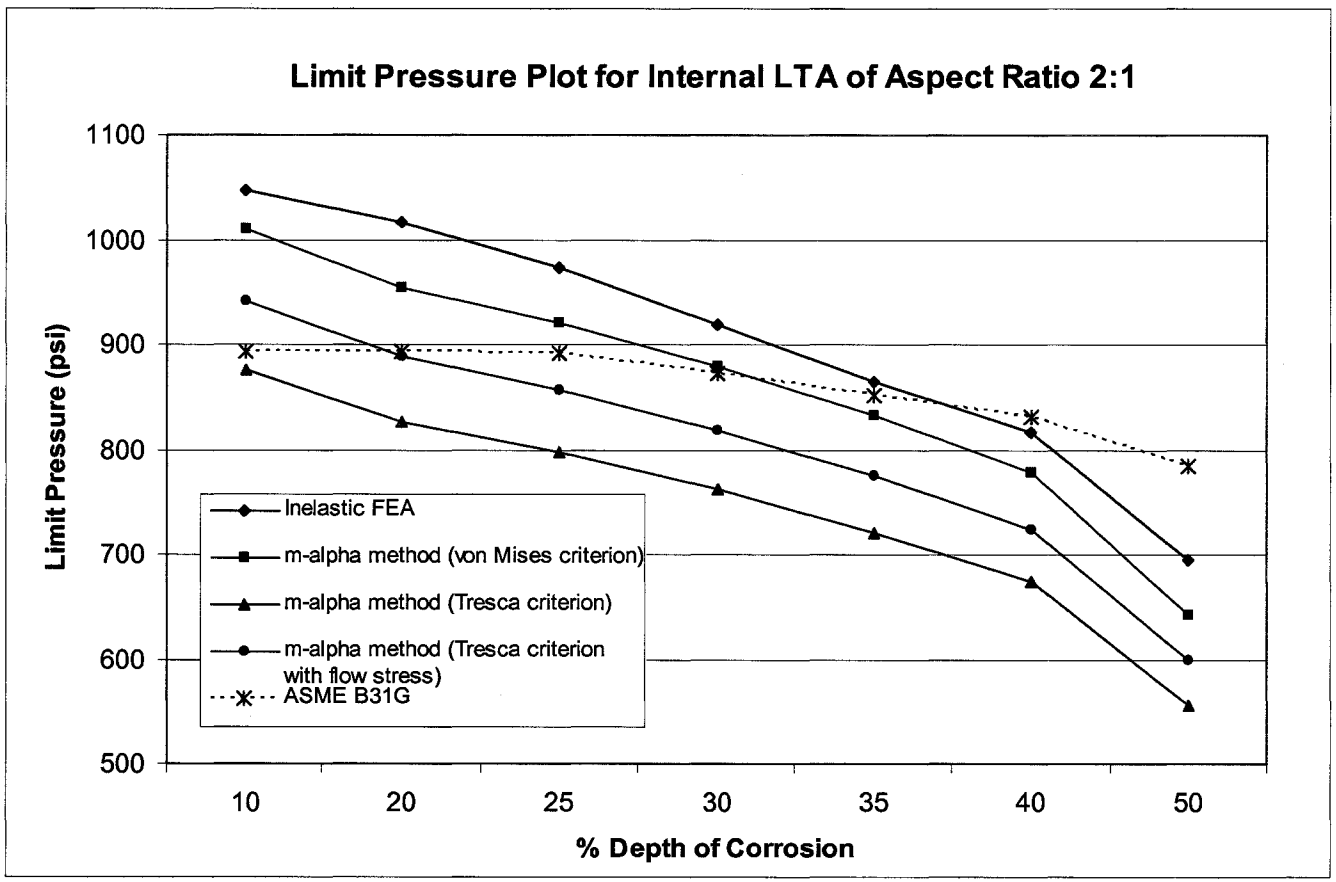
Limit Pressure Plot for Internal LTA of Aspect Ratio 2:1
Limit Pressure (psi)
1100
1000
900
800
700
600
500
10
20
25
30
35
40
50
% Depth of Corrosion
Inelastic FEA
m-alpha method (von Mises criterion)
m-alpha method (Tresca criterion)
m-alpha method (Tresca criterion with flow stress)
ASME B31G

Figure 4.7 (b)

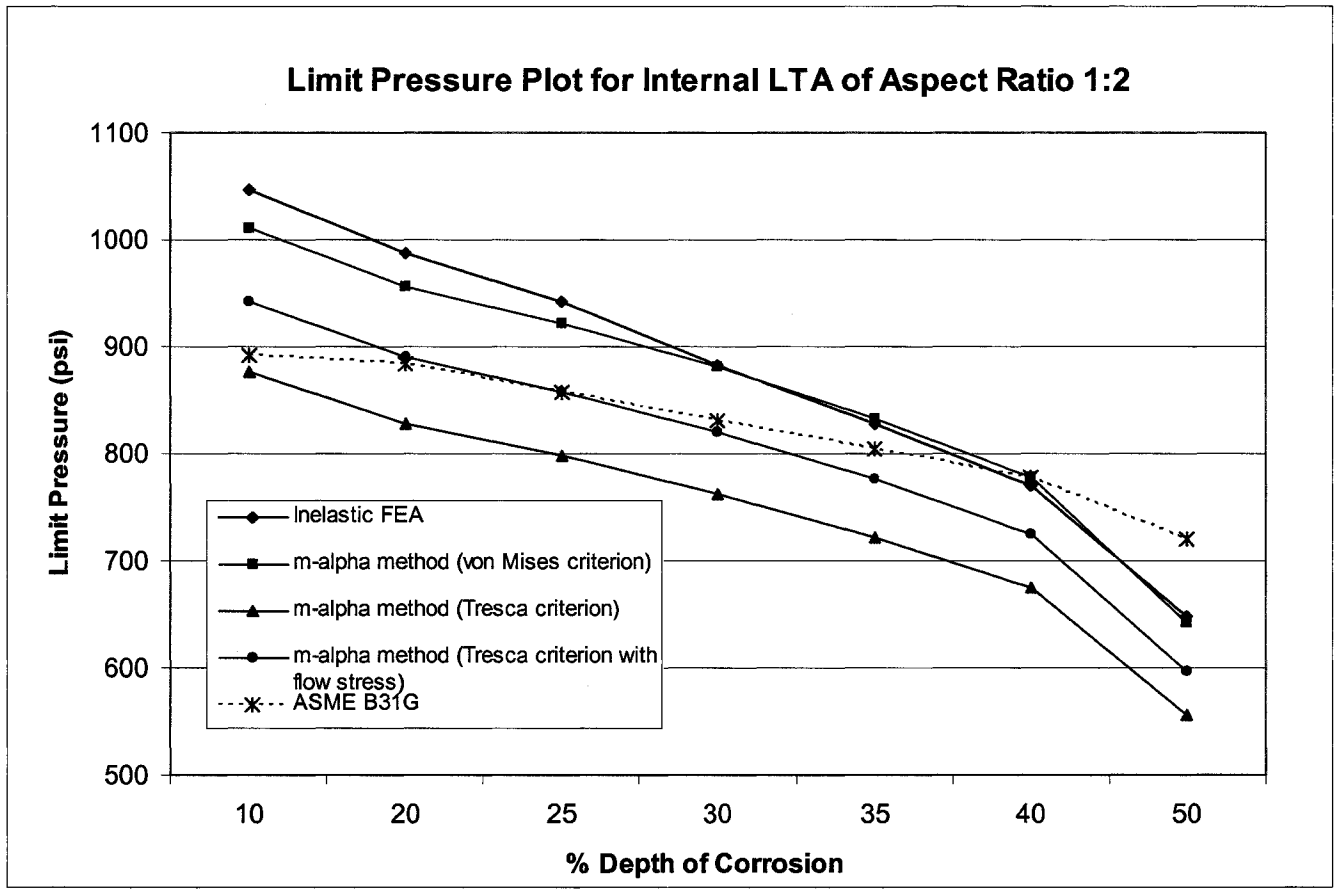
Limit Pressure Plot for Internal LTA of Aspect Ratio 1:2
Limit Pressure (psi)
1100
1000
900
800
700
600
500
10
20
25
30
35
40
50
% Depth of Corrosion
Inelastic FEA
m-alpha method (von Mises criterion)
m-alpha method (Tresca criterion)
m-alpha method (Tresca criterion with flow stress)
ASME B31G

Figure 4.7 (c)

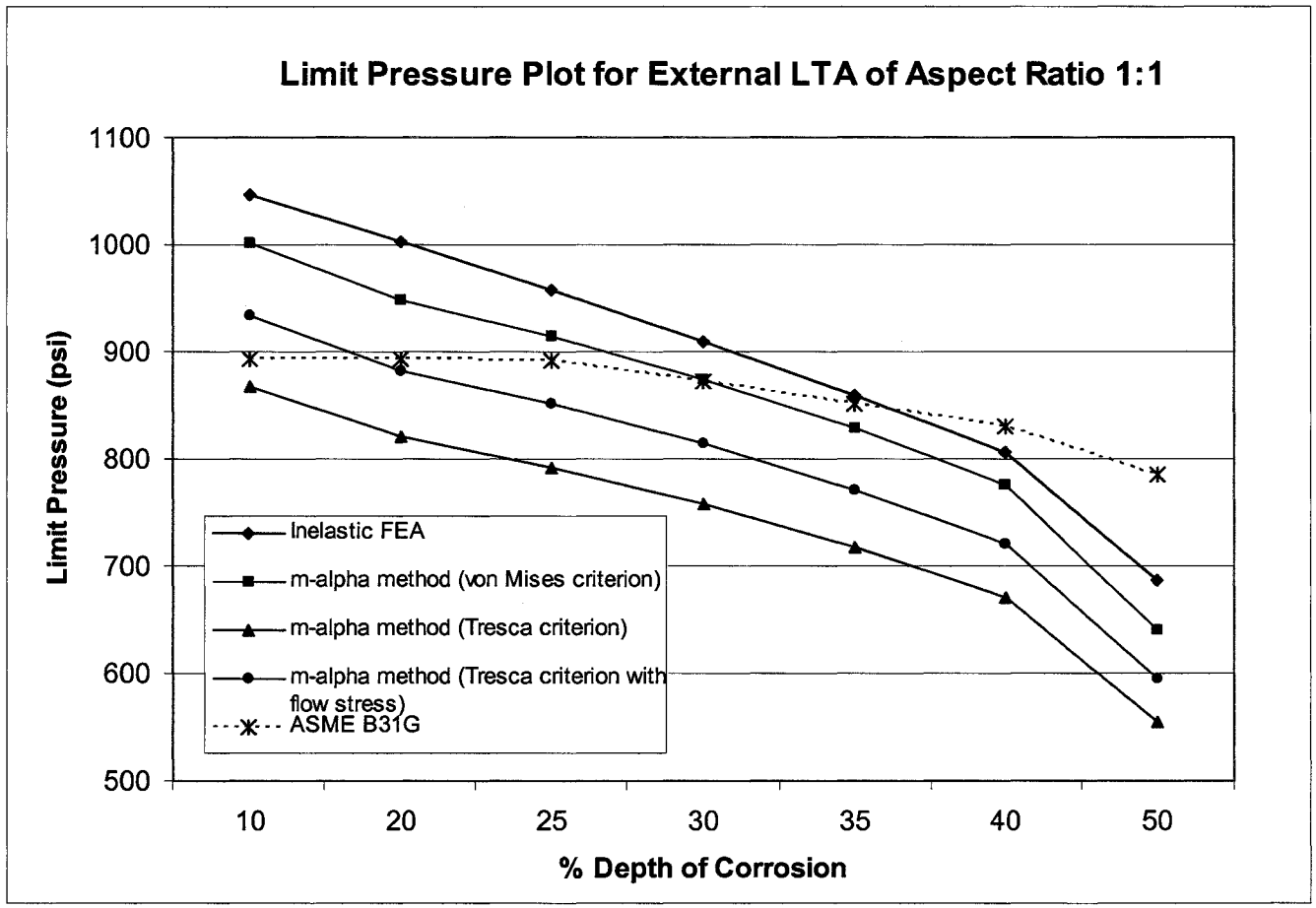
Limit Pressure Plot for External LTA of Aspect Ratio 1:1
Limit Pressure (psi)
1100
1000
900
800
700
600
500
10
20
25
30
35
40
50
% Depth of Corrosion
Inelastic FEA
m-alpha method (von Mises criterion)
m-alpha method (Tresca criterion)
m-alpha method (Tresca criterion with flow stress)
ASME B31G

Figure 4.8 (a)

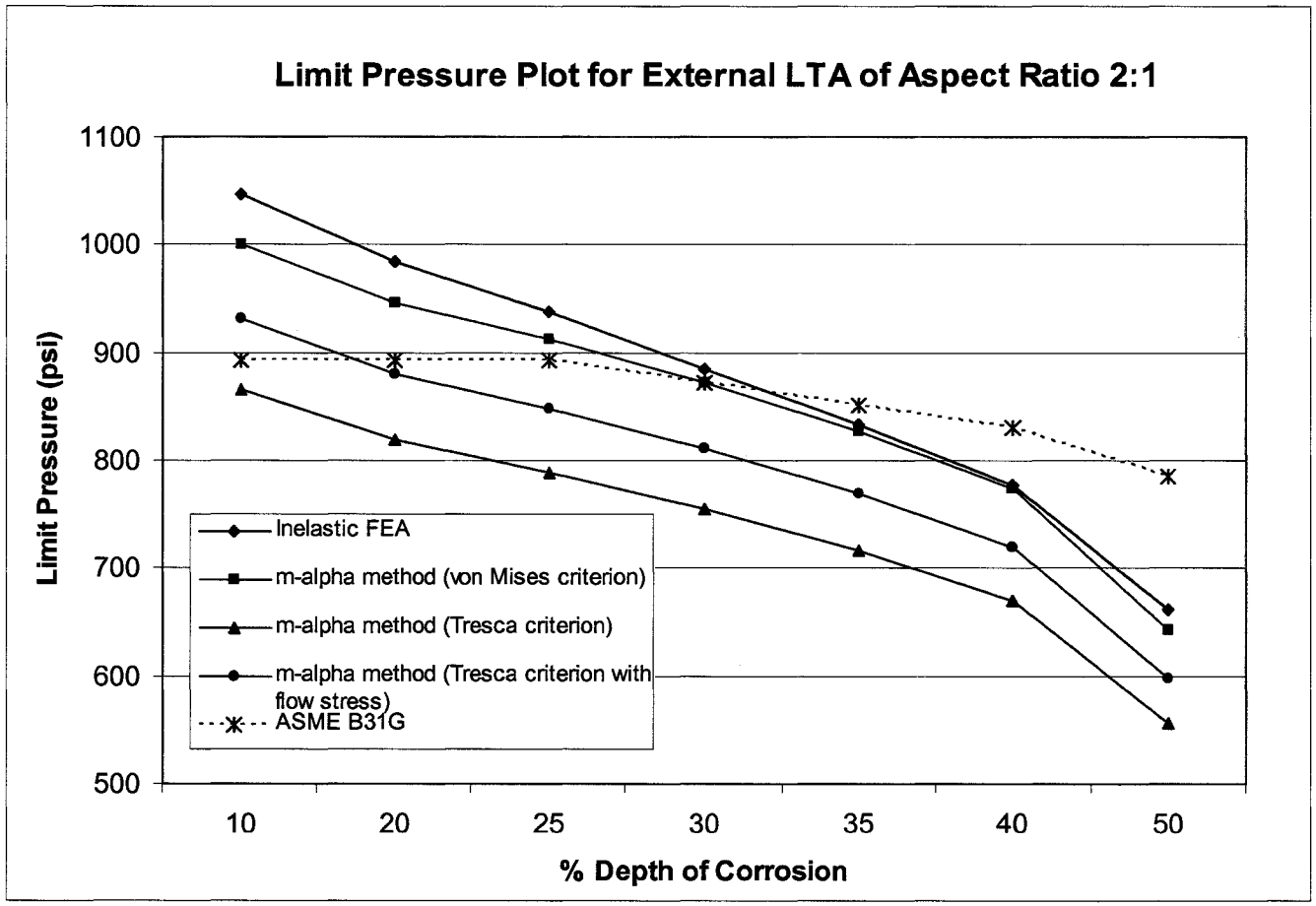
Limit Pressure Plot for External LTA of Aspect Ratio 2:1
Limit Pressure (psi)
1100
1000
900
800
700
600
500
10
20
25
30
35
40
50
% Depth of Corrosion
Inelastic FEA
m-alpha method (von Mises criterion)
m-alpha method (Tresca criterion)
m-alpha method (Tresca criterion with flow stress)
ASME B31G

Figure 4.8 (b)

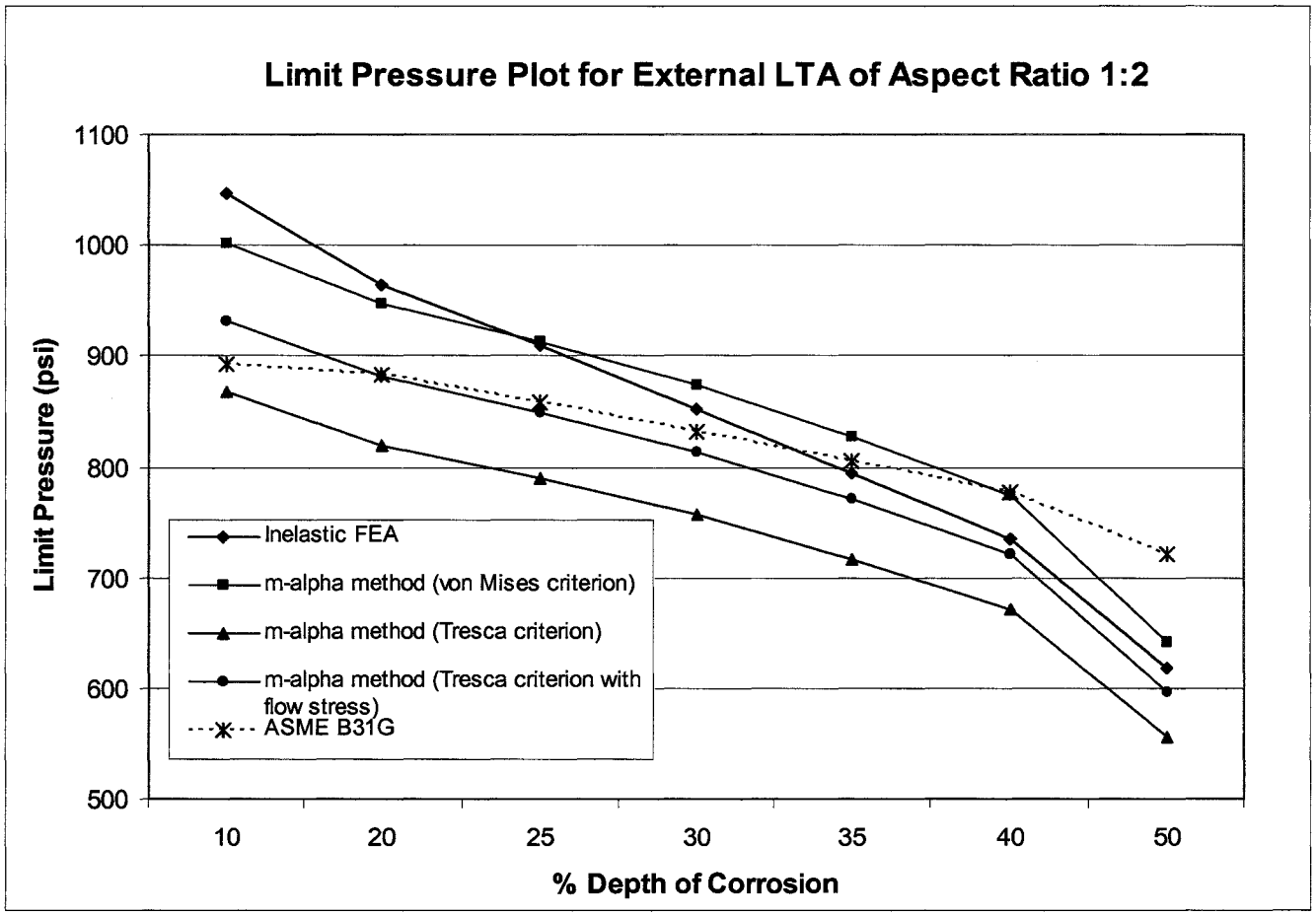
Limit Pressure Plot for External LTA of Aspect Ratio 1:2
Limit Pressure (psi)
1100
1000
900
800
700
600
500
10
20
25
30
35
40
50
% Depth of Corrosion
Inelastic FEA
m-alpha method (von Mises criterion)
m-alpha method (Tresca criterion)
m-alpha method (Tresca criterion with flow stress)
ASME B31G

Figure 4.8 (c)

4.6 Closure

A Level 2 method using variational principles of plasticity, in conjunction with the reference volume approach, has been found to be a simple and straight forward method for integrity assessment purposes. This thesis has presented a simple method to evaluate the effects of damage due to corrosion profiles and contours. The reference volume approach overcomes the limitation of other evaluation methods by considering the circumferential extent of corrosion. The method also provides a better understanding of the influence of damage on the integrity of the pipeline. The method is applied to a pipe with $r_i/t = 32.6$, and validated with inelastic FEA for different geometric configurations of internal and external corrosion. A sample calculation procedure to calculate RSF and limit pressure is presented. The results have been found to be conservative in most cases because of the apparent lower boundedness of m_α multiplier. The limit pressure has been predicted with reduced conservatism in most cases when compared with the ASME B31G criterion, which serves as the benchmark for comparison of various assessment procedures. It is to be noted that the damage implied by ASME B31G is underestimated for all aspect ratios and depths of corrosion. Because of its simplicity, the m_α method should be an attractive, easy to use procedure for engineers and can be programmed on a spread sheet.

CHAPTER 5

CONCLUSION

5.1 Contributions of the Thesis

The contributions of the thesis includes the extension of the Level 2 method, based on variational concepts in plasticity and reference volume, to pipelines with both internal and external corrosion. The application of robust limit load solutions for the assessment of LTA has yielded a direct, theoretical, simplified and improved evaluation procedure with a good understanding of the behaviour of LTA. Although the exact derivation of the relaxation lengths based on the classical shell theory is complex, it has been shown that the decay lengths can be conveniently used to define the reference volume. Introduction of the concept of reference volume to identify the kinematically active portion of the pipeline which participates in plastic action in the presence of damage has overcome the significant limitation of the existing methods by considering the circumferential extent of corrosion. This Level 2 solution has been implemented with

three yield criterions. Introduction of the flow stress (average of the yield stress and stress at 1% strain) as a failure stress has lead to the third criterion when it is applied with the Tresca criterion. This is done to obtain a less conservative prediction of the limit load when compared with the Tresca criterion.

Inelastic finite element analysis also has been carried out in this thesis in order to compare the results obtained by the variational method for validation purposes. Strain hardening was accounted in this material model to take advantage of the post yield behaviour of high strength pipeline steels. Although pipelines with LTA were traditionally assumed to fail by ductile tearing, limiting the membrane strain in the LTA to 1% would be a satisfactory failure criterion even in the case of pipelines made of low toughness materials or for pipelines that encounter loss of ductility due to service environment conditions. Permitting primary loads more than this limiting level would result in large deformations of the thinned section, which may result in a potential failure.

The study as a part of this thesis also involved a comparison of the remaining strength factor and limit pressure obtained using the ASME B31G criterion. This comparison showed the underestimation of the effect of corrosion damage by the ASME B31G criterion in the context of remaining strength factor. The variation of the limit pressure and RSF for various configurations of the LTA followed a similar pattern when variational method and inelastic FEA were used. The variational method gives an improved prediction of the limit pressure in most cases when compared with the ASME B31G criterion.

5.2 Future Research

This research can be extended in the direction of providing methods to calculate the reference volume of actual corrosion profiles. The corrosion profiles observed in pipelines in-service are usually irregular. A more accurate determination of the actual corrosion profile and determination of the reference volume will lead to a more accurate determination of the limit pressure and MAOP. A study has to be undertaken to validate different possibilities of considering the corroded volume and the reference volume with various shapes. This problem is complex due to the arbitrary variation of the corrosion profile dimensions in three dimensions: longitudinal, circumferential and radial (thickness) as seen in the pipelines in the field. A more optimized solution in this respect will yield a better method of assessing the structural integrity of corroded pipelines, which will be of great interest to the industry

This research can also be extended to analyze pipelines with multiple corrosion spots to evaluate their interaction effects. The decay lengths can be taken as a measure of the minimum required distance to avoid interactions. The interaction of LTA's is one of the problems encountered in the industry.

Another potential area of research is the extension of this method for the assessment of components of various shapes like spherical shells, elbows and conical shells with locally thinned areas. The challenge to this research lies in the determination of the reference volume for these shells of different geometries. A new expression for the

reference volume should be derived and used in conjunction with the variational method as done for cylindrical shells. This research can then be extended to assess composite structures such as storage tanks and vessels fabricated by welding different geometries. These recommended future research possibilities will set an evolutionary direction for the fitness-for-service assessment of industrial components with locally thinned areas (LTA's).

PUBLICATION

1. Ramkumar, B., and Seshadri, R., Q2, 2005, "Fitness-for-Service Assessment of Corroded Pipelines Based on Variational Concepts in Plasticity", The Journal of Pipeline Integrity.

REFERENCES

1. Office of Pipeline Safety website (http://ops.dot.gov/stats/stats.htm#average)

2. Canadian Energy Pipeline Association website (http://www.cepa.com)

3. Office of Pipeline Safety website (http://ops.dot.gov/stats/stats.htm)

4. Krishnaswamy, P., Stephens, D.R., Mohan, R., Scott, P., Osage, D.A., Sims, J.R., and Wilkowski, G.M., 1997, "Technologies for Evaluation of Erosion/Corrosion, Pitting, Blisters, Shell Out-of-Roundness, Weld Misalignment, Bulges and Dents in Pressurized Components", Final Report to Pressure Vessel Research Council, Battelle Memorial Institute, Columbus, OH.

5. ASME, "Manual for Determining the Remaining Strength of Corroded Pipelines", ASME B31G, 2001.

6. Chouchaoui, B.A., and Pick, R.J., 1994, "A Three Level Assessment of the Residual Strength of Corroded Line Pipe", OMAE – Volume V, Pipeline Technology, pp. 9-18.

7. Kiefner, J.F., and Vieth, P.H., 1989, "A Modified Criterion for Evaluating the Remaining Strength of Corroded Pipe", Final Report on Project PR3-805, Battelle Memorial Institute, Columbus, OH.

8. David A. Osage, Jeremy Janelle, and Philip A Henry, 2000, "Fitness-For-Service Local Metal Loss Assessment Rules in API 579", ASME PVP-Vol. 411, pp. 143-176.

9. Sims, J.R., Hantz, B.F., and Kuehn, K.E., 1992, "A Basis for the Fitness for Service Evaluation of Thin Areas in Pressure Vessels and Storage Tanks", PVP-Vol 233, Pressure Vessel Fracture, Fatigue and Life Management, ASME 1992, pp. 51-58.

10. Kiefner, J.F., Maxey, W.A., Eiber, R.J., and Duffy, A.R., 1973, "Failure Stress Levels of Flaws in Pressurized Cylinders", Progress in Flaw Growth and Fracture Toughness Testing, ASTM STP 536, American Society for Testing and Materials, 1973, pp 461-481.

11. Kiefner, J.F., 1990, "The Remaining Strength of Corroded Pipe", API Pipeline Conference, April 1990.

12. Kiefner, J.F., and Duffy, A.R., 1971, "Summary of Research to Determine the Strength of Corroded Areas in Line Pipe", presented at a public hearing at the U.S. Department of Transportation, (July 20, 1971).

13. Cronin, D.S., and Pick, R.J., 2000, "Experimental Database for Corroded Pipe: Evaluation of RSTRENG and B31G", 2000 International Pipeline Conference – Vol 2, ASME, pp. 757-767.

14. Kanninen, M.F., Pagalthivarthi, K.V., and Popelar, C.H., 1992, "Theoretical Analysis for the Residual Strength of Corroded Gas and Oil Transmission pipelines", ASTM Special Technical Publication, n1137, pp. 183-198.

15. Cronin, D.S., and Pick, R.J., 2002, "Prediction of the Failure Pressure for Complex Corrosion Defects", International Journal of Pressure Vessels and Piping, Vol. 79, n4, pp. 279-287.

16. Svensson, N.L., 1959, "The Bursting Pressure of Cylindrical and Spherical Vessels", ASME Pressure Vessel and Piping Design.

17. David Batte, Bin Fu, Mike G Kirkwood, and Dan Vu, 1997, "Advanced Methods of Integrity Assessment of Corroded Pipelines", Pipes and Pipelines International, January – February 1997, pp 5 - 11.

18. Leis, B.N., Stephens, D.R., 1997, "An Alternative Approach to Assess the Integrity of Corroded Line Pipe – Part I: Current Status", Proceedings of the Seventh International Offshore and Polar Engineering Conference, pp 624 - 634.

19. Mura, T., Rimawi, W.H., and Lee, S.L., 1965, "Extended Theorems of Limit Analysis", Quarterly of Applied Mathematics, 23, pp. 171-179.

20. Seshadri, R., and Mangalaramanan, S.P., 1997, "Lower Bound Limit Loads using Variational Concepts: the m_α - method", International Journal of Pressure Vessel and Piping, 71, pp. 93-106.

21. Calladine, C.R., and Drucker, D.C., 1962, "Nesting Surfaces for Constant Rate of Energy Dissipation and Creep, Quarterly of Applied Mathematics, Vol. 20, pp. 79-84

22. Boyle, J.T., 1982, "The Theorem of Nesting Surfaces in Steady Creep and its Application to Generalized Models and Limit Reference Stresses", Res Mechanica, Vol. 4, pp. 275-294

23. Mura, T. and Lee, S.L., 1963, "Application of Variational Principles to Limit Analysis", Quarterly of Applied Mathematics, 21, pp. 243-248.

24. Pan, L., and Seshadri, R., 2001, "Limit Load Estimation Using Plastic Flow Parameter in Repeated Elastic Finite Element Analysis", ASME PVP-Vol. 430, pp. 145-150.

25. Reinhardt, W.D., and Seshadri, R., 2003, "Limit Load Bounds for the m_α - multiplier", ASME Journal of Pressure Vessel Technology, 125, pp. 34-56.

26. Seshadri, R., 2005, "Integrity Assessment of Pressure Components with Local Hot Spots", ASME Journal of Pressure Vessel Technology, ASME Journal of Pressure Vessel Technology, 127, pp. 137-142.

27. Indermohan, H., and Seshadri, R., 2005, "Fitness-For-Service Methodology Based on Variational Principles in Plasticity", ASME Journal of Pressure Vessel Technology, 127, pp. 92-97.

28. ANSYS, 2004, University Research Version, 7.1, SAS IP, Inc.

29. Noronha Jr., D.B., Benjamin, A.C., and Andrade, E.Q., 2002, "Finite Element Models for the Prediction of the Failure Pressure of Pipelines with Long Corrosion Defects", Proceedings of IPC'02, pp. 1751-1758.

30. Kim., Y.J., Shim, D.J., Lim, H., and Kim, Y.J., 2004, "Reference Stress Based Approach to Predict Failure Strength of Pipes with Local Wall Thinning Under Single Loading", ASME Journal of Pressure Vessel Technology, 126, pp. 194-201.

31. DePadova, T.A., and Sims, J.R., 1995, "Fitness for Service Local Thin Areas Comparison of Finite Element Analysis to Physical Test Results", ASME PVP-Vol 315, Fitness-For-Service and Decisions for Petroleum and Chemical Equipment.

APPENDIX A

ANSYS INPUT FILES

A.1 Inelastic analysis of Undamaged Pipe

```
/title, Inelastic Analysis of Undamaged Pipe

! *** Dimensions ***

Ro=12                ! Outer Diameter of the Pipe

t=0.375              ! Wall thickness

Len=75               ! Length of the Pipe

!*** Material Properties of the Pipe ***

E=30e6               ! Elastic modulus

Y=30000              ! Yield Stress

T=50e4               ! Plastic modulus or tangent modulus

P=0.3                ! Poisson's Ratio

! *** Applied Loading ***

P=1100               ! Internal Pressure

!*** Calculation of Longitudinal Stress ***

Ri=Ro-t              ! Inner Radius of the Pipe

Rm=(Ro+Ri)/2         ! Mean Radius of the Pipe

sigmaL=((P)*(Ri)*(Ri))/(2*Rm*t)    ! Longitudinal Stress

!*** Element Size ***

Lon_Div=50           ! Number of element divisions along longitudinal direction
```

```
Arc_Div=15          ! Number of element divisions along circumferential direction
Thk_Div=4           ! Number of element divisions along thickness

!*** Pre-processing ***
/PREP7

!*** Set element type ***
 ET,1,SOLID185

!*** Set Material Properties ***
MP,EX,1,E
MP,PRXY,1,P
TB,BKIN,1,1,2,1
TBDATA,,Y,T,,,,

!*** Solid Modeling ***
K,1,0,0,0,          ! Definition of key points
K,2,Ri,0,0,
K,3,,Ri,0,
K,4,,-Ri,0,
K,5,Ro,,0,
K,6,0,Ro,0,
K,7,0,-Ro,0,
K,8,0,,Len,
```

```
LARC,2,3,1,Ri,
LARC,5,6,1,Ro,
LARC,2,4,1,Ri,
LARC,5,7,1,Ro,
L,2,5
L,3,6
L,4,7
L,1,8
al,5,1,6,2                ! Definition of areas using lines and arcs
al,5,3,7,4
VDRAG, 1,2 , , , , ,8     ! Extrusion of areas to construct volumes
```

!* Finite Element Mode and Meshing ***

```
lesize,13, , ,Lon_Div     ! Define the number of element divisions for lines
lesize,15, , ,Lon_Div
lesize,1, , ,Arc_Div
lesize,2, , ,Arc_Div
lesize,3, , ,Arc_Div
lesize,4, , ,Arc_Div
lesize,6, , ,Thk_Div
lesize,7, , ,Thk_Div
vmesh,all                 ! Mesh the volume
```

!* Apply Loads and Boundary Conditions*****

```
SFA,6,1,PRES,P          ! Internal Pressure
SFA,10,1,PRES,P
SFA,1,1,PRES,-sigmaL    ! Longitudinal stress to simulate end capped condition
SFA,2,1,PRES,-sigmaL

DA,5,SYMM               ! Application of symmetric boundary conditions
DA,9,SYMM
DA,7,SYMM
DA,11,SYMM

DK,10,UY,0

DTRAN                   ! Transfer boundary conditions from solid to FE model
SFTRAN                  ! Transfer loads from solid to FE model
```

!* Solution *****

```
/SOLU
NSUBST,200              ! Set the number of substeps for incremental loading
OUTRES,ALL,ALL
solve
```

A.2 Inelastic analysis of Pipe with Internal Corrosion

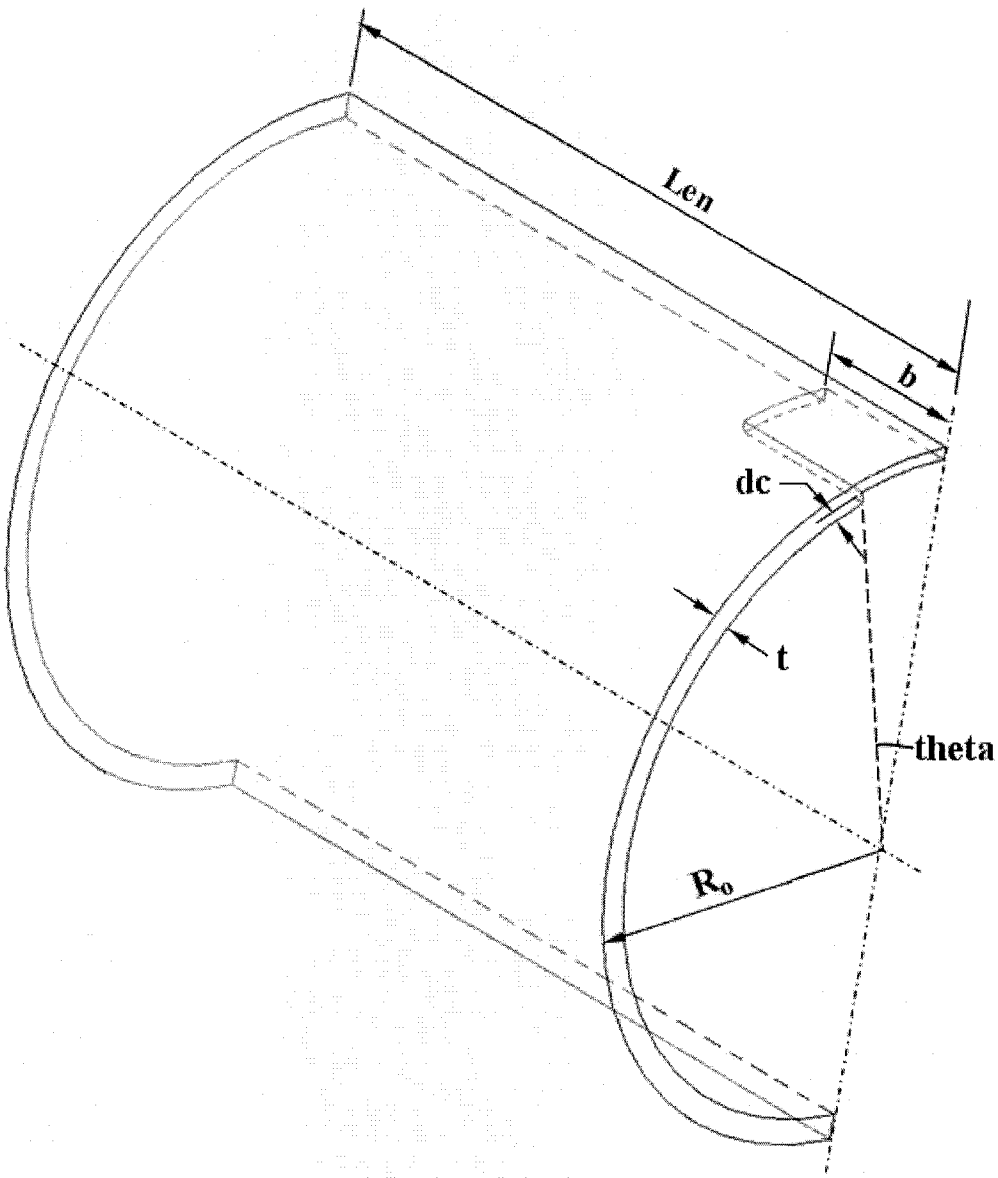

Figure A.1: Model of Pipe with Internal Corrosion

/title, Inelastic Analysis of Pipe with Internal Corrosion

! * Dimensions *****

Ro=12 ! Outer Diameter of the Pipe

t=0.375 ! Wall thickness

Len=75 ! Length of the Pipe

! * Corrosion Configuration *****

dc=0.25 ! Depth of corrosion

theta=13.89 ! Circumferential extent of corrosion (Half angle)

b=10 ! Longitudinal extent of corrosion (Half length)

!* Material Properties of the Pipe *****

E=30e6 ! Elastic modulus

Y=30000 ! Yield Stress

T=50e4 ! Plastic modulus or tangent modulus

P=0.3 ! Poisson's Ratio

! * Applied Loading *****

P=700 ! Internal Pressure

!* Calculation of Longitudinal Stress *****

Ri=Ro-t ! Inner Radius of the Pipe

Rm=(Ro+Ri)/2 ! Mean Radius of the Pipe

Rc=Ri+dc ! Inner radius of corrosion

```
sigmaL=((P)*(Ri)*(Ri))/(2*Rm*t)     ! Longitudinal Stress
```

!* Calculation of arc lengths ***

```
pi=3.141592654

arc1=(1.57*Rc)

arc4=(1.57*Ri)

arc5=(1.57*Ro)

arc2=(pi*theta*Rc)/180

arc3=(pi*theta*Ri)/180

arc6=(pi*theta*Ro)/180

a=arc2/arc1

a1=arc3/arc4

a2=arc6/arc5
```

!* Element Size ***

```
b_div=20              ! Number of elements along axial direction in the LTA

theta_div=10          ! Number of elements along circumferential direction in the LTA

Lon_Div=70            ! Number of elements along longitudinal direction in undamaged region

Arc_Div1=25         ! Number of elements along circumferential direction in undamaged region

arc_div2=18         ! Number of elements along circumferential direction in undamaged region

tc_Div=4              ! Number of elements along corrosion depth

t_div=3               ! Number of elements along remaining thickness of the pipe

lon_space_ratio=6     ! Longitudinal spacing ratio along the undamaged region
```

```
arc_space_ratio=5       ! Circumferential spacing ratio along the undamaged region

!*** Pre-processing ***

/PREP7

!*** Set element type ***

 ET,1,SOLID185

!*** Set Material Properties ***

MP,EX,1,E

MP,PRXY,1,P

TB,BKIN,1,1,2,1

TBDATA,,Y,T,,,,

!*** Solid Modeling ***

!*** Basic Cylinder ***

K,1,0,0,0,              ! Definition of key points

K,2,Ri,0,0,

K,3,,Ri,0,

K,4,,-Ri,0,

K,5,Ro,,0,

K,6,0,Ro,0,

K,7,0,-Ro,0,

K,8,0,,Len,
```

```
LARC,2,3,1,Ri,
LARC,5,6,1,Ro,
LARC,2,4,1,Ri,
LARC,5,7,1,Ro,
L,2,5
L,3,6
L,4,7
L,1,8
al,5,1,6,2                ! Definition of areas using lines and arcs
al,5,3,7,4
VDRAG, 1,2 , , , , ,8     ! Extrusion of areas to construct volumes
```

!* Corrosion Construction ***

```
K,15,0,Rc,0,              ! Creation of key points defining the corrosion profile
K,16,Rc,0,0,
LARC,15,16,1,Rc,
LDIV,22,a,17
LDIV,1,1-a,18
L,17,18
LCSL,6,22
al,26,22,25,24
vext,12,,,,,b             ! Creation of corroded volume
vsbv,1,3          ! Subtraction of corroded volume from entire volume of the cylinder
```

!* Modification of Volumes for Mapped Meshing ***

```
LDIV,2,1-a2,51

L,18,51

LDIV,12,1-a2,52

LDIV,16,a1,53

L,52,53

A,52,53,18,51

VSBA,     4,     1          ! Dividing into individual volumes circumferentially

K,54,Ro+10,Ro+10,b,

K,55,-(Ro+10),(Ro+10),b,

K,56,-(Ro+10),-(Ro+10),b,

K,57,Ro+10,-(Ro+10),b,

A,54,55,56,57

VSBA,     3,     1          ! Dividing into individual volumes longitudinally

K,54,Ro+10,Ro+10,b,

K,55,-(Ro+10),(Ro+10),b,

K,56,-(Ro+10),-(Ro+10),b,

K,57,Ro+10,-(Ro+10),b,

A,54,55,56,57

VSBA,     1,     1          ! Dividing into individual volumes longitudinally

K,54,Ro+10,Ro+10,b,
```

K,55,-(Ro+10),(Ro+10),b,

K,56,-(Ro+10),-(Ro+10),b,

K,57,Ro+10,-(Ro+10),b,

A,54,55,56,57

VSBA, 2, 1 ! Dividing into individual volumes longitudinally

!* Finite Element Mode and Meshing ***

!* Set the Element Divisions ***

lesize,48, , ,Lon_Div,lon_space_ratio

lesize,35, , ,Lon_Div,lon_space_ratio

lesize,49, , ,Lon_Div,lon_space_ratio

lesize,40, , ,Lon_Div,lon_space_ratio

lesize,41, , ,Lon_Div,lon_space_ratio

lesize,42, , ,Lon_Div,lon_space_ratio

lesize,58, , ,Lon_Div,lon_space_ratio

lesize,59, , ,Lon_Div,lon_space_ratio

!lesize,62, , ,Lon_Div,lon_space_ratio

lesize,12, , ,Arc_Div1,arc_space_ratio

lesize,31, , ,Arc_Div1,arc_space_ratio

lesize,51, , ,Arc_Div1,arc_space_ratio

lesize,52, , ,Arc_Div1,arc_space_ratio

lesize,1, , ,Arc_Div1,arc_space_ratio

lesize,2, , ,Arc_Div1,arc_space_ratio

lesize,23, , ,Arc_Div1,arc_space_ratio

lesize,17, , ,Arc_Div2

lesize,21, , ,Arc_Div2

lesize,38, , ,Arc_Div2

lesize,56, , ,Arc_Div2

lesize,3, , ,Arc_Div2

lesize,4, , ,Arc_Div2

lesize,26, , ,theta_Div

lesize,16, , ,theta_Div

lesize,45, , ,theta_Div

lesize,28, , ,theta_Div

lesize,30, , ,theta_Div

lesize,15, , ,theta_Div

lesize,22, , ,theta_Div

lesize,27, , ,tc_Div

lesize,39, , ,tc_Div

lesize,46, , ,tc_Div

lesize,47, , ,tc_Div

lesize,25, , ,t_Div

```
lesize,29, , ,t_Div

lesize,6, , ,t_Div


lesize,43, , ,b_Div

lesize,32, , ,b_Div

lesize,44, , ,b_Div

lesize,33, , ,b_Div

lesize,34, , ,b_Div

lesize,53, , ,b_Div

lesize,54, , ,b_Div

lesize,37, , ,b_Div

lesize,55, , ,b_Div


LREVERSE,35      ! Reverse line directions to obtain the desired gradually varying mesh

LREVERSE,41

LREVERSE,42

LREVERSE,58

LREVERSE,59

LREVERSE,2

LREVERSE,1

LREVERSE,12
```

!* Concatenate Lines and Areas to Enable Mapped Meshing ***

```
LCCAT,25,39
```

LCCAT,47,29

LCCAT,46,6

LCCAT,15,2

LCCAT,43,48

LCCAT,44,49

LCCAT,40,34

LCCAT,37,59

LCCAT,54,42

LCCAT,53,41

ACCAT,12,2

ACCAT,16,19

ACCAT,18,13

vmesh,all ! Mesh the entire volume

!* Apply Loads and Boundary Conditions*****

SFA,15,1,PRES,P ! Internal Pressure

SFA,24,1,PRES,P

SFA,29,1,PRES,P

SFA,21,1,PRES,P

SFA,3,1,PRES,P

SFA,35,1,PRES,P

```
DA,23,SYMM              ! Symmetric boundary conditions
DA,12,SYMM
DA,2,SYMM
DA,7,SYMM
DA,26,SYMM
DA,14,SYMM
DA,34,SYMM
SFA,22,1,PRES,-sigmaL       ! Longitudinal stress to simulate end capped condition
SFA,6,1,PRES,-sigmaL
SFA,11,1,PRES,-sigmaL

DK,5,UY,0

DTRAN                   ! Transfer boundary conditions from solid to FE model
SFTRAN                  ! Transfer loads from solid to FE model

!*** Solution ***
/SOLU
NSUBST,200              ! Set the number of substeps for incremental loading
OUTRES,ALL,ALL
Solve
```

A.3 Inelastic analysis of Pipe with External Corrosion

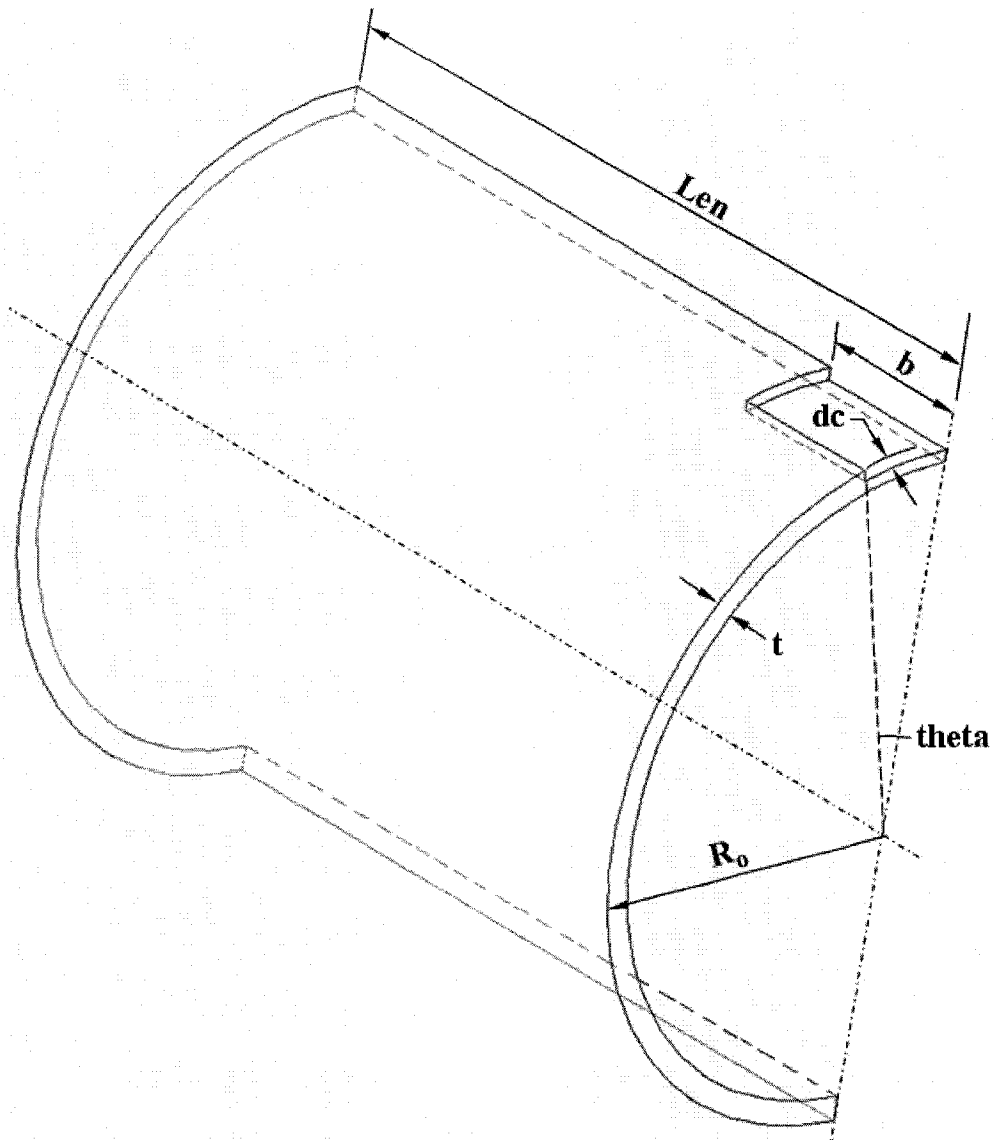

Figure A.1: Model of Pipe with External Corrosion

/title, Inelastic Analysis of Pipe with External Corrosion

! * Dimensions *****

Ro=12 ! Outer Diameter of the Pipe

t=0.375 ! Wall thickness

Len=75 ! Length of the Pipe

! * Corrosion Configuration *****

dc=0.25 ! Depth of corrosion

theta=13.89 ! Circumferential extent of corrosion (Half angle)

b=10 ! Longitudinal extent of corrosion (Half length)

!* Material Properties of the Pipe *****

E=30e6 ! Elastic modulus

Y=30000 ! Yield Stress

T=50e4 ! Plastic modulus or tangent modulus

P=0.3 ! Poisson's Ratio

! * Applied Loading *****

P=700 ! Internal Pressure

!* Calculation of Longitudinal Stress *****

Ri=Ro-t ! Inner Radius of the Pipe

Rm=(Ro+Ri)/2 ! Mean Radius of the Pipe

Rc=Ro-dc ! Inner radius of corrosion

```
sigmaL=((P)*(Ri)*(Ri))/(2*Rm*t)     ! Longitudinal Stress
```

!* Calculation of arc lengths ***

```
pi=3.141592654

arc1=(1.57*Rc)

arc4=(1.57*Ri)

arc5=(1.57*Ro)

arc2=(3.14*theta*Rc)/180

arc3=(3.14*theta*Ri)/180

arc6=(3.14*theta*Ro)/180

a=arc2/arc1

a1=arc3/arc4

a2=arc6/arc5
```

!* Element Size ***

```
b_div=20              ! Number of elements along axial direction in the LTA

theta_div=10          ! Number of elements along circumferential direction in the LTA

Lon_Div=70            ! Number of elements along longitudinal direction in undamaged region

Arc_Div1=25         ! Number of elements along circumferential direction in undamaged region

arc_div2=18         ! Number of elements along circumferential direction in undamaged region

tc_Div=4              ! Number of elements along corrosion depth

t_div=3               ! Number of elements along remaining thickness of the pipe

lon_space_ratio=6     ! Longitudinal spacing ratio along the undamaged region
```

```
arc_space_ratio=5       ! Circumferential spacing ratio along the undamaged region

!*** Pre-processing ***

/PREP7

!*** Set element type ***

 ET,1,SOLID185

!*** Set Material Properties ***

MP,EX,1,E

MP,PRXY,1,P

TB,BKIN,1,1,2,1

TBDATA,,Y,T,,,,

!*** Solid Modeling ***

!*** Basic Cylinder ***

K,1,0,0,0,              ! Definition of key points

K,2,Ri,0,0,

K,3,,Ri,0,

K,4,,-Ri,0,

K,5,Ro,,0,

K,6,0,Ro,0,

K,7,0,-Ro,0,

K,8,0,,Len,
```

```
LARC,2,3,1,Ri,
LARC,5,6,1,Ro,
LARC,2,4,1,Ri,
LARC,5,7,1,Ro,
L,2,5
L,3,6
L,4,7
L,1,8
al,5,1,6,2                ! Definition of areas using lines and arcs
al,5,3,7,4
VDRAG, 1,2 , , , , ,8     ! Extrusion of areas to construct volumes
```

!*Corrosion Construction*****

```
K,15,0,Rc,0,              ! Creation of key points defining the corrosion profile
K,16,Rc,0,0,
LARC,15,16,1,Rc,
LDIV,22,a,17
LDIV,2,1-a2,18
L,17,18
LCSL,6,22
al,22,27,24,25
vext,12,,,,,b             ! Creation of corroded volume
vsbv,1,3          ! Subtraction of corroded volume from entire volume of the cylinder
```

!* Modification of Volumes for Mapped Meshing ***

LDIV,1,1-a1,51

L,18,51

LDIV,12,1-a2,52

LDIV,16,a1,53

L,52,53

A,52,53,51,18

VSBA, 4, 1 ! Dividing into individual volumes circumferentially

K,54,Ro+10,Ro+10,b,

K,55,-(Ro+10),(Ro+10),b,

K,56,-(Ro+10),-(Ro+10),b,

K,57,Ro+10,-(Ro+10),b,

A,54,55,56,57

VSBA, 3, 1 ! Dividing into individual volumes longitudinally

K,54,Ro+10,Ro+10,b,

K,55,-(Ro+10),(Ro+10),b,

K,56,-(Ro+10),-(Ro+10),b,

K,57,Ro+10,-(Ro+10),b,

A,54,55,56,57

VSBA, 1, 1 ! Dividing into individual volumes longitudinally

K,54,Ro+10,Ro+10,b,

K,55,-(Ro+10),(Ro+10),b,

K,56,-(Ro+10),-(Ro+10),b,

K,57,Ro+10,-(Ro+10),b,

A,54,55,56,57

VSBA, 2, 1 ! Dividing into individual volumes longitudinally

!* Finite Element Mode and Meshing ***

!* Set the Element Divisions ***

lesize,48, , ,Lon_Div,lon_space_ratio

lesize,35, , ,Lon_Div,lon_space_ratio

lesize,49, , ,Lon_Div,lon_space_ratio

lesize,40, , ,Lon_Div,lon_space_ratio

lesize,41, , ,Lon_Div,lon_space_ratio

lesize,42, , ,Lon_Div,lon_space_ratio

lesize,58, , ,Lon_Div,lon_space_ratio

lesize,59, , ,Lon_Div,lon_space_ratio

lesize,12, , ,Arc_Div1,arc_space_ratio

lesize,34, , ,Arc_Div1,arc_space_ratio

lesize,51, , ,Arc_Div1,arc_space_ratio

lesize,52, , ,Arc_Div1,arc_space_ratio

lesize,2, , ,Arc_Div1,arc_space_ratio

lesize,23, , ,Arc_Div1,arc_space_ratio

lesize,1, , ,Arc_Div1,arc_space_ratio

lesize,17, , ,Arc_Div2

lesize,21, , ,Arc_Div2

lesize,38, , ,Arc_Div2

lesize,56, , ,Arc_Div2

lesize,3, , ,Arc_Div2

lesize,4, , ,Arc_Div2

lesize,27, , ,theta_Div

lesize,16, , ,theta_Div

lesize,29, , ,theta_Div

lesize,6, , ,theta_Div

lesize,45, , ,theta_Div

lesize,13, , ,theta_Div

lesize,22, , ,theta_Div

lesize,26, , ,tc_Div

lesize,43, , ,tc_Div

lesize,39, , ,tc_Div

lesize,44, , ,tc_Div

lesize,25, , ,t_Div

lesize,28, , ,t_Div

lesize,30, , ,t_Div

lesize,31, , ,b_Div

lesize,46, , ,b_Div

lesize,33, , ,b_Div

lesize,32, , ,b_Div

lesize,47, , ,b_Div

lesize,54, , ,b_Div

lesize,53, , ,b_Div

lesize,37, , ,b_Div

lesize,55, , ,b_Div

!* Concatenate Lines and Areas to Enable Mapped Meshing ***

LCCAT,43,30

LCCAT,28,44

LCCAT,25,39

LCCAT,46,48

LCCAT,1,13

LCCAT,3,1

LCCAT,4,2

LCCAT,49,47

LCCAT,33,40

LCCAT,27,12

LCCAT,12,17

```
LCCAT,16,34

LCCAT,34,21

LCCAT,41,53

LCCAT,42,54

LCCAT,58,55

LCCAT,59,37

ACCAT,15,19

ACCAT,6,13

LREVERSE,35     ! Reverse line directions to obtain the desired gradually varying mesh

LREVERSE,41

LREVERSE,42

LREVERSE,58

LREVERSE,59

LREVERSE,1

LREVERSE,2

LREVERSE,12

vmesh,all                    ! Mesh the entire volume
```

!* Apply Loads and Boundary Conditions*****

```
SFA,7,1,PRES,P               ! Internal Pressure

SFA,25,1,PRES,P
```

```
SFA,29,1,PRES,P
SFA,21,1,PRES,P
SFA,3,1,PRES,P
SFA,35,1,PRES,P

DA,22,SYMM              ! Symmetric boundary conditions
DA,12,SYMM
DA,2,SYMM
DA,26,SYMM
DA,18,SYMM
DA,16,SYMM
DA,34,SYMM

DK,5,UY,0

SFA,23,1,PRES,-sigmaL       ! Longitudinal stress to simulate end capped condition
SFA,5,1,PRES,-sigmaL
SFA,11,1,PRES,-sigmaL

DTRAN                   ! Transfer boundary conditions from solid to FE model
SFTRAN                  ! Transfer loads from solid to FE model

!*** Solution ***
/SOLU
NSUBST,200              ! Set the number of substeps for incremental loading
```

OUTRES,ALL,ALL

solve